Linking bacterial symbiont physiology to the ecology of hydrothermal vent symbioses

Linking bacterial symbiont physiology to the ecology of hydrothermal vent symbioses

A dissertation presented

by

Roxanne Abra Beinart

to

The Department of Organismic and Evolutionary Biology

in partial fulfillment of the requirements
for the degree of
Doctor of Philosophy
in the subject of
Biology

Harvard University
Cambridge, Massachusetts

November 2013

Dissertation advisor: Peter R. Girguis Roxanne Abra Beinart

Linking bacterial symbiont physiology to the ecology of hydrothermal vent symbioses

Symbioses between prokaryotes and eukaryotes are ubiquitous in our biosphere, nevertheless, the effects of such associations on the partners' ecology and evolution are poorly understood. At hydrothermal vents, dominant invertebrate species typically host bacterial symbionts, which use chemical energy to fix carbon to nourish their hosts and themselves. In this dissertation, I present evidence that symbiont metabolism plays a substantive, if not major, role in habitat use by vent symbioses. A study of nearly 300 individuals of the symbiotic snail *Alviniconcha* sp. showed specificity between three host species and three specific symbiont phylotypes, as well as a novel lineage of Oceanospirillales. Additionally, this study revealed a structured distribution of each *Alviniconcha*-symbiont combination across ~300 km of hydrothermal vents that exhibited a gradient in geochemical composition, which is consistent with the physiological tendencies of the specific symbiont phylotypes. I also present a comparison of the *in situ* gene expression of the symbionts of *Alviniconcha* across that same geochemical gradient, which further implicates symbiont energy and nitrogen metabolism in governing the habitat partitioning of *Alviniconcha*. Finally, I present data that allies productivity and sulfur metabolism in three coexisting vent symbioses, demonstrating specific interaction with the environment. Three symbioses, namely the snails *Alviniconcha* and *Ifremeria*, and the mussel *Bathymodiolus*, are found around vents with differing concentrations of sulfide, thiosulfate and polysulfide. Using high-pressure, flow-through incubations and stable isotopic tracers, I quantified symbiont productivity via sulfide and thiosulfate oxidation, and provided the first demonstration of thiosulfate-dependent autotrophy in intact hydrothermal vent symbioses. I further demonstrated that vent symbioses can excrete

thiosulfate and/or polysulfides, implicating them in substantively influencing the sulfur chemistry of their habitats. In summary, this dissertation demonstrates the importance of symbiont physiology to the ecology of prokaryote-eukaryote symbioses by revealing that symbiont activity may be critically important to the distribution of symbioses among specific niches, as well as can alter the geochemical environment through uptake and excretion of chemicals.

Linking bacterial symbiont physiology to the ecology of hydrothermal vent symbioses

Table of Contents

Acknowledgements

All that I have accomplished as a PhD student was made possible with the help and support of amazing people, both in my professional and personal life. I will always be beyond grateful to my advisor, Peter Girguis, for the faith he had in me from the very beginning, his continued patience and attention throughout my time in graduate school, and above all else, the fact that that he always treated me as a peer. The scope of skills I learned in the Girguis lab is beyond what I ever predicted I would as a graduate student: from wiring an outlet to identifying a pipe-fitting to writing a proposal. I am thankful for all that I have learned from Pete, and I know that I will only appreciate these things more as I move forward into other research. I also thank my committee, Andrew Knoll, Colleen Cavanaugh and Christopher Marx ; their questions were always balanced by encouragement and my dissertation is inestimably better because of their input and help.

I must also express gratitude to the past and current members of the Girguis lab, as well as others in the department of Organismic and Evolutionary Biology. I have been so fortunate to be part of such a supportive and inspiring lab group; I now can't imagine preparing a talk without their invaluable insight and direction. I must especially thank Jon Sanders, who has contributed, in both large and small ways, to every project I have worked on during my dissertation; I am lucky to have found both a friend and colleague in Jon. And of course there are my labmates, officemates, friends, and, at least in Kiana's case, roommate, Kiana Frank and Heather Olins; as well as my friend and lab neighbor, Dipti Nayak. They always challenged and supported me, and made every day fun. I am grateful for their friendship, which I know will be life-long.

Thank you to the many, many collaborators and coauthors that I have worked with as a graduate student. The list is long, but special thanks to Charles Fisher, Erin Becker, George

Luther, Amy Gartman, Nicole Dubilier, Spencer Nyholm, and Frank Stewart. Additionally, this work could have been done without the crew of the R/V *Thomas G. Thompson* and the ROV *JASON II*. I am also grateful to the staff of the Ernst Mayr Library of the Museum of Comparative Zoology at Harvard University for their acquisition of countless obscure articles and books for me. And in terms of logistical and moral support, I am particularly indebted to Jennifer Delaney and Stephanie Hillsgrove, who made lab logistical and administrative tasks immeasurably easier.

I am so appreciative of the incredible friends and family that I have encouraging me behind the scenes. Thank you to my extended family June and Steve Jones, Dana Jones, Erin Cooper, Jordan Kunkes and Eve Boltax for their love and support. My old friends Kara Gaughen, Jessica Russell, Alicia Widge, Laurel Aquadro and Christine Sun brighten my life in so many ways and nobody makes me laugh as hard. My husband Andy Jones has been an inspiration; I admire him for his unending optimism and constant curiosity. I am so grateful for our partnership and could not have done this without him. Thank you to my sister Nina Kunkes, whose wit and focus I admire, and whose love and support has been unwavering.

And finally, thank you to my parents, Daniel and Phyllis Beinart. My father always encouraged my scientific interests, whether he was teaching me binary code at the kitchen table or driving me to a before-school lab class in fourth grade. He gave me the skeptical, analytical mind that makes science fun. My mother is my greatest cheerleader, and never fails to make me feel like my work is important. She is why I strive to go as far as I can as a woman in this field, and make the path easier for those coming after me. I will always be grateful, for they are the reason I have made it this far.

Chapter 1
Introduction

There is a growing appreciation for the ubiquity of microbial symbioses on Earth, yet for most of these we only have a basic understanding of symbiont physiology and the impact of these partnerships on ecosystem ecology and biogeochemistry. Eukaryotes in many ecosystems have evolved specific associations with prokaryotes that allow them to capitalize on the relative diversity of prokaryotic metabolisms. Via the metabolic activities of their symbionts, host eukaryotes stand to gain a number of benefits including: access to novel nutritional or energy resources, detoxification of their surroundings, and/or metabolic processes that facilitate or complement their own metabolism. Thus, symbionts have the potential to mediate an organism's interaction with its biotic and abiotic environment. For example, symbiont physiology has the potential to influence the association's use of a specific habitat (Tsuchida et al. 2004), to affect interactions with predators (Lopanik et al. 2004), or, through metabolic activity, to alter local biogeochemical cycles (van der Heide et al. 2012).

Despite the potential significance of their activities on ecosystems, we have characterized the interaction between symbiont physiology and habitat in relatively few symbiotic taxa. This is particularly startling when we consider the prevalence of prokaryote-eukaryote symbioses in many environments, particularly in some marine ecosystems. To this end, the thesis presented here advances our understanding of the functioning of bacterial-animal symbioses at deep-sea, hydrothermal vent ecosystems through surveys characterizing the abundance and distribution of both symbiont and host in differing habitats (Ch.2 & 4), interrogation of symbiont physiological poise via transcriptomic analysis (Ch.3), and direct experimental measurement of symbiont metabolism (Ch.5).

Mutualistic associations between prokaryotes and eukaryotes predominate at hydrothermal vent habitats (Fisher et al. 2007). At these deep-sea hotsprings, invertebrates from many phyla have evolved partnerships with bacteria that enable them to thrive in the typically

resource-limited deep ocean (Dubilier et al. 2008; Cavanaugh et al. 2006). Symbiosis with bacteria allows animals to access chemical energy in venting fluid, which is otherwise unavailable to them as eukaryotes. Hydrothermal fluid is enriched in reduced substrates such as sulfide, methane and hydrogen that can be oxidized by chemoautotrophic bacteria providing energy for carbon fixation (Tsuchida et al. 2004; Tivey 2007). Through partnerships with chemoautotrophs, many vent invertebrates indirectly access this process, which ultimately provides the bulk of their nutrition (Lopanik et al. 2004; Cavanaugh et al. 1981; Fisher et al. 1989; Felbeck 1981; Belkin et al. 1986; Nelson et al. 1995; Polz et al. 1998; Ponsard et al. 2012; Watsuji et al. 2012). At almost all hydrothermal vents explored to date, dense assemblages of host animals are found clustered around vent orifices in order to provide their symbionts access to chemicals in venting fluid (van der Heide et al. 2012; Stewart et al. 2005).

Despite this common need for contact with vent fluid, their structured distribution within and among vent fields suggests habitat specialization by the holobionts (i.e., host and symbiont together). Vents are well-known for their variability in physico-chemical characteristics at both of these scales (Fisher et al. 2007; Le Bris et al. 2000; Mottl et al. 2011; Butterfield et al. 1994), providing a wealth of habitats that would enable regional or local environmental sorting. Indeed, differences in symbiotic communities are often observed among vent fields within the same region that have differing chemistry or geology (Dubilier et al. 2008; Desbruyeres et al. 2000; Cavanaugh et al. 2006; Galkin 1997; Desbruyeres et al. 1994). Additionally, within a vent field, vent holobionts are often found in discrete, mono-specific or –generic zones or patches that are associated with particular physico-chemical features (Marsh et al. 2012; Podowski et al. 2010; Luther et al. 2001; Waite et al. 2008; Cuvelier et al. 2011; Sarrazin et al. 1997; Tokeshi 2011; Sarrazin et al. 2002; Sarrazin & Juniper 1999). Typically, these patterns have been attributed to interactions between the environment and host physiology or traits – for example, differences in

tolerance to temperature or sulfide – that would lead to niche specialization (Podowski et al. 2010; Luther et al. 2001; Waite et al. 2008; Cuvelier et al. 2011; Sarrazin et al. 1997). However, it is equally likely that symbiont traits influence habitat specialization in these organisms, with the potential to drive the observed environmental sorting. Because most host taxa specifically associate with only one or two lineages of symbiont (Dubilier et al. 2008; Cavanaugh et al. 2006), the attributes of their particular partners may determine the niche of the holobiont.

In addition to affecting host ecology, the activities of chemoautotrophic vent symbionts may have a significant impact on their abiotic environment. Given the density of symbionts in host tissue, symbiont population sizes may rival or exceed those of similar free-living prokaryotes in their environment (Yamamoto et al. 2002; Pranal et al. 2009; Belkin et al. 1986; Powell & Somero 1986); therefore, symbiont metabolism has the potential to drastically influence local geochemistry. In situ manipulations that have measured the water chemistry before and after removal of vent symbioses have shown that they significantly deplete the reductants in venting fluid (Podowski et al. 2010; Waite et al. 2008; Le Bris et al. 2006). This has been reinforced with experimental measurements of the rates of sulfur, methane and hydrogen oxidation by a few intact symbioses and physically isolated symbionts (Girguis & Childress 2006; Henry et al. 2008; Childress et al. 1991; Petersen et al. 2011; Fisher et al. 1987; Wilmot & Vetter 1990; Goffredi et al. 1997). Input of metabolic end-products by vent symbioses into the environment is less well-characterized than their utilization of vent fluid reductants. Hydrogen sulfide oxidation by the symbionts of vent tubeworms has been shown to lower the pH of the surrounding water through the excretion of hydrogen ions (Girguis et al. 2002). In addition, in vitro experiments on symbionts show that some might only partially oxidize sulfide, excreting the resulting partially oxidized sulfur (Wilmot & Vetter 1990). Since insight into the ecology of vent symbioses and their effect on the environment is bound to our understanding of symbiont activity, more work is

needed to characterize the range of symbiont metabolism.

Among the symbionts of vent animals, high phylogenetic diversity, as well as widespread horizontal gene transfer, likely corresponds to ecologically significant physiological diversity (Kleiner et al. 2012). Vent symbionts are derived from many lineages of Proteobacteria, mainly γ-proteobacteria, that have independently evolved from various free-living lineages (Cavanaugh et al. 2006; Dubilier et al. 2008; Petersen et al. 2012). Though they converge in basic chemoautotrophic function, they can diverge in biochemical pathways or entire metabolisms that may have ecological implications for the host with which they associate. A comparison of the genomic content among some of the γ-proteobacterial symbionts of vent animals has shown that they can differ in genes for energy metabolism, carbon fixation and nitrogen acquisition (Kleiner et al. 2012). Moreover, experiments comparing the metabolism of vent symbioses have shown that they can differ in their use of substrates like sulfur compounds (Belkin et al. 1986; Wilmot & Vetter 1990). Whether and how these differences translate into niche preference by the holobionts is still unknown, but these characteristics potentially affect their distribution. In addition, differences among symbiont metabolism have the potential to differentially affect local geochemistry.

The work comprising this thesis focuses on the diverse chemoautotrophic symbionts of three mollusc genera found in dense communities at vents along the Eastern Lau Spreading Center (ELSC), which is part of the Lau back-arc basin. The ELSC comprises a series of vent fields that are found fairly linearly along a north-south spreading center, separated by 10s to 100s of kilometers. Vents along the ELSC span geological and geochemical gradients that result from the increasing influence of the subducting Pacific plate on crustal composition in the southward direction (Tivey et al. 2012). Vents in the northern part of the Lau Basin are mainly basaltic, while those in the south primarily andesitic. This geological shift has been linked to a north-south

gradient in vent fluid geochemistry, as well as concurrent changes in vent biological communities (Podowski et al. 2010; Kim & Hammerstrom 2012).

Because the ELSC vent fields are located in relative proximity to one another, span a gradient in physico-chemical conditions, and have no known barriers to biological dispersal (Speer & Thurnherr 2012), this region presented an ideal opportunity to investigate interactions between habitat and the ecology of vent symbioses. At ELSC vents, as well as others in the southwestern Pacific, two symbiotic provannid snail genera (*Ifremeria* and *Alviniconcha*), as well as the symbiotic mussel *Bathymodiolus brevior*, predominate (Podowski et al. 2009; Podowski et al. 2010; Desbruyeres et al. 1994). The genus *Ifremeria* is monotypic, containing only the species I. nautilei, while *Alviniconcha* comprises at least six cryptic lineages that were recently described as species (S. Johnson & B. Vrijenhoek, pers. comm.). In this dissertation, I discovered that three of the *Alviniconcha* host types (now thought to be species) co-occur at the ELSC vents (Ch.1). In Chapter 2, I surveyed the distribution of *Alviniconcha* host and symbiont types at vents along the ELSC, linking observed changes in geochemistry to a structured distribution of host-symbiont associations. Subsequent investigation of symbiont physiological poise through transcriptomic sequencing allowed me to assess the in situ gene expression of *Alviniconcha* symbionts from across the geochemical gradient (Ch. 3). In addition, my survey of the diversity of ELSC *Alviniconcha* symbionts and quantitative assessment of their association with the three host species, revealed an additional bacterial inhabitant of some *Alviniconcha* types which could be ecologically important via metabolic interactions with the symbioses or as a parasite (Ch.4).

On a much smaller spatial scale, observed patterns in intra-field habitat differentiation by the symbiotic molluscs of the ELSC suggest specific interactions and chemical exchanges with the abiotic environment. Surveys of the animal assemblages at ELSC vents have shown that these genera predictably occur in zones around hydrothermal vent flows with *Alviniconcha* nearest to the

vent orifice, *Ifremeria* comprising the next zone, and *B. brevior* being found at the very edges (Waite et al. 2008; Podowski et al. 2009; Podowski et al. 2010). For these holobionts, energy resources are directly tied to the physical space they occupy. As vent fluid emerges from the crust, it can be quickly diluted by the surrounding seawater and/or oxidized, either abiotically by reacting with metals or through the activities of free-living microorganisms (Santos Afonso & Stumm 1992; Pyzik & Sommer 1981; Luther et al. 2011; Gartman et al. 2011). Accordingly, proximity to the fluid flow is essential for productivity in these symbioses, since chemical reductants may quickly disappear. However, their need for fluid exposure is balanced by their tolerances to heat and/or toxic chemicals found in venting fluid, as well as by competitive interactions among the holobionts. At the ELSC, both these abiotic and biological processes are thought to shape the zonation of the three symbiotic mollusc genera (Sen et al. 2013; Podowski et al. 2010).

However, at the ELSC vents, another factor may enable the observed community structure. In this region, vent symbionts are hypothesized to supplement chemoautotrophy based on the highly-reduced chemicals from the venting fluid with the use of partially oxidized sulfur, which is reasonably abundant in the seawater around the symbiotic animals (Waite et al. 2008; Mullaugh et al. 2008; Gartman et al. 2011). For example, though undetectable amounts of sulfide are often found around *B. brevior*, concentrations of the partially oxidized compound thiosulfate are often high (Mullaugh et al. 2008; Waite et al. 2008). If low tolerance to high temperatures or sulfide concentrations or competitive exclusion by the other symbioses prevents *B. brevior* from inhabiting areas of high fluid flow, thiosulfate has the potential to serve as an important energy source. To address whether this is the case, in Chapter 5, I used high-pressure, flow-through respirometry to directly test the ability of all three ELSC molluscs to fuel autotrophy with the oxidation of thiosulfate. In addition, because the source of partially oxidized sulfur in situ is unknown, I measured the excretion of sulfur compounds by the three symbioses

when provided different sulfur substrates. The results of these experiments yield important insights into the chemoautotrophic metabolism of hydrothermal vent organisms and their potential to influence the pool of reductants in their habitats through excretion.

This dissertation demonstrates the importance of symbiont physiology to the ecology of prokaryote-eukaryote symbioses. Though the effects of symbiont activity on organismal ecology may be readily apparent at symbioses-dominated ecosystems like hydrothermal vents, given the prevalence of prokaryote-eukaryote symbioses on earth, they are likely to be significant in other biological systems as well. Here, I underscore that the activities of microbial symbionts may be imperative to a) the distribution of symbioses into specific niches and b) exchange with the geochemical environment through uptake and excretion of chemicals. In sum, my efforts advance our understanding of the fundamental influence of symbiont activity on hydrothermal vent ecosystem processes, providing valuable insight into the physiology of chemoautotrophic symbionts and their effects on host ecology and local geochemistry.

References

Belkin, S., Nelson, D.C. & Jannasch, H.W., 1986. Symbiotic assimilation of CO_2 in the two hydrothermal vent animals, the mussel *Bathymodiolus thermophilus* and the tubeworm *Riftia pachyptila*. Biol Bull, 170(1), pp.110–121.

Butterfield, D.A. et al., 1994. Gradients in the composition of hydrothermal fluids from the Endeavour segment vent field: Phase separation and brine loss. J. Geophys. Res., 99(B5), pp.9561–9583.

Cavanaugh, C. et al., 2006. Marine Chemosynthetic Symbioses. In The Prokaryotes. pp. 475–507.

Cavanaugh, C.M. et al., 1981. Prokaryotic Cells in the Hydrothermal Vent Tube Worm *Riftia pachyptila* Jones: Possible Chemoautotrophic Symbionts. Science, 213, pp.340–342.

Childress, J.J. et al., 1991. Sulfide and Carbon Dioxide Uptake by the Hydrothermal Vent Clam, *Calyptogena magnifica*, and Its Chemoautotrophic Symbionts. Physiological Zoology, 64(6), pp.1444–1470.

Cuvelier, D. et al., 2011. Hydrothermal faunal assemblages and habitat characterisation at the Eiffel Tower edifice (Lucky Strike, Mid-Atlantic Ridge). Marine Ecology, 32(2), pp.243–255.

Desbruyeres, D. et al., 2000. A review of the distribution of hydrothermal vent communities along the northern Mid-Atlantic Ridge: dispersal vs. environmental controls. Hydrobiologia, 440(1), pp.201–216.

Desbruyeres, D. et al., 1994. Deep-sea hydrothermal communities in southwestern Pacific back-arc basins (The North Fiji and Lau Basins) - composition, microdistribution and food-web. Marine Geology, 116(1-2), pp.227–242.

Dubilier, N., Bergin, C. & Lott, C., 2008. Symbiotic diversity in marine animals: the art of harnessing chemosynthesis. Nat Rev Micro, 6(10), pp.725–740.

Felbeck, H., 1981. Chemoautotrophic Potential of the Hydrothermal Vent Tube Worm, *Riftia pachyptila* Jones (Vestimentifera). Science (New York, N.Y.), 213(4505), pp.336–338.

Fisher, C.R. et al., 1987. The importance of methane and thiosulfate in the metabolism of the bacterial symbionts of two deep-sea mussels. Marine Biology, 96(1), pp.59–71.

Fisher, C.R., Childress, J.J. & Minnich, E., 1989. Autotrophic Carbon Fixation by the Chemoautotrophic Symbionts of *Riftia pachyptila*. Biol Bull, 177(3), pp.372–385.

Fisher, C.R., Takai, K. & Le Bris, N., 2007. Hydrothermal vent ecosystems. Oceanography, 20(1), pp.14–23.

Galkin, S.V., 1997. Megafauna associated with hydrothermal vents in the Manus Back-Arc Basin (Bismarck Sea). Marine Geology, 142(1-4), pp.197-206

Gartman, A. et al., 2011. Sulfide Oxidation across Diffuse Flow Zones of Hydrothermal Vents. Aquatic Geochemistry, 17(4-5), pp.583–601.

Girguis, P.R. & Childress, J.J., 2006. Metabolite uptake, stoichiometry and chemoautotrophic function of the hydrothermal vent tubeworm *Riftia pachyptila*: responses to environmental variations in substrate concentrations and temperature. Journal of Experimental Biology, 209(18), pp.3516–3528.

Girguis, P.R. et al., 2002. Effects of metabolite uptake on proton-equivalent elimination by two species of deep-sea vestimentiferan tubeworm, *Riftia pachyptila* and *Lamellibrachia* cf *luymesi*: proton elimination is a necessary adaptation to sulfide-oxidizing chemoautotrophic symbionts. Journal of Experimental Biology, 205(19), pp.3055–3066.

Goffredi, S. et al., 1997. Sulfide acquisition by the vent worm *Riftia pachyptila* appears to be via uptake of HS-, rather than H2S. J Exp Biol, 200(20), pp.2609–2616.

Henry, M.S., Childress, J.J. & Figueroa, D., 2008. Metabolic rates and thermal tolerances of chemoautotrophic symbioses from Lau Basin hydrothermal vents and their implications for species distributions. Deep Sea Research Part I: Oceanographic Research Papers, 55(5), pp.679–695.

Kim, S. & Hammerstrom, K., 2012. Hydrothermal vent community zonation along environmental gradients at the Lau back-arc spreading center. Deep Sea Research Part I: Oceanographic Research Papers, 62(0), pp.10–19.

Kleiner, M., Petersen, J.M. & Dubilier, N., 2012. Convergent and divergent evolution of metabolism in sulfur-oxidizing symbionts and the role of horizontal gene transfer. Current Opinion in Microbiology, 15(5), pp.621–631.

Le Bris, N. et al., 2000. A new chemical analyzer for in situ measurement of nitrate and total sulfide over hydrothermal vent biological communities. Marine Chemistry, 72(1), pp.1-15

Le Bris, N. et al., 2006. Variability of physico-chemical conditions in 9 50′N EPR diffuse flow vent habitats. Marine Chemistry, 98, pp.167-182

Lopanik, N., Gustafson, K.R. & Lindquist, N., 2004. Structure of Bryostatin 20: A Symbiont-Produced Chemical Defense for Larvae of the Host Bryozoan, *Bugulaneritina*. Journal of Natural Products, 67(8), pp.1412–1414.

Luther, G.W. et al., 2011. Thermodynamics and kinetics of sulfide oxidation by oxygen: a look at inorganically controlled reactions and biologically mediated processes in the environment. Frontiers in microbiology, 2, p.62.

Luther, G.W., III et al., 2001. Chemical speciation drives hydrothermal vent ecology. Nature, 410, p.813.

Marsh, L. et al., 2012. Microdistribution of Faunal Assemblages at Deep-Sea Hydrothermal Vents in the Southern Ocean H. Browman, ed. PLoS ONE, 7(10), p.e48348.

Mottl, M.J. et al., 2011. Chemistry of hot springs along the Eastern Lau Spreading Center. Geochimica Et Cosmochimica Acta, 75, pp.1013–1038.

Mullaugh, K.M. et al., 2008. Voltammetric (Micro)Electrodes for the In Situ Study of Fe^{2+} Oxidation Kinetics in Hot Springs and S_2O Production at Hydrothermal Vents. Electroanalysis, 20(3), pp.280–290.

Nelson, D.C., Hagen, K.D. & Edwards, D.B., 1995. The gill symbiont of the hydrothermal vent mussel *Bathymodiolus thermophilus* is a psychrophilic, chemoautotrophic, sulfur bacterium. Marine Biology, 121(3), pp.487–495.

Petersen, J.M. et al., 2011. Hydrogen is an energy source for hydrothermal vent symbioses. Nature, 476(7359), pp.176–180.

Petersen, J.M. et al., 2012. Origins and evolutionary flexibility of chemosynthetic symbionts from deep-sea animals. Biol Bull, 223(1), pp.123–137.

Podowski, E.L. et al., 2010. Biotic and abiotic factors affecting distributions of megafauna in diffuse flow on andesite and basalt along the Eastern Lau Spreading Center, Tonga. Marine Ecology Progress Series, 418, pp.25–45.

Podowski, E.L. et al., 2009. Distribution of diffuse flow megafauna in two sites on the Eastern Lau Spreading Center, Tonga. Deep-Sea Research Part I, 56(11), pp.2041–2056.

Polz, M.F. et al., 1998. Trophic ecology of massive shrimp aggregations at a Mid-Atlantic Ridge hydrothermal vent site. Limnology and Oceanography, 43(7), pp.1631–1638.

Ponsard, J. et al., 2012. Inorganic carbon fixation by chemosynthetic ectosymbionts and nutritional transfers to the hydrothermal vent host-shrimp *Rimicaris exoculata*. The ISME journal, 7(1), pp.96–109.

Powell, M.A. & Somero, G.N., 1986. Adaptations to Sulfide by Hydrothermal Vent Animals - Sites and Mechanisms of Detoxification and Metabolism. Biological Bulletin, 171(1), pp.274–290.

Pranal, V., Fiala-Medioni, A. & Guezennec, J., 2009. Fatty acid characteristics in two symbiont-bearing mussels from deep-sea hydrothermal vents of the south-western Pacific. Journal of the Marine Biological Association of the UK, 77(02), pp.473–492.

Pyzik, A.J. & Sommer, S.E., 1981. Sedimentary iron monosulfides: Kinetics and mechanism of formation. Geochimica Et Cosmochimica Acta, 45(5), pp.687-698

Santos Afonso, Dos, M. & Stumm, W., 1992. Reductive dissolution of iron (III)(hydr) oxides by hydrogen sulfide. Langmuir, 8(6), pp.1671-1675

Sarrazin, J. & Juniper, S.K., 1999. Biological characteristics of a hydrothermal edifice mosaic community. Marine Ecology Progress Series, 185, pp.1-19

Sarrazin, J., Levesque, C. & Juniper, S., 2002. Mosaic community dynamics on Juan de Fuca Ridge sulphide edifices: substratum, temperature and implications for trophic structure. CBM-Cahiers de Biologie Marine, 43, pp.279-275

Sarrazin, J., Robigou, V. & Juniper, S.K., 1997. Biological and geological dynamics over four years on a high-temperature sulfide structure at the Juan de Fuca Ridge hydrothermal observatory. Marine Ecology Progress Series, 153, pp.5-24

Sen, A. et al., 2013. Distribution of mega fauna on sulfide edifices on the Eastern Lau Spreading Center and Valu Fa Ridge. Deep Sea Research Part I: Oceanographic Research Papers, 72, pp.48–60.

Speer, K. & Thurnherr, A.M., 2012. The Lau Basin Float Experiment (LAUB-FLEX). Oceanography, 25(1), pp.284–285.

Stewart, F.J.F., Newton, I.L.G.I. & Cavanaugh, C.M.C., 2005. Chemosynthetic endosymbioses: adaptations to oxic-anoxic interfaces. Trends in Microbiology, 13(9), pp.439–448.

Tivey, M. et al., 2012. Links from Mantle to Microbe at the Lau Integrated Study Site: Insights from a Back-Arc Spreading Center. Oceanography, 25(1), pp.62–77.

Tivey, M.K., 2007. Generation of Seafloor Hydrothermal Vent Fluids and Associated Mineral Deposits. Oceanography, 20(1), pp.50–65.

Tokeshi, M., 2011. Spatial structures of hydrothermal vents and vent-associated megafauna in the back-arc basin system of the Okinawa Trough, western Pacific. Journal of Oceanography, 67(5), pp.651-665

Tsuchida, T., Koga, R. & Fukatsu, T., 2004. Host Plant Specialization Governed by Facultative Symbiont. Science, 303, pp.1989–1989.

van der Heide, T. et al., 2012. A Three-Stage Symbiosis Forms the Foundation of Seagrass Ecosystems. Science, 336, pp.1432–1434.

Waite, T.J. et al., 2008. Variation in sulfur speciation with shellfish presence at a Lau Basin diffuse flow vent site. Journal of Shellfish Research, 27(1), pp.163–168.

Watsuji, T.-O. et al., 2012. Cell-Specific Thioautotrophic Productivity of Epsilon-Proteobacterial Epibionts Associated with *Shinkaia crosnieri*, PLoS ONE, 7(10), p.e46282.

Wilmot, D.B., Jr & Vetter, R.D., 1990. The bacterial symbiont from the hydrothermal vent tubeworm *Riftia pachyptila* is a sulfide specialist. Marine Biology, 106(2), pp.273–283.

Yamamoto, H. et al., 2002. Phylogenetic characterization and biomass estimation of bacterial endosymbionts associated with invertebrates dwelling in chemosynthetic communities of hydrothermal vent and cold seep fields. Marine Ecology Progress Series, 245, pp.61–67.

Chapter 2

Evidence for the role of endosymbionts in regional-scale habitat partitioning by hydrothermal vent symbioses

(as published in Proceedings of the National Academy of Sciences)

Evidence for the role of endosymbionts in regional-scale habitat partitioning by hydrothermal vent symbioses

Roxanne A. Beinart[a], Jon G. Sanders[a], Baptiste Faure[b,c], Sean P. Sylva[d], Raymond W. Lee[e], Erin L. Becker[b], Amy Gartman[f], George W. Luther III[f], Jeffrey S. Seewald[d], Charles R. Fisher[b], and Peter R. Girguis[a,1]

[a]Department of Organismic and Evolutionary Biology, Harvard University, Cambridge, MA 02138; [b]Biology Department, Pennsylvania State University, University Park, PA 16802; [c]Institut de Recherche pour le Développement, Laboratoire d'Ecologie Marine, Université de la Réunion, 97715 Saint Denis de La Réunion, France; [d]Department of Marine Chemistry and Geochemistry, Woods Hole Oceanographic Institution, Woods Hole, MA 02543; [e]School of Biological Sciences, Washington State University, Pullman, WA 99164; and [f]School of Marine Science and Policy, University of Delaware, Lewes, DE 19958

Edited* by Paul G. Falkowski, Rutgers, The State University of New Jersey, New Brunswick, NJ, and approved September 26, 2012 (received for review February 21, 2012)

Deep-sea hydrothermal vents are populated by dense communities of animals that form symbiotic associations with chemolithoautotrophic bacteria. To date, our understanding of which factors govern the distribution of host/symbiont associations (or holobionts) in nature is limited, although host physiology often is invoked. In general, the role that symbionts play in habitat utilization by vent holobionts has not been thoroughly addressed. Here we present evidence for symbiont-influenced, regional-scale niche partitioning among symbiotic gastropods (genus *Alviniconcha*) in the Lau Basin. We extensively surveyed *Alviniconcha* holobionts from four vent fields using quantitative molecular approaches, coupled to characterization of high-temperature and diffuse vent-fluid composition using gastight samplers and in situ electrochemical analyses, respectively. Phylogenetic analyses exposed cryptic host and symbiont diversity, revealing three distinct host types and three different symbiont phylotypes (one ε-proteobacteria and two γ-proteobacteria) that formed specific associations with one another. Strikingly, we observed that holobionts with ε-proteobacterial symbionts were dominant at the northern fields, whereas holobionts with γ-proteobacterial symbionts were dominant in the southern fields. This pattern of distribution corresponds to differences in the vent geochemistry that result from deep subsurface geological and geothermal processes. We posit that the symbionts, likely through differences in chemolithoautotrophic metabolism, influence niche utilization among these holobionts. The data presented here represent evidence linking symbiont type to habitat partitioning among the chemosynthetic symbioses at hydrothermal vents and illustrate the coupling between subsurface geothermal processes and niche availability.

chemoautotrophy | symbiosis | endosymbiosis

Niche partitioning, the process wherein coexisting organisms occupy distinct niches, is thought to be essential in structuring many biological communities (1–3). Classic studies of ecological niche partitioning have focused on how the intrinsic traits of organisms allow them to occupy or use distinct habitats or resources (4, 5). However, species also can access novel niche space via symbiotic associations with other organisms. In these cases, the niche of the host is expanded through the addition of the symbiont's physiological capabilities. With increasing awareness of the prevalence of microbe–animal associations, the effect of the symbiont(s) on niche utilization may prove to be key to understanding the coexistence of organisms in many biological communities. This effect is likely to be especially important in ecosystems structured by coexisting symbiotic associations, such as hydrothermal vents. Therefore, we looked for habitat-utilization patterns reflective of symbiont-influenced niche partitioning among a group of closely related snail–bacterial symbioses in the Eastern Lau Spreading Center (ELSC) hydrothermal vent system.

Hydrothermal vents are extremely productive environments wherein primary production occurs via chemolithoautotrophy, the generation of energy for carbon fixation from the oxidation of vent-derived reduced inorganic chemicals (6). The dense communities of macrofauna that populate these habitats typically are dominated by invertebrates that form symbiotic associations with chemolithoautotrophic bacteria (7). In these chemosynthetic associations, the endosymbionts oxidize reduced vent-derived compounds—usually hydrogen sulfide (H_2S)—and fix inorganic carbon, which is shared with their host for biosynthesis and growth (8–12). Symbiotic associations between chemolithoautotrophic bacteria and invertebrates have been described for multiple invertebrate taxa from three phyla (13), and these associations often coexist within given vent fields, systems of vent fields (regions), and biogeographic provinces (14).

It is well established that hydrothermal fluid can exhibit marked spatial and temporal differences in temperature, pH, and chemical composition, the result of numerous subsurface geological, chemical, physical, and biological factors (15–18). This heterogeneity across both space and time provides myriad physicochemical niches and ample ecological opportunity to support a diversity of chemosynthetic symbioses via niche specialization. Previous studies have examined successional changes within a community of chemosynthetic symbioses in relation to temporal changes in vent-fluid chemistry (19, 20), the distribution of the symbioses in relation to physicochemical conditions within a vent field (21–27), and the distribution of chemosynthetic symbioses among different vent fields (28, 29). Host tolerance, growth rates, and physiological capacities often are invoked when explaining the observed distribution. Given the reliance of chemosynthetic symbioses on vent-derived chemicals for symbiont function (30), variations in symbiont physiological activity have the potential to result in distinct habitat-utilization patterns by holobionts. However, no study has yet comprehensively interrogated both

Author contributions: R.A.B., J.G.S., and P.R.G. designed research; R.A.B., J.G.S., B.F., A.G., and P.R.G. performed research; R.A.B., J.G.S., B.F., S.P.S., R.W.L., E.L.B., A.G., G.W.L., J.S.S., and C.R.F. analyzed data; and R.A.B. and P.R.G. wrote the paper.

The authors declare no conflict of interest.

*This Direct Submission article had a prearranged editor.

Freely available online through the PNAS open access option.

Data deposition: The sequences reported in this paper have been deposited in the GenBank database [accession nos. JN402310, JN402311, JQ624362–JQ624411 (*Alviniconcha* spp. host mitochondrial CO1 sequences), and JN377487, JN377488, JN377489 (symbiont 16S rRNA gene sequences)].

[1]To whom correspondence should be addressed. E-mail: pgirguis@oeb.harvard.edu.

This article contains supporting information online at www.pnas.org/lookup/suppl/doi:10.1073/pnas.1202690109/-/DCSupplemental.

host and symbiont to ascertain whether there is evidence for symbiont-influenced niche partitioning at vents.

Despite a convergence of general function among chemosynthetic symbioses in which the endosymbionts provide primary nutrition for the host, chemolithoautotrophic symbiont lineages have evolved multiple times from distinct lineages of free-living Proteobacteria (13, 31), and the genetic distance within and among symbiont lineages is sufficient to posit that physiological differences exist among them. Indeed, ongoing studies of chemosynthetic symbioses continue to reveal diverse modes of energy metabolism, such as hydrogen and carbon monoxide oxidation (32, 33). Given the obligate nature of these associations, the ecological implications of differences in symbiont physiological capacity are quite significant, because they may enable niche partitioning that results in previously inexplicable or unrecognized distribution patterns. If there are physiological differences among the symbionts of given groups (genera or species) of hosts, symbiont physiological activity would have the potential to constrain host habitat utilization via differences in chemolithotrophic metabolism.

Provannid gastropods of the genus *Alviniconcha* provide a unique opportunity to study symbiont-driven host niche partitioning. *Alviniconcha* are widely distributed at vents in the western Pacific (Manus Basin, Marianas Trough, North Fiji Basin, and the Lau Basin) as well as in the Indian Ocean at vents along the Central Indian Ridge. In addition to the described species of *Alviniconcha*, previous studies have found additional host "types" which are sufficiently divergent that they may represent undescribed species (34–36). These species and host types have been observed to host either intracellular γ- or ε-proteobacterial symbionts in the gill (36–40). Studies of the distribution of these species and types among vent fields examined a modest number of specimens per site (e.g., two individuals from each sampling site), with little or no contextual habitat information. As such, it is impractical to infer from these data the relationship between host type, symbiont type, and habitat utilization.

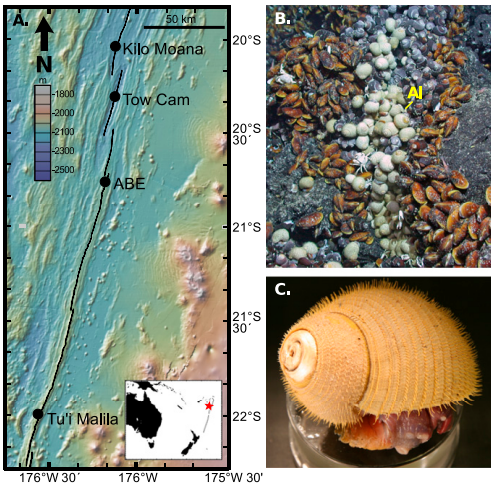

Fig. 1. (*A*) Map of ELSC depicting the five vent fields sampled herein. (*Inset*) Location of ELSC in the South Pacific. (*B*) A typical assemblage of *Alviniconcha* (Al) and other vent animals in the Lau Basin (Image courtesy of James Childress, University of California, Santa Barbara). (*C*) An individual *Alviniconcha* snail.

To look for patterns indicative of symbiont-influenced habitat partitioning, we collected 288 *Alviniconcha* individuals from the walls of hydrothermal chimneys and diffuse-flow habitats (where hydrothermal fluid is emitted from cracks in the seafloor) (Fig. 1 and Table S1). *Alviniconcha* were sampled from four vent fields spanning a regional geological gradient, where the two northernmost fields (Tow Cam and Kilo Moana) are dominated by basaltic lava, and the two southernmost vents (ABE and Tu'i Malila) are dominated by andesitic lava (41–45). Coregistered measurements of the physicochemical habitat within the animal collections, as well as characterization of vent end-member fluids from within each field, provide contextual geochemical information for these samples. Both host and symbionts were subject to phylogenetic analyses, and the composition of the symbiont population of all individuals was determined via quantitative PCR (qPCR). Select samples were also analyzed for stable-carbon isotopic content. Collectively, these data reveal striking patterns of both host and symbiont (holobiont) distribution along an ∼300-km length of the ELSC. The observed patterns in holobiont distribution correlate with differences in vent-fluid composition along the ELSC, implicating *Alviniconcha* symbionts in governing the distribution of their hosts among vent fields. These data provide evidence that symbiont complement might influence niche partitioning within a closely related group of animals and might in this case, as a consequence of differences in geochemical composition along the entire spreading center, yield regional-scale patterns of holobiont distribution.

Results

Phylogenetic Analysis of the Host Mitochondrial Cytochrome C Oxidase Subunit 1 Gene. We successfully amplified partial mitochondrial cytochrome C oxidase subunit 1 (CO1) from 274 host individuals and recovered a total of 56 haplotypes (Table S2). These haplotypes were distributed among three major clades with high (>0.95) posterior support, corresponding to three host types from the southwestern Pacific, and are called type 1 (HT-I), type 2 (HT-II), and type Lau (which we renamed here HT-III) (Fig. 2). Only HT-III has been previously described from the Lau Basin (38). Our results corroborate the *Alviniconcha* phylogeny as published in ref. 38, in which one major clade includes HT-I, HT-III, and *Alviniconcha hessleri* (from the Mariana trench), and the second major clade includes HT-II and *A.* aff. *hessleri* (from the Indian Ocean). For HT-I and HT-II, reference sequences AB235211 and AB235212 were each identical to the most common experimental haplotype in their respective clade; AB235215, representing HT-III, was identical to a relatively rare haplotype in our dataset but had only one nucleotide difference from the most common HT-III haplotype. The three host types found on the ELSC were divergent from those observed in the northwestern Pacific (Mariana Trench) and the Indian Ocean.

Some structure was apparent within the major host types in our sample. Within HT-III, a clade including 11 of the 22 HT-III haplotypes was supported with a posterior probability approaching 1.0. Although structure also was apparent in other host types, none was resolved with a posterior probability exceeding 0.9.

Phylogenetic Analyses of Symbiont 16S rRNA Genes. Based on 16S rRNA gene sequences, three symbiont phylotypes were found to be associated with ELSC *Alviniconcha*, only one of which had been previously observed in this region. Longer sequences were generated from clones of each phylotype for phylogenetic analysis (Fig. 3) and revealed that the three phylotypes are closely related to the previously published sequences for the γ- and ε-proteobacterial endosymbionts from *Alviniconcha* in this and other hydrothermal systems in the southwestern Pacific (Manus and North Fiji basins) (36–38). One of the γ-proteobacterial symbiont phylotypes, γ-Lau, was most closely related to the previously published symbiont sequence from *Alviniconcha* in the Lau Basin

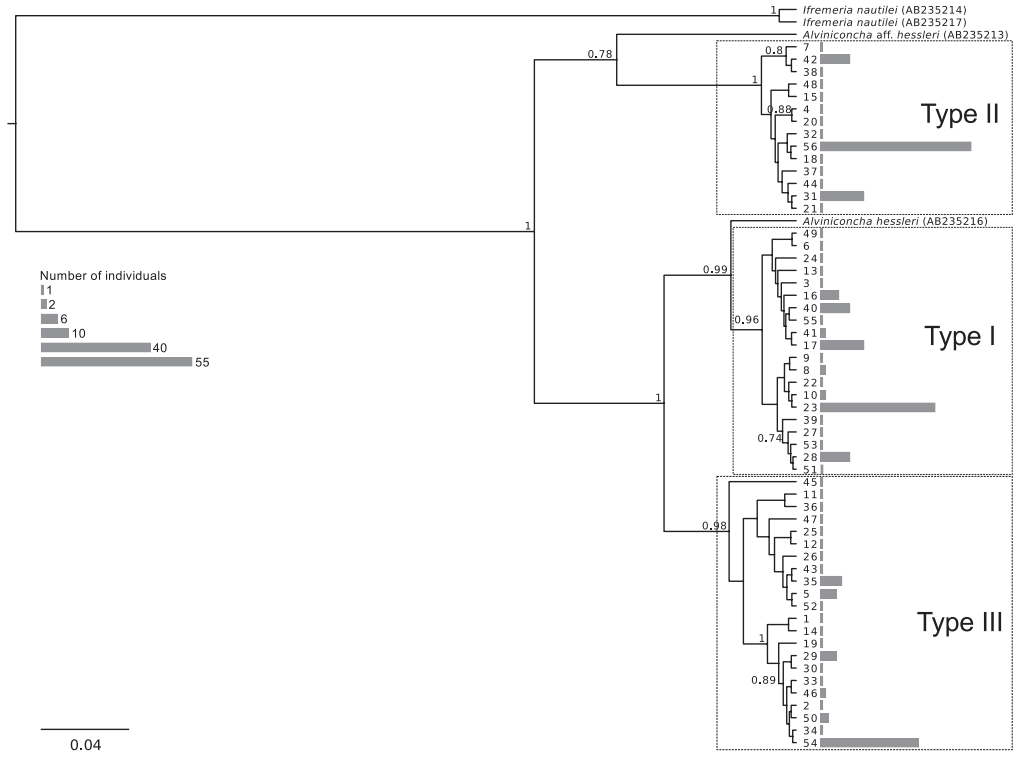

Fig. 2. Bayesian inference phylogeny of the *Alviniconcha* host mitochondrial CO1 haplotypes from this and previous studies and sequences from the sister genus *Ifremeria*. Boxes show the three *Alviniconcha* host types reported here. The haplotype ID number is shown at the tip of each branch, and the gray bars represent the total number of individuals recovered for each haplotype. Accession numbers for haplotypes found in this study are given in Table S2. Posterior probabilities are indicated above the nodes if >0.7.

(98% sequence identity) (38). The second γ-proteobacterial symbiont, phylotype γ-1, and an ε-proteobacterial symbiont phylotype were most closely related (96–97% and 97% sequence identity, respectively) to *Alviniconcha* symbionts previously observed in the North Fiji and Manus basins (38).

Proportion of Symbiont Phylotypes Within *Alviniconcha*. Quantification via qPCR revealed that all *Alviniconcha* individuals analyzed were dominated (>67% of total detected 16S rRNA genes) by either γ- or ε-proteobacterial endosymbionts. The dominant phylotype on average represented 99.5 ± 2.2% of the total symbiont gene counts within all individuals (Fig. 4). We never observed individual snails with approximately equal representation of γ- and ε-proteobacteria, although we did observe individuals with roughly equal representation of the two γ-proteobacterial phylotypes. Accordingly, we refer to *Alviniconcha* individuals as primarily hosting either γ- or ε-proteobacterial endosymbionts.

Relationships Among Symbiont Phylotypes and Host Types. Our qPCR analysis also revealed specificity among the three host types and three symbiont phylotypes. One-way analysis of similarity (ANOSIM) comparing the symbiont composition among the different host types demonstrated that each host type associated with significantly different symbiont populations (global $R = 0.789$, $P < 0.001$) (Fig. 4). HT-II were exclusively dominated by ε-proteobacteria, with ε-proteobacteria always representing >99% of the detected symbiont genes. Accordingly, we found no significant differences in the symbiont population among HT-II from three different vent fields (one-way ANOSIM; global $R = 0.312$, $P = 0.07$). HT-III, conversely, were exclusively dominated by γ-proteobacteria, either γ-1 or γ-Lau. A small number of HT-III individuals ($n = 7$, hereafter called "γ-Both") had relatively equal proportions of both γ-proteobacterial phylotypes. HT-III was found at the two southernmost vent fields (ABE and Tu'i Malila); however, because of the presence of only one HT-III individual at ABE, we were unable to statistically test the effect of geography on symbiont population composition in this host type. Finally, HT-I was dominated by either γ-1 or ε-proteobacteria but moret commonly dominated by γ-1, not the ε-proteobacteria ($n = 93$ vs. 6 individuals respectively). In this host type, the associated symbiont population displayed different patterns of symbiont fidelity according to geography. HT-I was found at all four vent fields; however, the dominant symbiont phylotype changed from north to south. Five of 12 HT-I individuals in the northern vent fields were dominated by ε-proteobacteria, compared with only 1 of 87 HT-I individuals in the southern vent fields. This finding was confirmed via one-way ANOSIM comparing the symbiont population of HT-I by location, which

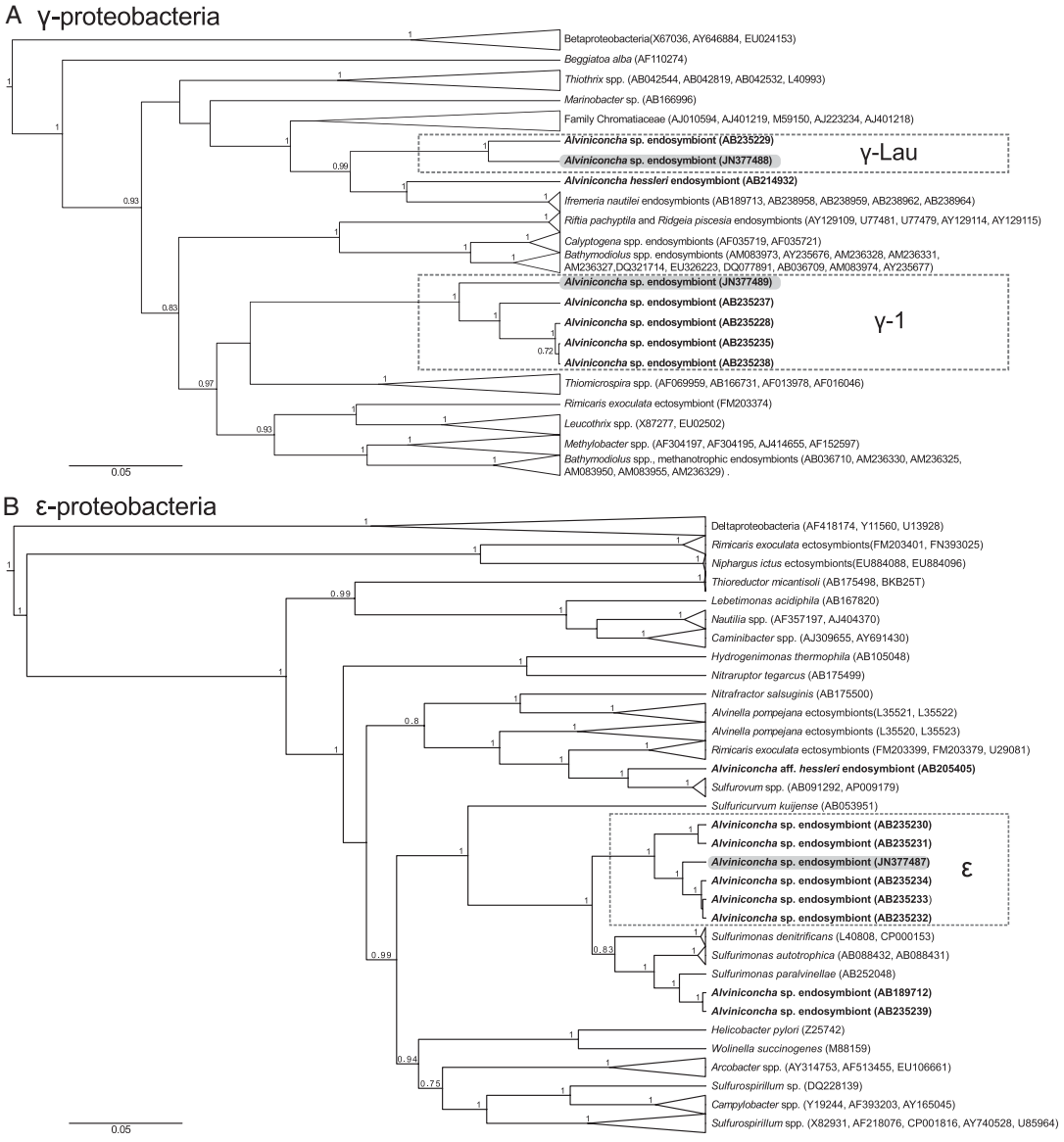

Fig. 3. Bayesian inference phylogenies of 16S rRNA sequences showing the three *Alviniconcha* symbiont phylotypes found at the ELSC. All *Alviniconcha* symbionts, from this study and others, are shown in bold. Gray highlighting indicates the representative sequences from this study. Boxes show the *Alviniconcha* symbiont phylotypes defined here and in other studies. Posterior probabilities are indicated above the nodes if >0.7. (*A*) γ-proteobacterial phylogeny, with β-proteobacteria as the outgroup. (*B*) ε-proteobacterial phylogeny, with δ-proteobacteria as the outgroup.

demonstrated that there were significant differences among HT-I individuals from the different vent fields (global $R = 0.385$, $P < 0.001$).

Geographic Patterns in the Abundance of *Alviniconcha* Host Types. The distribution and abundance of each host type varied geographically from north to south (Fig. 5). HT-I was found at all four vent fields, HT-II was found at three vent fields but not Tu'i Malila, and HT-III was found at the two southernmost vent fields, ABE and Tu'i Malila. With respect to their relative abundance, *Alviniconcha* populations at the northern vent fields were mainly HT-II, whereas populations at the southern vent fields were mainly HT-I and HT-III. The relative abundances of host types in the two northern vent fields (Kilo Moana and Tow

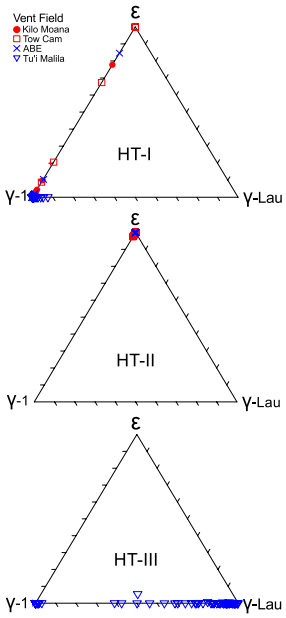

Fig. 4. Ternary plots of the symbiont composition of each *Alviniconcha* host type, with each point showing the symbiont composition of a single individual. The vertices of the triangle represent 100% of each symbiont phylotype, and the tick marks on the axes represent decreasing intervals of 10%. The symbiont phylotypes are indicated by γ-1 (γ-proteobacteria type 1), γ-Lau (γ-proteobacteria type Lau), and ε (ε-proteobacteria). Vent fields are indicated by ● (Kilo Moana), □ (Tow Cam), X (ABE), and ▽ (Tu'i Malila).

Cam) versus two southern vent fields (ABE and Tu'i Malila) were significantly different (global $R = 0.34$, $P = 0.03$).

Geographic Abundance of Symbiont Phylotypes. The abundance of symbiont phylotypes associated with *Alviniconcha* changed along the spreading center (Fig. 5). Individuals dominated by symbiont γ-1 were present at all four vent fields. Individuals dominated by ε-proteobacteria were present three vent fields but not Tu'i Malila. Individuals dominated by γ-Lau were observed only at Tu'i Malila. The dominant symbiont phylotypes in *Alviniconcha* from the two northern vent fields (Kilo Moana and Tow Cam) were significantly different from those of the southern two vent fields (ABE and Tu'i Malila) (one-way ANOSIM, global $R = 0.409$, $P = 0.024$). Specifically, the majority of *Alviniconcha* at the northern vent fields (Kilo Moana and Tow Cam) were dominated by ε-proteobacteria, whereas the majority of *Alviniconcha* at the southern vent fields (ABE and Tu'i Malila) were dominated by one of the two γ-proteobacterial phylotypes.

Chemistry and Temperature at *Alviniconcha* Habitats. Chemical and thermal measurements were taken upon the cleared substratum after *Alviniconcha* collections were completed (Table S1 and Fig. 6). Free sulfide concentrations in the vent fluids of the northernmost *Alviniconcha* habitats were significantly greater than those of the southernmost habitats (Mann–Whitney U, $P = 0.038$). Although we happened to sample more chimney wall habitats in the north, this difference in sampling does not explain the significant difference in sulfide concentrations between northern and southern fields. Indeed, when grouped by habitat type regardless of region, diffuse flows and chimney wall habitats measured here did not have significantly different sulfide concentrations (Mann–Whitney U, $P = 0.126$) (Table S1 and Fig. 6), nor did diffuse flows and chimneys within the same region (Mann–Whitney U, $P = 0.182$ and $P = 0.102$, north and south respectively). We also did not detect any significant differences in the oxygen concentrations or temperature of the vent fluids among the sample collection sites in the northern and southern vent fields ($P = 0.180$ and $P = 0.118$ respectively).

End-Member Vent-Fluid Chemistry. End-member aqueous concentrations of H_2S and hydrogen (H_2) reveal along-axis geochemical variations from north to south (Fig. 7). End-member aqueous H_2 concentrations varied from 220–498 μM in the northernmost vents (at Kilo Moana) and decreased to concentrations that varied from 35–135 μM in the southernmost (at Tu'i Malila) vents, nearly an order-of-magnitude difference in concentration. End-member dissolved H_2S concentrations exhibit a similar trend from north to south, although the ~twofold change in concentration of 4.9–2.8 mM from north to south is substantially

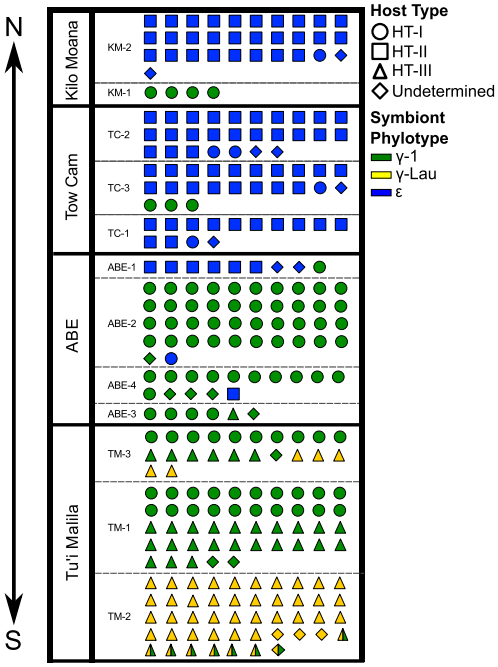

Fig. 5. The distribution of *Alviniconcha* host types and dominant symbiont type across the ELSC, with each individual colored according to dominant symbiont phylotype (>67% of the total detected 16S rRNA genes) and shaped according to host type. The four vent fields are separated by solid lines, and distinct collections from within each vent field are divided by dashed lines, with the collection ID indicated (Table S1). Symbiont phylotypes are indicated as follows: green, γ-proteobacteria type 1 (γ-1); yellow, γ-proteobacteria type Lau (γ-Lau); blue, ε-proteobacteria (ε).The individuals that had relatively equal proportions of two of the symbiont phylotypes are shown as two colors. Host types are indicated by shapes: ●, host type 1 (HT-I); ■, host type II (HT-II); ▲, host type III (HT-III); ◆, host type undetermined.

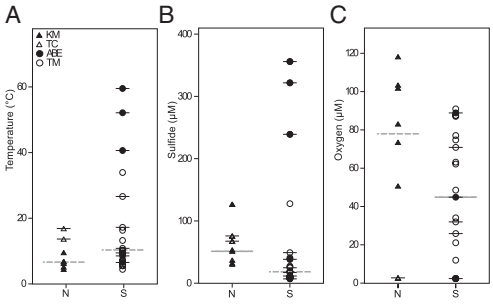

Fig. 6. Cyclic voltammetry measurements made on the cleared substratum after *Alviniconcha* collections, showing (*A*) temperature, (*B*) free sulfide concentration (sulfide), and (*C*) oxygen concentration at northern collections versus the southern collections. North (N) includes the vent fields Kilo Moana (KM) and Tow Cam (TC); South (S) includes ABE and Tu'i Malila (TM). Symbols with horizontal lines represent samples from diffuse vent flows; symbols without lines represent chimney wall habitats. Median values for each region are indicated by a dashed horizontal line.

less than that observed for aqueous H_2. In contrast to H_2 and H_2S, end-member methane (CH_4) concentrations in 2009 occupied a very narrow range of 33–44 μM and showed no along-axis trends (Fig. 7). End-member aqueous dissolved inorganic carbon (DIC) concentrations were highest in the Tu'i Malila vent fluid, reaching a value of 15 mM, and lowest in ABE vent fluids where concentrations varied from 5.4–7.0 mM, with fluids from the other vent fields containing intermediate concentrations of DIC (Fig. 7). End-member CH_4 and DIC concentrations did not change markedly from 2005 to 2009.

Stable Carbon Isotopic Composition According to Dominant Symbiont Phylotype. Across the ELSC, the average $\delta^{13}C$ value for gill tissue from *Alviniconcha* dominated by ε-proteobacteria (−11.6 ± 0.4‰) was much less depleted than the average value of *Alviniconcha* dominated by γ-proteobacteria (−27.6 ± 2.3‰) (Table S3). A one-way ANOVA of Tu'i Malila γ-proteobacteria hosting individuals grouped by dominant symbiont phylotype (γ-1, n = 23; γ-Lau, n = 21; γ-Both, n = 8), irrespective of host type, showed that there were significant differences among the groups ($P < 0.001$). Tukey's multiple pairwise comparisons showed that the $\delta^{13}C$ value in individuals dominated by γ-Lau was not significantly different from that in γ-Both individuals ($P = 0.834$), whereas individuals dominated by either γ-Lau or γ-Both were significantly less depleted than individuals dominated by γ-1 (P = 0.001 and $P = 0.004$, respectively). We were unable to compare the possible effects of host type on the stable-carbon isotopic composition in this subset of individuals, because we did not have enough individuals of different host types with the same dominant symbiont phylotype for statistical analysis.

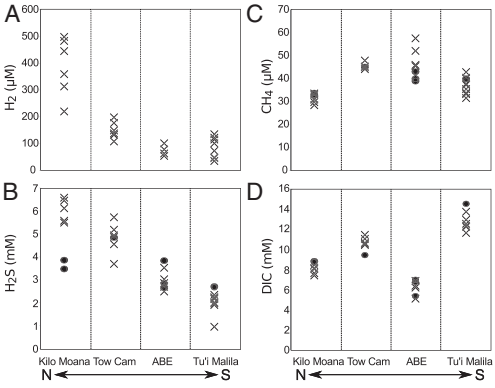

Fig. 7. The end-member fluid concentrations of (*A*) H_2, (*B*) H_2S, (*C*) CH_4, and (*D*) DIC at the four vent fields along the ELSC from which *Alviniconcha* were collected. Symbols indicate year of sampling: X, 2005; ●, 2009. DIC and H_2S data from 2005 were published previously by Mottl et al. (44).

Discussion

These analyses, which were based on an extensive sampling effort in four different vent fields along the length of the ELSC, uncover previously cryptic, regional-scale patterns in the distribution of *Alviniconcha* holobionts. Our results suggest that regional-scale gradients in geochemistry, which are the surficial expression of subsurface tectonic processes and water–rock interactions, respectively, influence niche availability—and thus partitioning—among hydrothermal vent symbioses. Specifically, we observed striking patterns in the distribution of *Alviniconcha* host types, wherein *Alviniconcha* associated with ε-proteobacteria were substantially more abundant at the northernmost, basaltic vent fields (Kilo Moana and Tow Cam). Conversely, *Alviniconcha* associated with γ-proteobacteria were more abundant at the andesitic southern vent fields (ABE and Tu'i Malila) (42, 43). We observed further basin-wide geographic trends in *Alviniconcha* individuals hosting different γ-proteobacterial symbionts, including the absence of individuals dominated by the γ-Lau phylotype from all except the Tu'i Malila vent fields. Together, with geochemical data from high-temperature and diffuse vent fluids from these vent fields, our results indicate that niche partitioning within a genus of chemosynthetic symbioses at deep sea hydrothermal vents is linked to subsurface geological/geochemical processes. These data suggest that interactions between symbionts and the physicochemical habitat, rather than host physiology alone, can govern the distribution of hydrothermal vent symbioses across a biogeographical province.

Symbiont and Host Diversity and Association. The cryptic diversity revealed here reshapes our understanding of the biogeography of this genus. Before this study, only HT-III (previously called "host type Lau") and one symbiont phylotype (γ-Lau) had been documented in the Lau Basin (38). Our phylogenetic surveys uncovered two additional host types (HT-I and HT-II) and two additional symbiont phylotypes (γ-1 and ε-proteobacterial) within the ELSC. Collectively, these data establish the ELSC as the geographic area with the highest documented diversity for this genus, with a greater number of host types and symbiont phylotypes than in any other region. [It is possible that *Alviniconcha* hosts and symbionts are comparably diverse at other western Pacific and Indian Ocean vent systems, although this remains to be determined (36–38, 40).] Regardless, the data herein show unforeseen holobiont diversity within the genus *Alviniconcha* and emphasize the value of interrogating both host and symbiont identity at an appropriate sampling scale to capture cryptic phylogenetic diversity.

The observed patterns of association among the host and symbiont phylotypes were most surprising. 16S rRNA gene qPCR of all sampled individuals revealed that *Alviniconcha* host types exhibited varying degrees of specificity for their symbionts. *Alviniconcha* HT-II associated solely with ε-proteobacteria. HT-III hosted mixed populations of the two γ-proteobacterial phylotypes (γ-Lau and γ-1). Notably, HT-I associated with both γ- or ε-proteobacterial endosymbionts, sometimes within the same individual (although one endosymbiont always dominated).

Although some species of *Bathymodiolus* hydrothermal vent mussels are known to associate with two endosymbiotic γ-proteobacterial phylotypes (46–48), the ability of an *Alviniconcha* individual to host endosymbionts from two distinct bacterial classes is unprecedented among chemosynthetic symbioses. These symbionts are thought to be environmentally acquired (49), and the observed patterns of symbiont distribution among host types suggest interplay between host specificity and environmental determinants. This interplay may have a profound role in structuring the distribution of *Alviniconcha* host types across available niche space.

Holobiont Distribution and Basin-Wide Geochemical Gradients. Further investigation revealed that the holobionts exhibited a structured pattern of distribution across the four vent fields. Although *Alviniconcha* HT-I and the symbiont γ-1 were represented at all four vent fields, individuals dominated by the symbiont γ-Lau were observed at only one vent field (Tu'i Malila), and only one HT-III individual was found outside of Tu'i Malila. Structured distributions of marine fauna often result from geographical isolation or other barriers to dispersal (50, 51). However, the representation of host HT-I and symbiont phylotype γ-1 among all of the vents studied here, combined with our recovery of host haplotypes identical to previously collected individuals from thousands of kilometers away, suggests that the existence of such barriers is unlikely. *Alviniconcha* are thought to produce far-dispersing planktotrophic larvae (52), and studies of deepwater circulation in the ELSC have revealed continuity among the sites (53). Thus, the potential for geographic isolation caused by limitations on larval dispersal or deepwater circulation along the ELSC seems low.

Geological and geochemical gradients along the spreading center better explain the observed holobiont distributions. The ELSC comprises a series of vent fields in the Lau back-arc basin created by the subduction of the Pacific plate under the Indo-Australian plate. As the ELSC proceeds from north to south, it approaches the volcanic arc, resulting in an increased influence of the subducting Pacific plate on the crustal rocks (54–56). Consequently, there is a change in crustal rock type, with vent fields in the north being dominated by basalt and vent fields in the south being dominated by basaltic-andesite and andesitic lavas (42, 43). The increasing influence of the subducting slab is reflected in the changing geochemical composition of vent fluids north to south along the spreading center, including sizeable differences in dissolved volatile concentrations (28, 44, 45). Our analyses of high-temperature vent effluents from among the sampling sites revealed variations in gross geochemical composition along the ELSC that appear to be stable over time (44, 45). Both H_2 and H_2S concentrations decrease from north to south, with H_2 showing about an order-of-magnitude difference in concentration in end-member fluids from Kilo Moana in the north (~500 μM) to Tu'i Malila in the south (~43 μM). Because there often is a correspondence between the geochemical composition of a diffuse flow and nearby high-temperature flow (57–59), the elevated H_2 and H_2S concentrations in the high-temperature fluids at the northern vent sites likely correspond to higher concentrations of these chemical species in the cooler vent fluids bathing the *Alviniconcha* at these fields. Indeed, in situ voltammetry of vent fluids from among the collections corroborated the above geochemical trend and established that sulfide concentrations were higher among the *Alviniconcha* aggregations in the northern vent fields, although temperature and oxygen concentrations were not significantly different among the collection sites.

Niche Partitioning. If there are functional differences among *Alviniconcha* symbionts, then each host type's specificity for a particular symbiont would influence its capacity to exploit different physicochemical niches. Given the aforementioned distribution of phylotypes and the seeming lack of barriers to dispersal, we posit that the observed patterns of distribution of *Alviniconcha* across the ELSC relates to the gradients in vent-fluid geochemistry (Fig. 7). Holobionts with ε-proteobacterial symbionts dominated in fields with higher H_2 and H_2S concentrations, and conversely holobionts with γ-proteobacterial symbionts were in greater abundance at fields with lower H_2 and H_2S. This observation is consistent with studies of free-living ε- and γ-proteobacteria in sulfidic environments, which found that ε-proteobacteria dominate over γ-proteobacteria in habitats with higher sulfide (60–62). Both H_2 and sulfur oxidation are known to be common metabolisms among the close relatives (i.e., *Sulfurimonas* spp.) of the ε-proteobacterial symbionts (60, 63–65), and we hypothesize that one or both of these mechanisms supports autotrophy in this phylotype. Previous studies of *Alviniconcha* symbiont metabolism have focused on sulfide oxidation in vivo and in vitro (39, 66) but did not identify the symbionts, so it is unclear which phylotypes are engaged in this metabolism. We observed that holobionts with ε-proteobacteria did not have visible sulfur granules (a known intermediate in some sulfur oxidation pathways) in their gills. In contrast, holobionts with γ-proteobacteria had elemental sulfur in their gills, suggesting different modes of sulfur metabolism. This finding, too, is consistent with studies of sulfur oxidation by ε- and γ-proteobacteria, which are known to use different pathways (reviewed in ref. 60). We recognize that other factors, yet to be determined, could influence the north-to-south partitioning of ε- and γ-proteobacterial symbionts as well as the distribution of holobionts with γ-Lau and γ-1, along the ELSC. Further work identifying the specific reductants and pathways used by the three symbiont phylotypes is needed to better understand the connection between symbiont physiology and the observed habitat partitioning.

We also observed evidence for niche partitioning at a local (vent-field) scale. Most collections were dominated by holobionts associating with one particular symbiont type (e.g., HT-I and II both hosting ε-proteobacterial symbionts in collection TC-2) (Fig. 5). This patchiness does not correspond strictly to habitat type (chimney wall vs. diffuse flows), because collections from both habitat types were dominated by ε-proteobacterial symbionts in the north and, conversely, by γ-proteobacterial symbionts in the south. There are anomalous collections from Kilo Moana and ABE that deviate from the overarching patterns of distribution in this study and that reflect local patchiness in geochemistry. Indeed, if these patterns are driven by habitat conditions, we would expect local variation in chemistry to result in patchy holobiont distribution even within a vent field. Unfortunately, we did not collect environmental data at these specific sites, so we cannot determine whether these collections were associated with different geochemistry. Although higher-resolution sampling of *Alviniconcha* with associated fine-scale chemical measurements is necessary to understand the extent of intrafield habitat partitioning by these symbioses, the existing data suggest interactions between the symbionts and the environment.

Previous studies have hypothesized that differences in the oxygen tolerance of the carbon fixation pathways used by the γ- and ε-proteobacterial symbionts could influence habitat utilization by the different *Alviniconcha* symbioses (38, 61). Indeed, our measurements of carbon-stable isotopic composition are consistent with the use of different carbon-fixation pathways by the γ- and ε-proteobacterial symbionts (Table S3). However, the oxygen concentrations were not significantly different in the habitats occupied by individuals with the γ- and ε-proteobacterial symbionts. Moreover, it is unlikely that environmental oxygen concentrations are experienced by the symbionts, because host oxygen-binding proteins, such as the gill hemoglobin of *Alviniconcha* (67), have a high affinity for oxygen and will govern its partial pressure within the host's tissues. With respect to whether differences in host physiology influence the observed distribution patterns, little is known about differences in thermal tolerance or

chemotolerance among *Alviniconcha* host types (66). Sulfide tolerance has been suggested to affect animal distribution at vents (23, 27, 68) and is significantly different among collections dominated by the different *Alviniconcha* holobionts at the ELSC. However, the highest sulfide levels detected among the snails in our collections are well below the tolerance limits reported from shipboard experiments on *Alviniconcha*, and thus host tolerance for sulfide is unlikely to be responsible for the patterns we report (66). Additionally, temperature and oxygen concentrations—two key factors often invoked in governing the distribution of animals at vents (23)—were not significantly different among our collection sites. Although both host and symbiont physiology undoubtedly influence the overall niche of these holobionts, we suggest that host physiology is unlikely to play a major role in the habitat partitioning observed here.

Conclusions

For vent holobionts, access to vent-derived chemical resources (reduced compounds for chemolithoautotrophy) requires physical proximity to the emitted vent fluid, as evidenced by the strong association of chemosynthetic symbioses with vent-fluid emissions (e.g., ref. 28). Competition among these holobionts for chemical resources takes the form of competition for the limited space near vent flows. Within a chemically heterogeneous vent system such as the ELSC, with spatial variability in the composition of vent fluid, resource partitioning among symbioses appears to occur via the differential distribution of the symbioses across the range of geochemical milieus. Here, we observed this process occurring both within a genus and at a regional scale, with differential distribution of holobionts among distinct vent fields that are tens of kilometers apart.

In many ecosystems, niche partitioning has been shown to facilitate the coexistence of ecologically similar taxa (reviewed in ref. 3) but generally has been considered in the context of the intrinsic differences in organisms, not in differences in their symbionts. Despite growing knowledge of the ubiquity of symbioses in the natural world, evidence for their effects on niche partitioning among similar hosts is surprisingly rare. In a few animal–microbial symbioses, namely coral–algal and aphid–bacterial associations, studies have correlated microbial symbiont genetic and physiological diversity with niche partitioning by the symbioses. In these cases, specificity in partnering among physiologically distinct endosymbiont phylotypes and genetically distinct hosts has been found to correspond to the distribution of corals in different light and temperature regimes on reefs (69–74) and to the distribution of aphids on different plant types (75–77). Previous research on the relationship between symbiont identity and environmental geochemistry at hydrothermal vents examined how differences in symbiont phylotype and abundance varied within a single species of mussel as a function of habitat (47, 78–80). It now is apparent that the process of symbiont-influenced niche partitioning among genetically distinct hosts is likely to play a role in structuring vent ecosystems and is driven by subsurface geological and geochemical interactions. The influence of symbiont metabolism on host niche utilization is fundamental to our understanding of hydrothermal vent symbioses and vent ecosystems. With increasing awareness of the prevalence of microbe–animal interactions in our biosphere, the process of symbiont-driven niche partitioning is likely to be elemental in other biological systems as well.

Methods

***Alviniconcha* Specimens.** A total of 288 *Alviniconcha* specimens were collected from four vent fields in the ELSC using the remotely operated vehicle (ROV) *Jason II* during expedition TM-235 in 2009 on board the R/V *Thomas G. Thompson* (Fig. 1 and Table S1). Sites were chosen randomly, and live specimens were collected using modified "mussel pots" (81, 82) or large scoop nets and were returned to the ship in insulated containers. On board ship, live specimens were kept in chilled (4 °C) seawater until dissection. Symbiont-containing gill tissues were dissected on shipboard and were frozen immediately at −80 °C. The frozen tissue remained at −80 °C until it was subsampled for DNA extraction and carbon isotope analysis.

Free Sulfide, Oxygen, and Temperature Determination via in Situ Voltammetry. In situ voltammetry and a temperature probe were used to determine free sulfide and oxygen concentrations as well as fluid temperatures associated with a subset of the *Alviniconcha* collections (Table S1) (83, 84). Measurements were made in the same manner for both diffuse flows and chimney walls. Briefly, animals were collected, and then 1–12 scan sets were performed with the tip of the probe directly on the cleared substrate. Each scan set was comprised of 7–12 discrete measurements (scans), which then were averaged. At the diffuse-flow sites, measurements were made on the cleared substratum after animals were collected. At the chimney wall sites, after animals were collected, the probe was positioned directly along the side of the perpendicular to chimney wall structure, so that the tip touched or was within 1 cm of touching the chimney wall (based on the laser scale from the ROV *Jason*). In all cases, shimmering water often was visible, and temperatures never were higher than 60 °C. The instrument's quantitative limits of detection for free sulfide and oxygen are 0.2 μM and 15 μM, respectively. For statistical analyses, values below the quantitative limits of detection were treated as in ref. 28.

End-Member Vent-Fluid Sampling and Analyses. Hydrothermal fluids were recovered from high-temperature orifices (temperatures ranged from 268–320 °C) using the ROV *Jason II* and isobaric gas-tight fluid samplers (85) during expedition TM-236 in June–July 2009 on the R/V *Thomas G. Thompson.* Samples were analyzed for dissolved CH_4, H_2S, and DIC. Dissolved CH_4, DIC, and H_2 also were measured at the vent fields sampled during this study during expedition TUIM05MV on the R/V *Melville* (April–May 2005) (see ref. 44 for 2005 sample information). All fluid samples were processed via gas chromatography or gravimetry as in ref. 44. See *SI Methods* for details of end-member calculations.

DNA Extraction. Approximately 25 mg of gill tissue was subsampled while frozen for DNA extraction. Each subsample was placed into one well of a 96-well plate containing a proprietary lysis buffer from the AutoGenprep 965/960 Tissue DNA Extraction kit (AutoGen, Inc.), and DNA was extracted with the AutoGenprep 965 automatic extraction system. Before downstream analysis, all DNA extracts were diluted 1:100 in molecular-grade sterile water to minimize the effect of any coextracted inhibitors on downstream molecular analysis.

Phylogenetic Analysis of the Host Mitochondrial CO1 Gene. DNA extracts from all *Alviniconcha* individuals were used as template to partially amplify the CO1 mitochondrial gene, and the resulting sequences were cleaned, trimmed, and aligned and then were used to produce a Bayesian inference phylogeny using the SRD06 model of nucleotide evolution (86), which partitions the protein coding sequence into first plus second and third codon positions, estimating parameters for each. Details of these analyses can be found in *SI Methods*. Host CO1 gene sequences were deposited in GenBank, and accession numbers are given in Table S2.

Phylogenetic Analysis of Symbiont 16S rRNA Genes. Universal bacterial primers were used to amplify symbiont 16S rRNA genes from the DNA extracts of 30 individuals from ABE and Tu'i Malila. A clone library was constructed from the pooled amplicons of individuals from each vent field, and sequence diversity was assessed via partial sequencing of clones (see *SI Methods* for GenBank accession numbers). The clones were found to represent three phylotypes with >96% identity to previously sequenced *Alviniconcha* symbionts. Bidirectional sequencing of clones representative for each symbiont phylotype yielded longer sequences (accession numbers JN377487, JN377488, JN377489), which were cleaned, trimmed, and aligned with other 16S rRNA gene sequences from both free-living and symbiotic Proteobacteria and then were used to produce a Bayesian inference phylogeny with BEAST (87) implementing the GTR+I+G model of substitution. Details of these analyses can be found in *SI Methods*.

Symbiont qPCR Assay Development. SYBR Green qPCR primers (Table S4) were designed for the three symbiont phylotypes using the aforementioned 16S rRNA gene alignment. Each phylotype assay was designed to target *Alviniconcha* symbiont 16S rRNA gene sequences from this study and others to capture intraphylotype sequence diversity. Details of qPCR assay design and optimization are given in *SI Methods*.

Assessing Symbiont Composition via qPCR. To confirm that our subsamples yielded symbiont populations typical of the entire gill, we took three subsamples (from either end and the middle of each gill) from the whole gills of six individuals, extracted DNA as described above, and found that the proportion of symbiont phylotypes varied by <1% among subsamples (Table S5). We accordingly estimated the proportion of each symbiont phylotype in the original *Alviniconcha* gill DNA extracts by applying all three qPCR assays to 2 μL of each sample (in duplicate), which were compared against duplicate standard curves and no-template controls and then were averaged to determine copy number. Reactions in which the cycle threshold (C_t) was greater than the C_t for the lowest standard (10 copies) were documented as zero copies. Additionally, all quantities were adjusted for amplification inhibition (*SI Methods*). Symbiont populations within an individual were assessed by assuming each 16S rRNA gene to represent a single symbiont genome (see *SI Methods* for discussion of this assumption).

Analysis of Carbon Isotopic Composition. Approximately 300 mg gill tissue was subsampled while frozen for carbon isotopic analysis. Samples were lyophilized for 24 h and then were acidified with 0.1 N HCl to remove any inorganic carbon contamination. The samples subsequently were dried for 24–48 h at 50–60 °C, homogenized to a fine powder, and sealed within tin capsules. The carbon isotopic composition was determined by combustion in an elemental analyzer (Eurovector, Inc.) and separating the evolved CO_2 by gas chromatography before introduction to a Micromass Isoprime isotope ratio mass spectrometer for determination of $^{13}C/^{12}C$ ratios. Measurements are reported in δ-notation relative to the Peedee belemnite in parts per thousand deviations (‰). Typical precision of analyses was ±0.2‰ for $\delta^{13}C$. Egg albumin was used as a daily reference standard.

Statistical Analyses. Comparisons of the symbiont composition of *Alviniconcha* individuals at different vent fields and among the four host types was assessed via ANOSIM using Bray–Curtis dissimilarity (88) (see *SI Methods* for details of ANOSIM). In these analyses, the symbiont composition for each individual represented an independent community profile. Additionally, the collections were compared by classifying each individual based on its dominant symbiont phylotype (γ-1, γ-Lau, ε, or γ-Both for the few individuals that hosted relatively equal proportions of the two γ-proteobacterial symbionts). In these analyses, Bray–Curtis dissimilarity from standardized collection profiles was used.

One-way ANOVAs with post hoc pairwise comparisons (Tukey's) were performed (SPSS Statistics v19) to compare the average carbon-stable isotope values among individuals from the same vent field (Tu'i Malila) with different dominant γ-proteobacterial symbiont phylotypes.

To compare the temperature and environmental sulfide and oxygen concentrations among the collections at all sites as measured via cyclic voltammetry, a nonparametric test (Mann–Whitney U; SPSS Statistics v19) was used.

ACKNOWLEDGMENTS. We thank E. Podowski and S. Hourdez for extensive assistance in the laboratory and on board ship; T. Yu and T. Galyean for preparing samples for stable isotopic analysis; K. Fontenaz for help with phylogenetic analysis; and the crews of the R/V *Thomas G. Thompson*, R/V *Melville*, and the ROV *Jason II*. This paper is based on work supported by National Science Foundation Grants OCE-0732369 (to P.R.G.), OCE-0732333 (to C.R.F.), OCE-1038124 and OCE-0241796 (to J.S.S.), and OCE-0732439 (to G.W.L.) under Graduate Research Fellowship DGE-1144152 (to R.A.B. and J.G.S.). J.S.S. also received support from the Woods Hole Oceanographic Institution. B.F. was supported by a Lavoisier Research Fellowship from the French Ministry of Foreign and European Affairs.

1. Chase JM, Leibold MA (2003) *Ecological Niches: Linking Classical and Contemporary Approaches* (Univ of Chicago Press, Chicago).
2. Leibold MA, McPeek MA (2006) Coexistence of the niche and neutral perspectives in community ecology. *Ecology* 87(6):1399–1410.
3. Chesson P (2000) Mechanisms of maintenance of species diversity. *Annual Review of Ecology and Systematics* 31:343–366.
4. Schoener TW (1974) Resource partitioning in ecological communities. *Science* 185 (4145):27–39.
5. Schoener TW (1986) Resource partitioning. *Community Ecology: Pattern and Process*, eds Kikkawa J, Anderson DJ (Blackwell Scientific Publications, Boston), pp 91–126.
6. Fisher CR, Takai K, Le Bris N (2007) Hydrothermal vent ecosystems. *Oceanography (Washington DC)* 20(1):14–23.
7. Van Dover CL (2000) *The Ecology of Deep-Sea Hydrothermal Vents* (Princeton Univ Press, Princeton).
8. Cavanaugh CM, Gardiner SL, Jones ML, Jannasch HW, Waterbury JB (1981) Prokaryotic cells in the hydrothermal vent tube worm *Riftia pachyptila* Jones: Possible Chemoautotrophic Symbionts. *Science* 213(4505):340–342.
9. Fisher CR, Childress JJ, Minnich E (1989) Autotrophic carbon fixation by the chemoautotrophic symbionts of *Riftia pachyptila*. *The Biological Bulletin* 177(3):372–385.
10. Felbeck H (1981) Chemoautotrophic potential of the hydrothermal vent tube worm, *Riftia pachyptila* Jones (Vestimentifera). *Science* 213(4505):336–338.
11. Belkin S, Nelson DC, Jannasch HW (1986) Symbiotic assimilation of CO2 in the two hydrothermal vent animals, the mussel *Bathymodiolus thermophilus* and the tubeworm *Riftia pachyptila*. *The Biological Bulletin* 170(1):110–121.
12. Nelson DC, Hagen KD, Edwards DB (1995) The gill symbiont of the hydrothermal vent mussel *Bathymodiolus thermophilus* is a psychrophilic, chemoautotrophic, sulfur bacterium. *Marine Biology* 121(3):487–495.
13. Dubilier N, Bergin C, Lott C (2008) Symbiotic diversity in marine animals: The art of harnessing chemosynthesis. *Nat Rev Microbiol* 6(10):725–740.
14. Ramirez-Llodra E, Shank TM, German CR (2007) Biodiversity and biogeography of hydrothermal vent species thirty years of discovery and investigations. *Oceanography (Washington DC)* 20(1):30–41.
15. Butterfield DA, et al. (1994) Gradients in the composition of hydrothermal fluids from the Endeavour segment vent field: Phase separation and brine loss. *Journal of Geophysical Research* 99(B5):9561–9583.
16. Butterfield DA, Massoth GJ, McDuff RE, Lupton JE, Lilley MD (1990) Geochemistry of hydrothermal fluids from axial seamount hydrothermal emissions study vent field, Juan-de-Fuca Ridge - subseafloor boiling and subsequent fluid-rock interaction. *Journal of Geophysical Research-Solid Earth and Planets* 95(B8):12895–12921.
17. Von Damm KL (1995) Controls on the chemistry and temporal variability of seafloor hydrothermal fluids. *Seafloor Hydrothermal Systems: Physical, Chemical, Biological, and Geological Interactions*, Geophys Monogr Ser (American Geophysical Union, Washington, DC), 91:222–247.
18. Tivey MK (2007) Generation of seafloor hydrothermal vent fluids and associated mineral deposits. *Oceanography (Washington DC)* 20(1):50–65.
19. Shank TM, et al. (1998) Temporal and spatial patterns of biological community development at nascent deep-sea hydrothermal vents (9°50′N, East Pacific Rise). *Deep Sea Research Part II: Topical Studies in Oceanography* 45(1–3):465–515.
20. Hessler RR, et al. (1988) Temporal change in megafauna at the Rose Garden hydrothermal vent (Galapagos Rift; eastern tropical Pacific). *Deep Sea Research Part A: Oceanographic Research Papers* 35(10–11):1681–1709.
21. Fisher CR, et al. (1988) Microhabitat variation in the hydrothermal vent mussel, *Bathymodiolus thermophilus*, at the Rose Garden vent on the Galapagos Rift. *Deep Sea Research Part A: Oceanographic Research Papers* 35(10–11):1769–1791.
22. Waite TJ, et al. (2008) Variation in sulfur speciation with shellfish presence at a Lau Basin diffuse flow vent site. *Journal of Shellfish Research* 27(1):163–168.
23. Luther GW, 3rd, et al. (2001) Chemical speciation drives hydrothermal vent ecology. *Nature* 410(6830):813–816.
24. Moore TS, Shank TM, Nuzzio DB, Luther GW III (2009) Time-series chemical and temperature habitat characterization of diffuse flow hydrothermal sites at 9°50′N East Pacific Rise. *Deep Sea Research Part II: Topical Studies in Oceanography* 56(19–20): 1616–1621.
25. Fisher CR, et al. (1988) Variation in the hydrothermal vent clam, *Calyptogena magnifica*, at the Rose Garden vent on the Galapagos spreading center. *Deep Sea Research Part A: Oceanographic Research Papers* 35(10-11):1811–1831.
26. Le Bris N, Govenar B, Le Gall C, Fisher CR (2006) Variability of physico-chemical conditions in 9°50′N EPR diffuse flow vent habitats. *Marine Chemistry* 98(2–4):167–182.
27. Le Bris N, Sarradin PM, Caprais JC (2003) Contrasted sulphide chemistries in the environment of 13°N EPR vent fauna. *Deep Sea Research Part I: Oceanographic Research Papers* 50(6):737–747.
28. Podowski EL, Ma S, Luther GW III, Wardrop D, Fisher CR (2010) Biotic and abiotic factors affecting distributions of megafauna in diffuse flow on andesite and basalt along the Eastern Lau Spreading Center, Tonga. *Marine Ecology Progress Series* 418: 25–45.
29. Podowski EL, Moore TS, Zelnio KA, Luther GW, Fisher CR (2009) Distribution of diffuse flow megafauna in two sites on the Eastern Lau Spreading Center, Tonga. *Deep-Sea Research Part I: Oceanographic Research Papers* 56(11):2041–2056.
30. Girguis PR, Childress JJ (2006) Metabolite uptake, stoichiometry and chemoautotrophic function of the hydrothermal vent tubeworm *Riftia pachyptila*: Responses to environmental variations in substrate concentrations and temperature. *Journal of Experimental Biology* 209(Pt 18):3516–3528.
31. Cavanaugh CM, McKiness ZP, Newton ILG, Stewart FJ (2007) Marine Chemosynthetic Symbioses. *The Prokaryotes*, eds Dworkin M, Falkow S, Rosenberg E, Schleifer K-H, Stackebrandt E (Springer, New York), pp 475–507.
32. Petersen JM, et al. (2011) Hydrogen is an energy source for hydrothermal vent symbioses. *Nature* 476(7359):176–180.
33. Kleiner M, et al. (2012) Metaproteomics of a gutless marine worm and its symbiotic microbial community reveal unusual pathways for carbon and energy use. *Proc Natl Acad Sci* 109(19):E1173–E1182.
34. Denis F, Jollivet D, Moraga D (1993) Genetic separation of two allopatric populations of hydrothermal snails *Alviniconcha* spp (Gastropoda) from two south western pacific back-arc basins. *Biochemical Systematics and Ecology* 21(4):431–440.
35. Kojima S, et al. (2001) Phylogeny of hydrothermal-vent-endemic gastropods *Alviniconcha* spp. from the western Pacific revealed by mitochondrial DNA sequences. *The Biological Bulletin* 200(3):298–304.
36. Suzuki Y, et al. (2005) Novel chemoautotrophic endosymbiosis between a member of the Epsilonproteobacteria and the hydrothermal-vent gastropod *Alviniconcha* aff. *hessleri* (Gastropoda: Provannidae) from the Indian Ocean. *Appl Environ Microbiol* 71 (9):5440–5450.
37. Suzuki Y, et al. (2005) Molecular phylogenetic and isotopic evidence of two lineages of chemoautotrophic endosymbionts distinct at the subdivision level harbored in one

host-animal type: The genus *Alviniconcha* (Gastropoda: Provannidae). *FEMS Microbiol Lett* 249(1):105–112.
38. Suzuki Y, et al. (2006) Host-symbiont relationships in hydrothermal vent gastropods of the genus *Alviniconcha* from the Southwest Pacific. *Appl Environ Microbiol* 72(2): 1388–1393.
39. Stein JL, et al. (1988) Chemoautotrophic symbiosis in a hydrothermal vent gastropod. *The Biological Bulletin* 174(3):373–378.
40. Urakawa H, et al. (2005) Hydrothermal vent gastropods from the same family (Provannidae) harbour epsilon- and gamma-proteobacterial endosymbionts. *Environ Microbiol* 7(5):750–754.
41. Martinez F, Taylor B, Baker ET, Resing JA, Walker SL (2006) Opposing trends in crustal thickness and spreading rate along the back-arc Eastern Lau Spreading Center: Implications for controls on ridge morphology, faulting, and hydrothermal activity. *Earth and Planetary Science Letters* 245(3–4):655–672.
42. Bézos A, Escrig S, Langmuir CH, Michael PJ, Asimow PD (2009) Origins of chemical diversity of back-arc basin basalts: A segment-scale study of the Eastern Lau Spreading Center. *Journal of Geophysical Research* 114(B6):B06212.
43. Escrig S, Bézos A, Goldstein SL, Langmuir CH, Michael PJ (2009) Mantle source variations beneath the Eastern Lau Spreading Center and the nature of subduction components in the Lau basin-Tonga arc system. *Geochemistry Geophysics Geosystems* 10(4):Q04014.
44. Mottl MJ, et al. (2011) Chemistry of hot springs along the Eastern Lau Spreading Center. *Geochimica Et Cosmochimica Acta* 75:1013–1038.
45. Hsu-Kim H, Mullaugh KM, Tsang JJ, Yucel M, Luther GW, 3rd (2008) Formation of Zn- and Fe-sulfides near hydrothermal vents at the Eastern Lau Spreading Center: Implications for sulfide bioavailability to chemoautotrophs. *Geochem Trans* 9(1):6.
46. Distel DL, Lee HK, Cavanaugh CM (1995) Intracellular coexistence of methano- and thioautotrophic bacteria in a hydrothermal vent mussel. *Proc Natl Acad Sci USA* 92(21):9598–9602.
47. Duperron S, et al. (2006) A dual symbiosis shared by two mussel species, *Bathymodiolus azoricus* and *Bathymodiolus puteoserpentis* (Bivalvia: Mytilidae), from hydrothermal vents along the northern Mid-Atlantic Ridge. *Environ Microbiol* 8(8): 1441–1447.
48. DeChaine EG, Cavanaugh CM (2006) Symbioses of Methanotrophs and Deep-Sea Mussels (Mytilidae: Bathymodiolinae). Molecular Basis of Symbiosis. *Progress in Molecular and Subcellular Biology*, ed Overmann J (Springer, Berlin), 41:227–249.
49. Endow K, Ohta S (1989) The symbiotic relationship between bacteria and a mesogastropod snail, *Alviniconcha hessleri*, collected from hydrothermal vents of the Mariana back-arc basin. *Bulletin of the Japanese Society of Microbial Ecology* 3(2): 73–82.
50. Vrijenhoek RC (2010) Genetic diversity and connectivity of deep-sea hydrothermal vent metapopulations. *Mol Ecol* 19(20):4391–4411.
51. Cowen RK, Sponaugle S (2009) Larval dispersal and marine population connectivity. *Annu Rev Mar Sci* 1(1):443–466.
52. Waren A, Bouchet P (1993) New records, species, genera, and a new family of gastropods from hydrothermal vents and hydrocarbon seeps. *Zoologica Scripta* 22(1):1–90.
53. Speer K, Thurnherr AM (2012) The Lau Basin float experiment (LAUB-FLEX). *Oceanography (Washington DC)* 25(1):284–285.
54. Martinez F, Taylor B (2002) Mantle wedge control on back-arc crustal accretion. *Nature* 416(6879):417–420.
55. Taylor B, Martinez F (2003) Back-arc basin basalt systematics. *Earth and Planetary Science Letters* 210(3-4):481–497.
56. Dunn RA, Martinez F (2011) Contrasting crustal production and rapid mantle transitions beneath back-arc ridges. *Nature* 469(7329):198–202.
57. Proskurowski G, Lilley MD, Olson EJ (2008) Stable isotopic evidence in support of active microbial methane cycling in low-temperature diffuse flow vents at 9°50′N East Pacific Rise. *Geochimica Et Cosmochimica Acta* 72(8):2005–2023.
58. Butterfield DA, Massoth GJ (1994) Geochemistry of north Cleft segment vent fluids: Temporal changes in chlorinity and their possible relation to recent volcanism. *Journal of Geophysical Research* 99(B3):4951–4968.
59. Butterfield DA, et al. (1997) Seafloor eruptions and evolution of hydrothermal fluid chemistry. *Philosophical Transactions of the Royal Society of London. Series A: Mathematical, Physical and Engineering Sciences* 355(1723):369–386.
60. Yamamoto M, Takai K (2011) Sulfur metabolisms in epsilon- and gamma-Proteobacteria in deep-sea hydrothermal fields. *Frontiers in Microbiology*, 10.3389/fmicb.2011.00192.
61. Nakagawa S, Takai K (2008) Deep-sea vent chemoautotrophs: Diversity, biochemistry and ecological significance. *FEMS Microbiol Ecol* 65(1):1–14.
62. Macalady JL, et al. (2008) Niche differentiation among sulfur-oxidizing bacterial populations in cave waters. *ISME J* 2(6):590–601.
63. Campbell BJ, Engel AS, Porter ML, Takai K (2006) The versatile epsilon-proteobacteria: Key players in sulphidic habitats. *Nat Rev Microbiol* 4(6):458–468.
64. Nakagawa S, et al. (2005) Distribution, phylogenetic diversity and physiological characteristics of epsilon-Proteobacteria in a deep-sea hydrothermal field. *Environ Microbiol* 7(10):1619–1632.
65. Nakagawa S, Takaki Y (2001) *Nonpathogenic Epsilonproteobacteria* (John Wiley and Sons, Ltd, Chichester). Available at http://www.els.net.
66. Henry MS, Childress JJ, Figueroa D (2008) Metabolic rates and thermal tolerances of chemoautotrophic symbioses from Lau Basin hydrothermal vents and their implications for species distributions. *Deep-Sea Research Part I: Oceanographic Research Papers* 55(5):679–695.
67. Wittenberg JB, Stein JL (1995) Hemoglobin in the symbiont-harboring gill of the marine gastropod Alviniconcha hessleri. *The Biological Bulletin* 188(1):5–7.
68. Matabos M, Le Bris N, Pendlebury S, Thiebaut E (2008) Role of physico-chemical environment on gastropod assemblages at hydrothermal vents on the East Pacific Rise (13°N/EPR). *Journal of the Marine Biological Association of the United Kingdom* 88(05):995–1008.
69. Thornhill DJ, Kemp DW, Bruns BU, Fitt WK, Schmidt GW (2008) Correspondence between cold tolerance and temperatre biogeography in a western Atlantic *Symbiodinium* (Dinophyta) lineage. *Journal of Phycology* 44(5):1126–1135.
70. Verde E, McCloskey L (2007) A comparative analysis of the photobiology of zooxanthellae and zoochlorellae symbiotic with the temperate clonal anemone *Anthopleura elegantissima* (Brandt). III. Seasonal effects of natural light and temperature on photosynthesis and respiration. *Marine Biology* 152(4):775–792.
71. Iglesias-Prieto R, Beltrán VH, LaJeunesse TC, Reyes-Bonilla H, Thomé PE (2004) Different algal symbionts explain the vertical distribution of dominant reef corals in the eastern Pacific. *Proc Biol Sci* 271(1549):1757–1763.
72. Loram JE, Trapido-Rosenthal HG, Douglas AE (2007) Functional significance of genetically different symbiotic algae Symbiodinium in a coral reef symbiosis. *Mol Ecol* 16(22):4849–4857.
73. Bongaerts P, et al. (2010) Genetic divergence across habitats in the widespread coral *Seriatopora hystrix* and its associated *Symbiodinium*. *PLoS ONE* 5(5):e10871.
74. Finney JC, et al. (2010) The relative significance of host-habitat, depth, and geography on the ecology, endemism, and speciation of coral endosymbionts in the genus Symbiodinium. *Microb Ecol* 60(1):250–263.
75. Ferrari J, et al. (2004) Linking the bacterial community in pea aphids with host-plant use and natural enemy resistance. *Ecol Entomol* 29(1):60–65.
76. Ferrari J, Scarborough CL, Godfray HC (2007) Genetic variation in the effect of a facultative symbiont on host-plant use by pea aphids. *Oecologia* 153(2):323–329.
77. Tsuchida T, Koga R, Shibao H, Matsumoto T, Fukatsu T (2002) Diversity and geographic distribution of secondary endosymbiotic bacteria in natural populations of the pea aphid, *Acyrthosiphon pisum*. *Mol Ecol* 11(10):2123–2135.
78. Halary S, Riou V, Gaill F, Boudier T, Duperron S (2008) 3D FISH for the quantification of methane- and sulphur-oxidizing endosymbionts in bacteriocytes of the hydrothermal vent mussel *Bathymodiolus azoricus*. *ISME J* 2(3):284–292.
79. Riou V, et al. (2008) Influence of CH_4 and H_2S availability on symbiont distribution, carbon assimilation and transfer in the dual symbiotic vent mussel *Bathymodiolus azoricus*. *Biogeosciences* 5(6):1681–1691.
80. Fujiwara Y, et al. (2000) Phylogenetic characterization of endosymbionts in three hydrothermal vent mussels: Influence on host distributions. *Marine Ecology Progress Series* 208:147–155.
81. Van Dover CL (2002) Community structure of mussel beds at deep-sea hydrothermal vents. *Marine Ecology Progress Series* 230:137–158.
82. Cordes EE, Becker EL, Hourdez S, Fisher CR (2010) Influence of foundation species, depth, and location on diversity and community composition at Gulf of Mexico lower-slope cold seeps. *Deep Sea Research Part II: Topical Studies in Oceanography* 57(21–23):1870–1881.
83. Luther GW III, et al. (2008) Use of voltammetric solid-state (micro)electrodes for studying biogeochemical processes: Laboratory measurements to real time measurements with an in situ electrochemical analyzer (ISEA). *Marine Chemistry* 108(3–4):221–235.
84. Gartman A, et al. (2011) Sulfide oxidation across diffuse flow zones of hydrothermal vents. *Aquatic Geochemistry* 17(4):583–601.
85. Seewald JS, Doherty KW, Hammar TR, Liberatore SP (2002) A new gas-tight isobaric sampler for hydrothermal fluids. *Deep Sea Research Part I: Oceanographic Research Papers* 49(1):189–196.
86. Shapiro B, Rambaut A, Drummond AJ (2006) Choosing appropriate substitution models for the phylogenetic analysis of protein-coding sequences. *Mol Biol Evol* 23(1): 7–9.
87. Drummond AJ, Rambaut A (2007) BEAST: Bayesian evolutionary analysis by sampling trees. *Australian Journal of Ecology* 7(1):214.
88. Clarke KR (1993) Non-parametric multivariate analyses of changes in community structure. *Australian Journal of Ecology* 18(1):117–143.

Chapter 3

Metatranscriptomics reveal differences in *in situ* energy and nitrogen metabolism among hydrothermal vent snail symbionts

(as published in The International Society for Microbial Ecology Journal)

The ISME Journal (2013) 7, 1556–1567

www.nature.com/ismej

OPEN

ORIGINAL ARTICLE

Metatranscriptomics reveal differences in *in situ* energy and nitrogen metabolism among hydrothermal vent snail symbionts

JG Sanders[1,4], RA Beinart[1,4], FJ Stewart[2], EF Delong[3] and PR Girguis[1]
[1]*Department of Organismic and Evolutionary Biology, Harvard University, Cambridge, MA, USA;* [2]*School of Biology, Georgia Institute of Technology, Atlanta, GA, USA and* [3]*Parsons Laboratory, Massachusetts Institute of Technology, Civil and Environmental Engineering, Cambridge, MA, USA*

Despite the ubiquity of chemoautotrophic symbioses at hydrothermal vents, our understanding of the influence of environmental chemistry on symbiont metabolism is limited. Transcriptomic analyses are useful for linking physiological poise to environmental conditions, but recovering samples from the deep sea is challenging, as the long recovery times can change expression profiles before preservation. Here, we present a novel, *in situ* RNA sampling and preservation device, which we used to compare the symbiont metatranscriptomes associated with *Alviniconcha*, a genus of vent snail, in which specific host–symbiont combinations are predictably distributed across a regional geochemical gradient. Metatranscriptomes of these symbionts reveal key differences in energy and nitrogen metabolism relating to both environmental chemistry (that is, the relative expression of genes) and symbiont phylogeny (that is, the specific pathways employed). Unexpectedly, dramatic differences in expression of transposases and flagellar genes suggest that different symbiont types may also have distinct life histories. These data further our understanding of these symbionts' metabolic capabilities and their expression *in situ*, and suggest an important role for symbionts in mediating their hosts' interaction with regional-scale differences in geochemistry.
The ISME Journal (2013) **7,** 1556–1567; doi:10.1038/ismej.2013.45; published online 25 April 2013
Subject Category: Microbe-microbe and microbe-host interactions
Keywords: symbiosis; hydrothermal vents; metatranscriptomics; chemoautotrophy; *Alviniconcha*

Introduction

Endosymbioses among marine invertebrates and chemoautotrophic bacteria have a key role in the ecology and biogeochemistry of deep-sea hydrothermal vents and similar environments. Symbionts derive energy by oxidizing reduced compounds (for example, sulfide, methane, hydrogen) and fix inorganic carbon, providing nutrition to their hosts (Felbeck, 1981; Fisher and Childress, 1984; Childress *et al.*, 1986, 1991; Girguis and Childress, 2006; Petersen *et al.*, 2011). Much is known about host biochemical and morphological adaptations to both their symbionts and the environment (reviewed in Stewart *et al.,* 2005; Childress and Girguis, 2011).

Surprisingly less, however, is known about the relationship between symbiont physiology and the environment, in particular how variations in environmental geochemistry influence symbiont metabolic activity and, in turn, how this affects the ecology of the animal–microbe association. The symbioses between the deep-sea snail *Alviniconcha* and its chemoautotrophic symbionts afford a unique opportunity to examine these relationships. *Alviniconcha* are provannid gastropods that are indigenous to vents in the Western Pacific and Indian Ocean and harbor chemoautotrophic symbionts within host cells located in the gill (Suzuki *et al.,* 2006). At the Eastern Lau Spreading Center in the southwestern Pacific (ELSC, Supplementary Figure S1), genetically distinct *Alviniconcha* 'types' (likely cryptic species) form associations with three lineages of chemoautotrophic Proteobacteria: two γ-proteobacteria (termed γ-1 and γ-Lau) and an ε-proteobacterium (Beinart *et al.*, 2012). A recent study of these host-symbiont associations (hereafter referred to as holobionts), found striking patterns of distribution along the ~300 km length of the ELSC, wherein snails hosting ε-proteobacteria dominated the northern vent fields and those hosting γ-proteobacteria dominated the southern fields (Beinart *et al.,* 2012). Vent fluids also showed marked changes in geochemistry along this range,

Correspondence: PR Girguis, Department of Organismic and Evolutionary Biology, Harvard University, 16 Divinity Avenue, Biolabs Rm 3085, Cambridge, MA 02138, USA.
E-mail: pgirguis@oeb.harvard.edu
[4]These authors contributed equally to this work.
Received 24 September 2012; revised 31 January 2013; accepted 11 February 2013; published online 25 April 2013

with substantially elevated hydrogen and hydrogen sulfide concentrations in the northernmost fields (Mottl *et al.,* 2011; Beinart *et al.,* 2012). This unprecedented pattern of holobiont distribution across this 300 km spreading center suggests a link between symbiont physiology and the environment; namely that differences in the availability of reduced compounds may influence the realized niche of the holobionts as a function of their symbionts' metabolic capacity.

Our understanding of these observed patterns would be facilitated by analyses that reveal the symbionts' physiological poise *in situ*. Transcriptomic studies have been used to relate changes in gene expression to environmental conditions (Gracey, 2007; Gracey *et al.,* 2008). Previous studies have also used transcriptomics to study gene expression in both host and chemoautotrophic symbionts (Harada *et al.,* 2009; Stewart *et al.,* 2011; Wendeberg *et al.,* 2012). However, using transcriptomics to study patterns of gene expression in the deep sea (that is, *in situ*) is especially challenging. Organisms are typically held in ambient seawater during sampling and recovery, so their transcriptional profiles likely change in the hours between collection and preservation (Wendeberg *et al.,* 2012).

To better examine the relationship between *Alviniconcha* symbiont physiology and the observed regional-scale differences in geochemistry, we developed a novel *in situ* sampling and preservation system that allowed us to quickly homogenize and preserve holobionts at the seafloor, simultaneously stopping transcription and stabilizing nucleic acids for downstream analysis. Using this device, we collected individual *Alviniconcha* from four vent fields spanning the previously observed geochemical gradient along the ELSC. Gene expression analyses revealed key differences among symbiont types in the expression of genes relating to hydrogen and sulfur oxidation. In contrast, similarities in patterns of gene expression relating to nitrogen metabolism—which deviate from canonical models of nitrate reduction—suggest a potentially unique strategy of nitrogen utilization that is shared among these symbionts. We also observed differences in gene expression that may be relevant to the maintenance and transmission of these associations. Our results clearly illustrate differences in physiological poise among these symbiont types, underscore the likely role of symbiont physiology in structuring holobiont distribution, and provide insights into how these phylogenetically distinct symbionts have evolved to exploit resources and niches in these highly dynamic environments.

Materials and methods

Instrument design

To preserve holobiont RNA *in situ*, we designed a sample container/homogenizer termed the *In Situ* Mussel And Snail Homogenizer (ISMASH; Figures 1a and b). The ISMASH consists of a 1 l stainless steel blending cylinder, the bottom of which contains a rotating blade assembly and preservative inlet. The top is open to permit sample insertion but is sealed post-collection via a magnetically-latched lid equipped with a one-way check valve. The ISMASH can be operated at any depth attainable by the submersible. During operations, the ISMASH is deployed open and empty on the submersible's working platform. When individual specimens are deposited in the cylinder, the operator places the magnetic lid on the cylinder, and RNALater (Ambion Inc., Grand Island, NY, USA) is pumped in from the bottom, displacing the less-dense seawater through the lid's check valve. After pumping sufficient RNALater to ensure thorough flushing, a hydraulic motor actuates the blade assembly and the sample is homogenized. For a complete instrument description and operational procedures, see Supplementary Information.

Sample collection

Alviniconcha holobionts (Figure 1c) were collected along the ELSC using the ROV Jason II aboard the R/V Thomas G Thompson during expedition TM-235 in 2009. One snail was collected randomly from among large aggregations at each of the four vent fields (Kilo Moana and Tow Cam in the north, ABE and Tu'i Malila in the south; Table 1, Supplementary Figure S1), then homogenized *in situ*. Time limitations prohibited additional sampling. Homogenization was completed within 4–10 min of collection. Upon recovery, the ~1 l homogenates were carefully transferred to sterile glass jars, incubated overnight at 4 °C, and then frozen and maintained at −20° for ~5 months before extraction.

Nucleic acid extraction, library preparation, and sequencing

Before extraction, homogenates were thawed and rehomogenized in a clean, sterile blender (Waring Inc., Torrington, CT, USA) to maximize uniformity. One 2-ml aliquot was taken from each sample and centrifuged at 14 000 × g for 10 min in a refrigerated centrifuge. RNA was extracted from the pellet using TRIzol (Invitrogen Inc., Grand Island, NY, USA) per the manufacturer's protocol. After each extraction, RNA was assessed with an Agilent 2100 Bioanalyzer (Santa Clara, CA, USA) to determine concentration and integrity.

To maximize mRNA representation in our metatranscriptomic libraries, we preferentially removed eukaryotic and bacterial ribosomal RNA (rRNA) using sample-specific rRNA probes as in Stewart *et al.* (2010). Each of the four libraries was sequenced in a separate, gasketed quadrant using Titanium chemistry, yielding a full plate on a

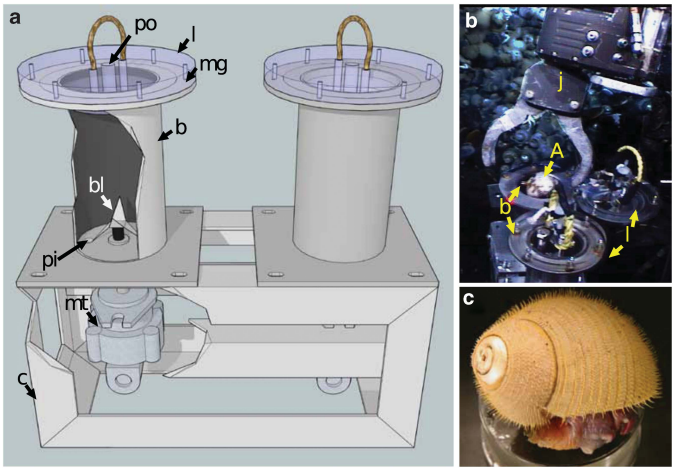

Figure 1 The *In Situ* Mussel and Snail Homogenizer (ISMASH). Cutaway schematic of the ISMASH design (**a**) and a photograph of the ROV JASON II manipulator arm depositing an *Alviniconcha* into the ISMASH body (**b**), with parts labeled: po, preservative outlet; l, magnetic sealing acrylic lid; mg, magnets; b, blender body; bl, blade assembly; pi, preservative inlet; mt, motor; c, chassis; j, ROV JASON II manipulator arm; A, *Alviniconcha*. An *Alviniconcha* snail, photograph taken shipboard (**c**).

Table 1 Sample information for each metatranscriptome: vent field, collection details, and host and symbiont type

Vent field	*Dive*	*Date, time (GMT)*	*Latitude, longitude*	*Depth (m)*	*Host type (accession)*	*Symbiont type*
Kilo Moana	J2-433	6/6/2009, 05:49	20 03.227 S, 176 8.008 W	2615	HT-II (JX134579)	ε
Tow Cam	J2-432	6/5/2009, 11:58	20 18.973 S, 176 8.195 W	2722	HT-II (JX134578)	ε
ABE	J2-431	6/3/2009, 14:29	20 45.794 S, 176 11.478 W	2146	HT-I (JX134580)	γ-1
Tu'i Malila	J2-430	6/2/2009, 09:50	21 59.363 S, 176 34.105 W	1869	HT-III (JX134581)	γ-1/ γ-Lau

Roche Genome Sequencer FLX (Roche Inc., Basel, Switzerland).

DNA was extracted from an additional 2 ml aliquot per sample using a DNeasy Blood & Tissue kit (Qiagen Inc., Venlo, Netherlands) per the manufacturer's protocol. DNA samples were used to assess host and symbiont identities, as well as microbial diversity (while the gill endosymbionts are typically monocultures, our technique would also include any epibionts or other microbes associated with the snail). We confirmed host genotypes by sequencing 500 bp of the mitochondrial cytochrome oxidase I gene (as in Beinart *et al.,* 2012; Table 1). The identity and abundances of the major symbiont types were assessed using SYBR Green qPCR assays on a Mx3005P real-time thermal cycler (Stratagene Inc., Santa Clara, CA, USA), using previously described primers and protocols (Beinart *et al.,* 2012). Microbial diversity was assessed via pyrosequencing of the V1–V3 region of the bacterial 16S rRNA gene (Dowd *et al.,* 2008).

Metatranscriptomic analyses

Sequences were filtered of rRNA sequences using BLASTN (cutoff bit score = 50) against a custom database of rRNA sequences derived from the SILVA LSU and SSU databases and microbial genomes (Pruesse *et al.,* 2007). Non-rRNA reads were further filtered for potentially artifactual duplicate sequences (reads of equal length sharing 100% sequence identity) using custom scripts as in the study of Gomez-Alvarez *et al.* (2009). The remaining reads were annotated using BLASTX against the NCBI nr database (as of 28 April 2011; bit score cutoff = 50). BLASTX results were examined for taxonomic representation, gene content, and functional pathways in MEGAN4 (Huson *et al.,* 2011).

Given the representation of both host and symbiont sequences in the libraries, we analyzed reads annotated as eukaryotic or bacterial separately. Each sample's eukaryotic and bacterial transcriptomes were normalized to the total number of non-rRNA reads assigned to their respective taxonomic division in MEGAN. Reads not assigned a division-level taxonomic identification were excluded from further analysis.

To validate the results from MEGAN, we submitted our entire raw transcriptomic data set and, separately, the fraction of non-rRNA reads identified as bacterial in origin to MG-RAST (Meyer *et al.,*

Table 2 Metatranscriptome sequence characteristics

	Kilo Moana	*Tow Cam*	*ABE*	*Tu'i Malila*
Total reads	199 679	165 105	182 311	171 587
rRNA reads	102 675	83 436	67 669	135 141
Non-rRNA reads	97 004	81 669	114 642	36 446
Taxon-assigned proteins	35 497	35 763	48 666	17 408
% Eukaryotic (MG-RAST accn.)	71% (4492532.3)	60% (4492531.3)	58% (4492530.3)	37% (4492529.3)
% Bacterial (MG-RAST accn.)	27% (4491348.3)	38% (4491346.3)	39% (4491347.3)	59% (4491344.3)
% γ-1[a] (16S)	0/0%	0/0%	87/98%	33/48%
% γ-Lau[a] (16S)	0/0%	0/0%	0/0%	59/51%
% ε[a] (16S)	84/100%	98/100%	0/2%	0/1%

[a]Proportion of symbiont 16S rRNA gene copies in ISMASH DNA as determined via 454 pyrosequencing/quantitative PCR.

2008). There was broad agreement between results derived from MEGAN and those from MG-RAST. Unless otherwise specified, all described results are derived from manual searches of the bacterial data sets with SEED/Subsystems annotations in MG-RAST (e-value $= 10^{-4}$). All eight datasets are now publicly available on MG-RAST (Table 2).

Bacterial 16S rRNA gene diversity from amplicon pyrosequencing was assessed in QIIME v1.4.0 (Caporaso *et al.,* 2010). Raw pyrosequencing flowgrams were denoised using the QIIME Denoiser (Reeder and Knight, 2010), then sequences were filtered for chimeras using the *de novo* implementation of the UCHIME chimera checker (Edgar *et al.,* 2011). Sequences were then clustered at 97% identity using UCLUST (Edgar, 2010), and the resulting operational taxonomic units were analyzed using the default QIIME pipeline.

Results and discussion

Transcriptome characteristics and taxonomic composition

The ISMASH was highly effective at preserving RNA *in situ*. Assessments of extracted RNA showed good preservation, with clearly defined eukaryotic and prokaryotic rRNA peaks (Supplementary Figure S2). Rapid *in situ* homogenization likely facilitated the penetration of preservative throughout the tissues of these large-shelled organisms. More importantly, *in situ* homogenization arrests metabolism and alleviates concerns about transcriptional changes that might arise if specimens are simply submerged in a preservative *in situ*, or are recovered in seawater and preserved on board ship.

Between 160 000 and 200 000 metatranscriptomic reads were recovered from each sample (Table 2). Of these, 37–79% matched the rRNA database. Between 10–27% of the total reads (17 000 and 49 000) matched to protein-coding genes in the NCBI nr database. In total, we recovered between 9450 and 18 915 putatively bacterial and between 6434 and 28 412 putatively eukaryotic protein-coding transcripts per sample. Approximately 50–60% of transcripts identified as bacterial in origin were successfully assigned a functional annotation, compared with just 12–13% of eukaryotic transcripts. Consistent with our objective of examining symbiont gene expression, subsequent analyses focused solely on genes of bacterial origin. Expression data presented hereafter are normalized to the total number of protein-coding transcripts assigned to bacteria in each sample, and scaled to represent a 10 000 read library.

Host genotyping and assessment of the symbiont compositions from DNA extracts demonstrated that the distribution of sampled holobionts along the spreading center—as well as the observed specificity among host and symbiont types—was concordant with previous results (Beinart *et al.,* 2012). Partial *Alviniconcha* mitochondrial cytochrome oxidase I gene sequences showed that all four sampled snails had $\geqslant$99% identity to genotypes previously described from the ELSC (Table 1). Taxonomic assignment of bacterial 16S rRNA genes amplified from DNA extracts revealed that 84–98% of bacteria in each sample matched *Alviniconcha* symbiont reference sequences, with the most abundant operational taxonomic units in each sample matching reference sequences at 99–100% identity (Table 2). ε-proteobacterial symbionts dominated the host type II samples from the two northern fields (Kilo Moana and Tow Cam), and γ-proteobacterial symbionts dominated the host type I and type III samples from the two southern fields (ABE and Tu'i Malila, respectively). Though three of the four samples were dominated by a single symbiont phylotype, the Tu'i Malila sample appeared to simultaneously host both γ-1 and γ-Lau phylotypes (Table 2).

To help confirm that the overall taxonomic composition of the data set was reflected in key metabolic pathways, taxonomic assignments for genes involved in sulfur metabolism, hydrogen oxidation, and nitrogen metabolism were manually reviewed in MEGAN (Supplementary Table S1). Despite the uncertainties associated with taxonomy assignment to individual short reads, there was very little evidence for expression of ε-proteobacterial transcripts in γ-dominated samples, or *vice versa*.

Sulfur metabolism

Sulfur oxidation genes were well represented in all metatranscriptomes, constituting 2–3% of the total bacterial transcripts in each sample (Figure 2, Supplementary Table S1). The γ-dominated samples showed expression of sulfur oxidation genes and pathways typical of chemoautotrophic γ-proteobacteria (Figure 3, Supplementary Table S1). From both γ-dominated samples, we recovered transcripts from the core periplasmic Sox genes, *soxXYZ*, though not the *soxCD* genes. The Sox complex without SoxCD is utilized for the incomplete

oxidation of sulfide or thiosulfate, resulting in the deposition of periplasmic elemental sulfur granules (Grimm *et al.,* 2008; Ghosh and Dam, 2009). The γ-dominated metatranscriptomes also contained transcripts for sulfide:quinone (oxido)reductases (Sqr) and sulfide dehydrogenases (Fcc), which

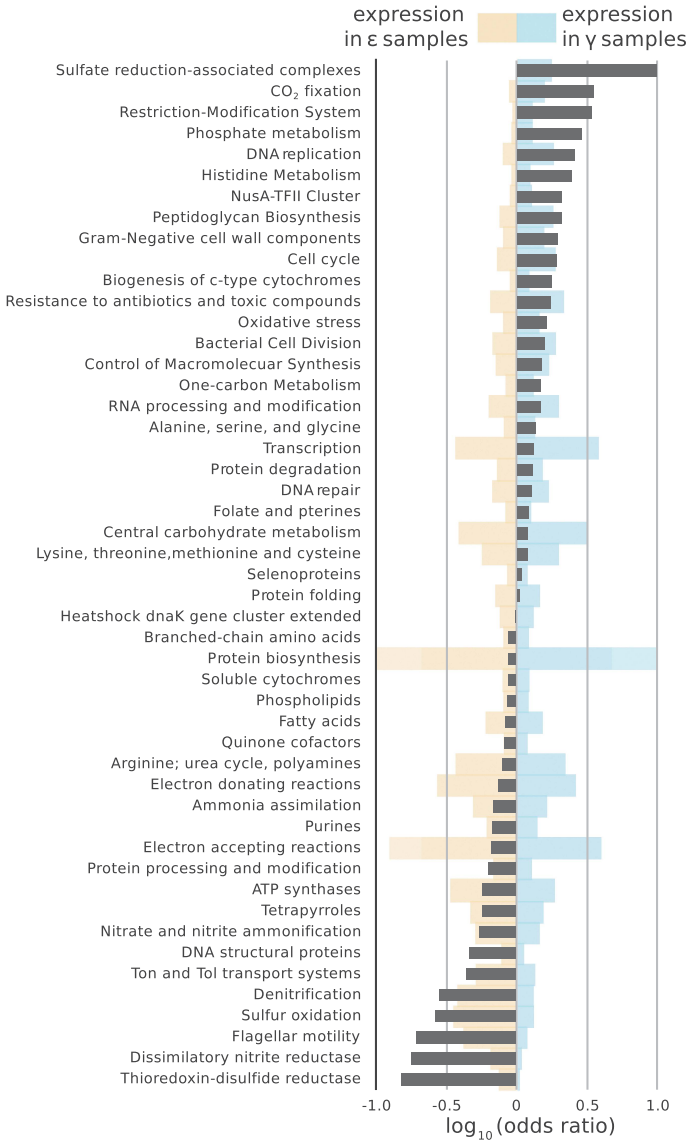

Figure 2 Summarized differences in expression of the most abundant categories of symbiont genes. Only gene categories with membership comprising >0.5% of the total data set are represented. Blue- and yellow-shaded bars indicate relative levels of expression in γ- or ε-dominated metatranscriptomes, respectively, on a linear scale. Dark gray bars indicate the base-10 logarithm of the odds ratio ((Gγ/Tγ)/(Gε/Tε), where G = no. reads in that category and T = total no. of reads). Positive log (odds ratios) indicate genes more likely to be expressed in γ-dominated metatranscriptomes ('Protein biosynthesis' abundance and 'Sulfate reduction' log ratio bars exceed the axis limits in the figure at the scale presented). Genes are summarized by the Level 2 of the SEED Subsystems ontology as annotated in MEGAN4.

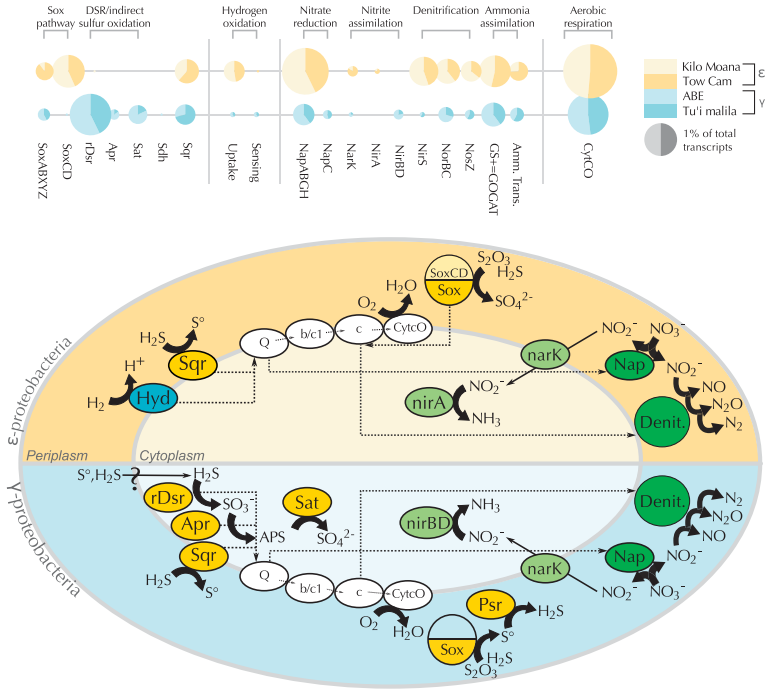

Figure 3 Energy metabolism pathways and levels of expression in γ- and ε-dominated metatranscriptomes. (**a**) Relative abundance of genes involved in sulfur oxidation, hydrogen oxidation, nitrogen reduction and assimilation, and aerobic respiration. Circle area reflects total normalized expression for each gene category for γ- or ε-dominated metatranscriptomes, respectively. Circles are divided according to relative contribution of each individual sample. ε-dominated metatranscriptomes are shaded yellow, while γ-dominated metatranscriptomes are shaded blue. (**b**) Energy metabolism models for γ- and ε-proteobacterial symbionts represented in a stylized cell. The upper, yellow half shows the model for ε-symbionts, while the blue lower half shows the model for γ-symbionts. Proteins and complexes are colored by metabolic category: yellow = sulfur metabolism; white = aerobic respiration; green = nitrogen metabolism; blue = hydrogen oxidation. Arrows show general direction of electron flux. Sox, Sox multienzyme complex; rDsr, reverse dissimilatory sulfur reduction pathway; Apr, adenylylsulfate reductase; Sat, sulfur adenylyltransferase; Sdh, sulfite dehydrogenase; Sqr, sulfide quinone (oxido)reductase; Psr, polysulfide reductase; Hyd, hydrogenase; Nap, periplasmic nitrate reductase; NarK, nitrate/nitrite transporter; NirA, ferredoxin-dependent nitrite reductase; NirBD, NADH-dependent siroheme nitrite reductase; NirS, membrane-bound respiratory nitrite reductase; Nor, nitric oxide reductase; Nos, nitrous oxide reductase; GS + GOGAT, glutamine synthetase + glutamate synthase; Amm. Trans., ammonium transporter; Q, quinone; b/c1, cytochrome bc1; c, cytochrome *c*; CytCO, cytochrome *c* oxidase.

oxidize sulfide to elemental sulfur in the periplasm (Frigaard and Dahl, 2008; Ghosh and Dam, 2009). Consistent with the expression of these genes and pathways, we frequently observe elemental sulfur granules in the gills of *Alviniconcha* hosting γ-proteobacteria. The further oxidation of this elemental sulfur to sulfate is thought to involve additional pathways (Ghosh and Dam, 2009), such as reverse dissimilatory sulfate reduction (rDSR). Indeed, the DSR genes *dsrABCEFJKMLOPS* were highly expressed in both γ-dominated samples, with *dsrFHR* genes present in at least one γ-dominated sample (*dsrEFHR* abundances determined via MG-RAST IMG annotation). The presence of *dsrEFH* transcripts indicates use of this pathway for the oxidation of reduced sulfur species. Here, the reverse DSR pathway is likely coupled to sulfite oxidation via an indirect pathway involving APS reductase and sulfate adenylyltransferase, both of which were identified in the γ-dominated metatranscriptomes.

Notably, the expression of an incomplete Sox complex along with reverse DSR and indirect sulfite oxidation pathways is common among γ-proteobacterial chemosynthetic endosymbionts (Harada *et al.,* 2009; Markert *et al.,* 2011; Stewart *et al.,* 2011). We detected transcripts from both pathways in the metatranscriptome derived from a snail dominated by the γ-1 phylotype, suggesting that both pathways are present and being expressed in this symbiont. However, as the other metatranscriptome was derived from a mixed symbiont community of two γ-proteobacterial phylotypes, we cannot say whether these pathways are expressed by one or both of the γ-proteobacterial symbionts.

In contrast to the γ-dominated metatranscriptomes, the ε-dominated metatranscriptomes from

the northern two vent fields lacked reverse DSR transcripts, but were replete with complete Sox–multienzyme complex and Sqr transcripts (Figure 3, Supplementary Table S1). The full Sox–multienzyme complex is employed by ε-proteobacteria for the complete oxidation of sulfide, thiosulfate, and/or elemental sulfur (Yamamoto and Takai, 2011). Additionally, we detected high expression of *sqr* genes, despite the fact that the ε-proteobacterial symbiont, like its free-living relatives from the genus *Sulfurimonas*, has not been observed to form visible sulfur granules (Sievert *et al.,* 2008). Many ε-proteobacterial genomes encode genes for Sqr in addition to the Sox complex, though the role of Sqr in sulfur oxidation and its relationship to the Sox pathway is still uncertain in these symbionts and other ε-proteobacteria.

Hydrogen metabolism

Previous work has shown that *Alviniconcha* hosting ε-proteobacterial symbionts dominate at the northern vent fields, where hydrogen concentrations are highest, suggesting that hydrogen might serve as an electron donor for these symbionts (Beinart *et al.,* 2012). The metatranscriptomes from the two ε-dominated, northernmost samples revealed the potential for respiratory hydrogen oxidation, with both samples expressing genes allied to Group 1 NiFe-hydrogenases (~0.5% of all transcripts, Figure 3 and Supplementary Table S1). This group of enzymes, often called uptake hydrogenases, are membrane-bound, respiratory enzymes that oxidize hydrogen and donate electrons to the quinone pool (Vignais and Billoud, 2007). Hydrogen oxidation transcripts for Group 1 NiFe-hydrogenases were also recovered—though with much lower representation—from the γ-dominated metatranscriptomes (Figure 3).

The presence of hydrogenase transcripts in all four of the *Alviniconcha* metatranscriptomes indicates that hydrogen could be an electron donor in both the γ- and ε-proteobacterial symbionts of *Alviniconcha*. However, the difference in expression of hydrogenases between the ε- and the γ-dominated individuals suggests that hydrogen oxidation potentially has a larger role in the energy metabolism of the holobionts with ε-proteobacteria (Figure 3, Supplementary Table S1). Phylogenetic analysis of the *Alviniconcha* ε-proteobacterial endosymbionts from the ELSC shows that they are closely allied to members of the genus *Sulfurimonas* (Beinart *et al.,* 2012), many of which are able to utilize both hydrogen and reduced sulfur compounds as electron donors (Nakagawa *et al.,* 2005). A recent study employed a suite of molecular, physiological, and geochemical approaches to show that vent mussels with γ-proteobacterial symbionts can oxidize hydrogen to support carbon fixation (Petersen *et al.,* 2011). Future studies will use similar approaches to elucidate the degree to which these *Alviniconcha* ε-proteobacterial endosymbionts rely on hydrogen for energy production.

Carbon fixation

Transcript representation and abundances revealed clear differences in carbon fixation pathways between γ- and ε-dominated individuals (Figure 4, Supplementary Table S1). Key genes of the Calvin-Benson-Bassham cycle, including those encoding Form II Ribulose-1,5-bisphosphate carboxylase/oxygenase and phosphoribulokinase, were enriched in γ-dominated metatranscriptomes. In contrast, the three key genes associated with the reductive tricarboxylic acid (rTCA) cycle (ATP citrate lyase, 2-oxoglutarate oxidoreductase, and fumarate reductase) were found only in snails hosting ε-proteobacteria.

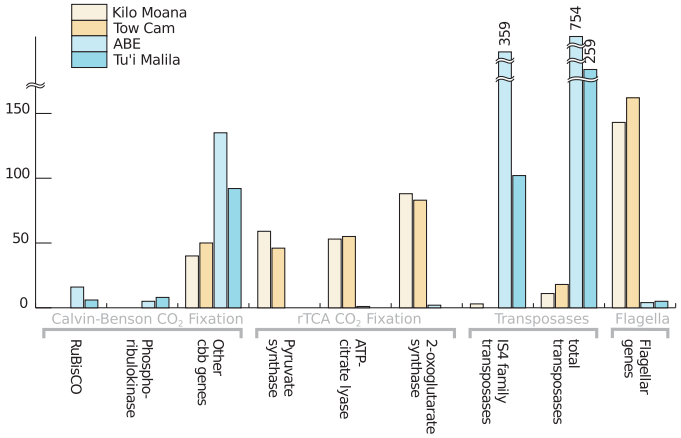

Figure 4 Summarized differences in expression of genes involved in carbon fixation, transposase and flagellar genes. Transcript abundance is normalized to 10 000 per sample.

These patterns are consistent with previous studies of carbon fixation in both free-living and symbiotic chemoautotrophs of these two major bacterial groups (Hugler *et al.,* 2005; Takai *et al.,* 2005; Woyke *et al.,* 2006; Nakagawa and Takai, 2008; Sievert *et al.,* 2008; Hügler *et al.,* 2011). Both the Calvin-Benson-Bassham cycle with Form II Ribulose-1,5-bisphosphate carboxylase/oxygenase and the reductive tricarboxylic acid cycle are typically associated with autotrophs from low-oxygen environments (Berg, 2011), suggesting that the symbionts of *Alviniconcha* are experiencing such conditions. This may be due to low environmental oxygen concentrations around *Alviniconcha* or limited provisioning to the symbionts by the snails' oxygen-binding proteins hemocyanin and hemoglobin (Wittenberg and Stein, 1995).

Nitrogen metabolism

All organisms need nitrogen for growth and biosynthesis, requiring the assimilation of an exogenous source of nitrogen. At vents, dissolved organic nitrogen (for example, free amino acids) is quite low (Johnson *et al.,* 1986), while inorganic nitrogen compounds are typically abundant. Some vent fluids contain nM to μM concentrations of dissolved ammonium, which is easily assimilated by many organisms. However, there are no data on ammonium concentrations at the ELSC (Tivey, 2007). Nitrate, however, is typically very abundant in seawater surrounding vents (occurring at ~40 μM; Johnson *et al.,* 1986).

Nitrate can be used both as a primary nitrogen source for biosynthesis and growth and as a respiratory terminal electron acceptor. Assimilatory nitrate reduction canonically utilizes the cytoplasmic nitrate reductase Nas. Dissimilatory nitrate reduction (DNR) frequently utilizes the membrane-bound respiratory nitrate reductase Nar, but in some bacteria may also be catalyzed via a periplasmic–enzyme complex (Nap) (Potter *et al.,* 2001). The nitrite generated by DNR may be further reduced to ammonia via dissimilatory nitrate reduction to ammonia (DNRA), which may then be utilized for biosynthesis (though Nap has not typically been associated with nitrate assimilation, Berks, 1995). In both assimilatory nitrate reduction and DNRA, the resulting ammonium is typically assimilated by the glutamine synthetase-glutamate synthase or glutamate dehydrogenase pathways (Reitzer, 2003).

In all of the metatranscriptomes, we found the expression of some genes typically associated with both assimilatory and dissimilatory nitrate reduction, as well as for ammonium assimilation. Curiously, though, we did not find evidence for complete expression of any of the canonical pathways. Instead, periplasmic nitrate reductase (Nap) appeared to catalyze nitrate reduction as the first step for both assimilation and respiration.

Genes involved in ammonium assimilation comprised a substantial portion of all metatranscriptomes, indicating that all *Alviniconcha* symbionts were poised to assimilate ammonium either from the reduction of nitrate or from the environment (Figure 3, Supplementary Table S1). Both ε- and γ-proteobacterial symbionts showed substantial expression of glutamine synthetase-glutamate synthase and ammonium transporters. As mentioned above, all symbionts were poised for nitrate reduction in the periplasm via the Nap complex. We did not detect the periplasmic nitrite reductase Nrf, which is typically the next step in Nap-catalyzed DNRA (Potter *et al.,* 1999). However, both γ- and ε-dominated transcriptomes showed expression of the narK nitrite/nitrate transporter and cytoplasmic ammonifying nitrite reductases, representing a potential mechanism for assimilation of periplasmically-reduced nitrate via the shuttling of nitrite into the cytoplasm and subsequent reduction to ammonium and assimilation by glutamine synthetase-glutamate synthase (Figure 3, Supplementary Table S1). This model represents an alternative to the typical pathway for DNRA.

The substantial expression of genes involved in respiratory denitrification suggests another possible fate for periplasmic nitrite (Figure 3, Supplementary Table S1), raising the possibility that *Alviniconcha* symbionts may be utilizing nitrate as an alternative electron acceptor to oxygen, potentially reducing competition for oxygen with the host (Hentschel and Felbeck, 1993; Hentschel *et al.,* 1996). Though we did not detect transcripts for the canonical dissimilatory nitrate reductase Nar, in other bacteria, Nap has been shown to catalyze the first step in aerobic denitrification, as the presence of oxygen inhibits activity of Nar (Potter *et al.,* 2001). We posit that Nap has a similar role in *Alviniconcha* symbionts. All of our samples contained transcripts for the rest of the denitrification pathway, including periplasmic respiratory cytochrome cd1 nitrite reductase NirS, the nitric oxide–reductase complex Nor, and the nitrous oxide–reductase complex Nos. Denitrification genes were more abundantly and consistently expressed in the ε-dominated transcriptomes, where they constituted around 2% of all reads. These genes were less abundant (0.3% of reads) in the γ-proteobacterial metatranscriptomes. Notably, NirS, which serves the reduction of nitrite to nitric oxide, and thus may serve to commit nitrite to a dissimilatory pathway, was ~50-fold more abundant in the ε-dominated samples (Figure 3).

Functionally, this assemblage of assimilatory and dissimilatory genes may represent a strategy well suited for life around hydrothermal vents, where fluid mixing leads to ammonium concentrations that are inversely correlated with availability of oxygen as a terminal electron acceptor. The model outlined in Figure 3 would permit purely respiratory reduction of nitrate in holobionts exposed to oxygen-poor and ammonium-rich vent fluid. Conversely, holobionts in more aerobic conditions, with less access to ammonium, could decrease complete denitrification to dinitrogen in favor of assimilating

nitrate to meet the needs of biosynthesis. Under this hypothesis, the expression differences we observed between γ- and ε-dominated metatranscriptomes would suggest that these symbionts were engaged primarily in either nitrogen assimilation or denitrification in response to variations in water chemistry in their respective habitats.

Despite differences in expression, the complement of nitrogen genes was remarkably consistent between ε- and γ-dominated metatranscriptomes. The similarities in nitrogen gene content were especially striking in light of the large differences we observed in sulfur and carbon pathways. Where the latter differences were typical of pathways found in free-living members of their respective proteobacterial classes, the combination of nitrogen-related genes we observed in both classes of *Alviniconcha* symbionts was fairly unusual, but could potentially catalyze functionally identical pathways in both classes of symbiont. At hydrothermal vents, the capacity to use nitrate for both biosynthesis and respiration is widespread among ε-proteobacteria (Sievert and Vetriani, 2012), including the free-living relatives of *Alviniconcha* ε-proteobacterial symbionts, *Sulfurimonas* (Takai *et al.,* 2006; Sievert *et al.*, 2008; Sikorski *et al.,* 2010). Nitrate respiration is less common among free-living vent γ-proteobacteria (Sievert and Vetriani, 2012), though, curiously, patterns of nitrogen gene expression similar to the *Alviniconcha* symbionts have been observed in other γ-proteobacterial symbionts, such as those associated with vent tubeworms (Markert *et al.,* 2011; Robidart *et al.,* 2011). Although this model remains to be validated, such functional convergence may reflect similar selective pressures imposed by life in this environment, as well as the symbiotic lifestyle.

Flagellar genes

Flagellar genes showed striking differences in expression between ε- and γ-proteobacterial metatranscriptomes (Figure 4, Supplementary Table S1), hinting at potential differences in host–symbiont interactions. The ε-dominated samples expressed transcripts for at least 30 flagellum-related genes, including flagellins *flaAB* and transcripts associated with the flagellar hook, ring, motor, basal body, and biosynthesis (Supplementary Table S1). Only 10 flagellum-related genes were recovered from γ-dominated metatranscriptomes and, in aggregate, were ~20-fold lower in abundance. While the diversity of roles that flagellar genes have in other symbiotic bacteria complicates interpretation (Anderson *et al.,* 2010), we propose three hypotheses that might explain the observed differences in expression.

First, if flagella are used primarily for motility, their abundant expression in mature-host associations may signal differences in symbiont motility and transmission dynamics between the ε- and γ-proteobacterial symbionts. *Riftia* tubeworm symbionts, while possessing a large number of genes related to motility and chemotaxis, do not appear to possess flagella while inhabiting the host trophosome (Harmer *et al.,* 2008; Robidart *et al.,* 2008). Instead, they may utilize flagella during horizontal transmission (Harmer *et al.,* 2008), when flagellar motility could be important in escaping from parental host tissue and/or chemotaxis towards a new host. Here, the abundant flagellar gene expression in ε-symbionts could indicate that they are actively transmitted throughout the lifetime of the host. The lower expression observed in the γ-hosting snails might in turn reflect either a different transmission strategy or, potentially, temporal differences in symbiont transmission.

Second, flagellar proteins are commonly used in host recognition and attachment. It is plausible that the expression of flagellar genes in ε-dominated metatranscriptomes relates to host recognition (that is, specificity). Flagellar proteins are critical to symbiont recognition and colonization in other systems: for example, the *Euprymna-Vibrio* symbioses (Nyholm *et al.,* 2000; Millikan and Ruby, 2004), another highly specific, horizontally transmitted marine symbiosis. A previous study found that one *Alviniconcha* host type nearly always hosted solely ε-proteobacterial symbionts, while others hosted mixed populations of the two γ-proteobacterial symbiont lineages and, occasionally, the ε-proteobacterial symbionts (Beinart *et al.,* 2012). The expression of flagellin in ε-proteobacterial symbionts may contribute to this specificity.

Finally, flagellar genes may also mediate nutritional export from symbiont to host. Ring- and hook-associated flagellar proteins have been shown to have an important secretory role in the intracellular symbionts of aphids (Maezawa *et al.,* 2006; Toft and Fares, 2008), though they have lost genes for the flagellin tail proteins, which were abundantly expressed in our ε-dominated samples. In *Alviniconcha*, the mode of nutrient transfer in γ-hosting individuals may predominantly be via digestion of symbiont cells, as is thought to be the case for γ-proteobacterial symbionts of other vent animals (Lee *et al.,* 1999). In contrast, translocation of small organic compounds from symbiont to host may have a bigger role in *Alviniconcha* hosting ε-proteobacteria. Compound-specific isotopic observations made by Suzuki *et al*. (2005) suggest as much, demonstrating that symbiont-associated fatty acids are detected in non-symbiotic host tissues of γ-, but not ε-hosting *Alviniconcha.*

Transposons

Another surprising difference between symbiont types was the increased abundance of transposases in the γ-dominated metatranscriptomes, where predicted transposases accounted for 3–7% of all bacterial transcripts via IMG in MG-RAST (SEED called around 2–5% of the transcripts transposons). Predicted transposases were present

in the ε-dominated samples, but were much lower in abundance and matched largely to different transposase families (Figure 4, Supplementary Table S1). The presence of transposons in the genomes of other chemoautotrophic symbionts is variable: they are undetected in the genomes of the vertically-transmitted endosymbiont of vent clams (Kuwahara *et al.,* 2007; Newton *et al.,* 2007), while those of the horizontally transmitted vent tubeworm endosymbionts contain at least one (Robidart *et al.,* 2008; Gardebrecht *et al.,* 2012), and nearly 20% of an endosymbiont genome from the oligochaete *Olavius algarvensis* is composed of transposable elements (Woyke *et al.,* 2006).

Moran and Plague (2004) have proposed that the proliferation of mobile genetic elements occurs early during the transition to an obligate intracellular lifestyle, as genetic bottlenecks during transmission decrease the effective population size of the symbionts, leading to decreased strength of selection. Combined with the lack of a free-living life stage, this is thought to relax purifying selection on the symbiont genome. Although conflicting with the current hypothesis that both γ-proteobacterial and ε-proteobacterial symbionts are transmitted via the environment, the dramatic differences in transposase expression observed among these metatranscriptomes hints at the possibility that these two distinct symbiont–host associations either represent different stages of evolutionary development, or exhibit differing transmission modes. When taken in conjunction with the corresponding differences in flagellar gene expression, these data raise the hypothesis that ε-proteobacterial symbionts in *Alviniconcha*, relative to the γ-proteobacterial symbionts, experience more frequent dispersal and fewer genetic bottlenecks.

Conclusions

Our results reveal that *Alviniconcha* symbionts exhibited marked differences in gene expression related to energy metabolism. The predominance of both hydrogen oxidation and DNR genes in the ε-dominated metatranscriptomes would suggest that these holobionts live in more highly reduced and potentially less oxygen-rich fluids. This is consistent with the previously observed patterns of distribution across a regional gradient, wherein ε-hosting *Alviniconcha* were most abundant in the more sulfidic, hydrogen-rich fluids found at the northern vent fields (Beinart *et al.,* 2012). Though these differences in expression do not necessarily imply differences in metabolic capability (this is better addressed via genomic sequencing of each symbiont type), their striking correlation with holobiont biogeography supports the hypothesis that symbiont physiology has an important role in habitat partitioning among the host types in this genus.

Unexpectedly, the observed differences in flagellar genes and transposons between ε- and γ-dominated metatranscriptomes hint at differences in symbiont life histories, potentially related to the dynamics of association between host and symbiont, including mode of transmission and nutrient exchange. Though other chemoautotrophic symbioses have been described with widely varying specificities and transmission mechanisms (reviewed in Dubilier *et al.,* 2008), *Alviniconcha* is thus far unique in that close relatives *within* the genus host unrelated symbionts, each with apparently variable degrees of specificity (Beinart *et al.,* 2012).

The data presented here illustrate the value of using *in situ* preservation and shore-based transcriptomics to examine symbiont physiological poise. This technology and methodology allowed us to test *a priori* hypotheses as well as to identify previously unrecognized differences among these symbionts. Future studies should employ such approaches when studying both host and symbiont gene expression within and among different geochemical habitats to better understand the complex relationships among symbionts, their hosts, and the environment.

Acknowledgements

This material is based upon work supported by the National Science Foundation (OCE-0732369 to PRG and GRF grant no. DGE-1144152 to JGS and RAB), as well as Moore Foundation Investigator and Agouron Institute grants to EFD. We thank the crews of the RV Thomas G Thompson and the ROV JASON II, C DiPerna and P Meneses for assisting with the design and building of the ISMASH and J Dang for assistance with sample processing. We also thank J Bryant, R Barry and T Palden for their help in complementary DNA preparation and pyrosequencing and J Delaney, C Cavanaugh, A Knoll and C Marx for their helpful comments and editing that improved this article.

References

Anderson JK, Smith TG, Hoover TR. (2010). Sense and sensibility: flagellum-mediated gene regulation. *Trends Microbiol* **18**: 30–37.

Beinart RA, Sanders JG, Faure B, Sylva SP, Lee RW, Becker EL *et al.* (2012). Evidence for the role of endosymbionts in regional-scale habitat partitioning by hydrothermal vent symbioses. *Proc Natl Acad Sci USA* **109**: E3241–E3250.

Berg I. (2011). Ecological aspects of the distribution of different autotrophic CO_2 fixation pathways. *Appl Environ Microbiol* **77**: 1925–1936.

Berks B. (1995). Enzymes and associated electron transport systems that catalyse the respiratory reduction of nitrogen oxides and oxyanions. *Biochim Biophys Acta* **1232**: 97–173.

Caporaso JG, Kuczynski J, Stombaugh J, Bittinger K, Bushman FD, Costello EK *et al.* (2010). QIIME allows

analysis of high-throughput community sequencing data. *Nat Meth* **7**: 335–336.

Childress JJ, Fisher CR, Brooks JM, Kennicutt MC, Bidigare R, Anderson AE. (1986). A methanotrophic marine molluscan (bivalvia, mytilidae) symbiosis: mussels fueled by gas. *Science* **233**: 1306–1308.

Childress JJ, Fisher CR, Favuzzi JA, Sanders NK. (1991). Sulfide and carbon dioxide uptake by the hydrothermal vent clam, *Calyptogena magnifica*, and its chemoautotrophic symbionts. *Physiol Zool* **64**: 1444–1470.

Childress JJ, Girguis PR. (2011). The metabolic demands of endosymbiotic chemoautotrophic metabolism on host physiological capacities. *J Exp Biol* **214**: 312–325.

Dowd S, Callaway T, Wolcott R, Sun Y, McKeehan T, Hagevoort R *et al.* (2008). Evaluation of the bacterial diversity in the feces of cattle using 16S rDNA bacterial tag-encoded FLX amplicon pyrosequencing (bTEFAP). *BMC Microbiol* **8**: 125.

Dubilier N, Bergin C, Lott C. (2008). Symbiotic diversity in marine animals: the art of harnessing chemosynthesis. *Nat Rev Micro* **6**: 725–740.

Edgar RC. (2010). Search and clustering orders of magnitude faster than BLAST. *Bioinformatics* **26**: 2460–2461.

Edgar RC, Haas BJ, Clemente JC, Quince C, Knight R. (2011). UCHIME improves sensitivity and speed of chimera detection. *Bioinformatics* **27**: 2194–2200.

Felbeck H. (1981). Chemoautotrophic potential of the hydrothermal vent tube worm, *Riftia pachyptila* jones (Vestimentifera). *Science* **213**: 336–338.

Fisher CR, Childress JJ. (1984). *Substrate Oxidation by Trophosome Tissue from Riftia pachyptila Jones (Phylum pogonophora* vol. 5. Elsevier: Amsterdam, PAYS-BAS.

Frigaard N-U, Dahl C. (2009). Sulfur Metabolism in phototrophic sulfur bacteria. *Adv Microb Physiol* **54**: 103–200.

Gardebrecht A, Markert S, Sievert SM, Felbeck H, Thurmer A, Albrecht D *et al.* (2012). Physiological homogeneity among the endosymbionts of *Riftia pachyptila* and *Tevnia jerichonana* revealed by proteogenomics. *ISME J* **6**: 766–776.

Ghosh W, Dam B. (2009). Biochemistry and molecular biology of lithotrophic sulfur oxidation by taxonomically and ecologically diverse bacteria and archaea. *FEMS Microbiol Rev* **33**: 999–1043.

Girguis PR, Childress JJ. (2006). Metabolite uptake, stoichiometry and chemoautotrophic function of the hydrothermal vent tubeworm *Riftia pachyptila*: responses to environmental variations in substrate concentrations and temperature. *J Exp Biol* **209**: 3516–3528.

Gomez-Alvarez V, Teal TK, Schmidt TM. (2009). Systematic artifacts in metagenomes from complex microbial communities. *ISME J* **3**: 1314–1317.

Gracey AY. (2007). Interpreting physiological responses to environmental change through gene expression profiling. *J Exp Biol* **210**: 1584–1592.

Gracey AY, Chaney ML, Boomhower JP, Tyburczy WR, Connor K, Somero GN. (2008). Rhythms of gene expression in a fluctuating intertidal environment. *Curr Biol* **18**: 1501–1507.

Grimm F, Franz B, Dahl C. (2008). *Thiosulfate and Sulfur Oxidation in Purple Sulfur Bacteria Microbial Sulfur Metabolism* In: Dahl C, Friedrich CG (eds).Springer: Berlin Heidelberg, pp 101–116.

Harada M, Yoshida T, Kuwahara H, Shimamura S, Takaki Y, Kato C *et al.* (2009). Expression of genes for sulfur oxidation in the intracellular chemoautotrophic symbiont of the deep-sea bivalve *Calyptogena okutanii*. *Extremophiles* **13**: 895–903.

Harmer TL, Rotjan RD, Nussbaumer AD, Bright M, Ng AW, DeChaine EG *et al.* (2008). Free-living tube worm endosymbionts found at deep-sea vents. *Appl Environ Microbiol* **74**: 3895–3898.

Hentschel U, Felbeck H. (1993). Nitrate respiration in the hydrothermal vent tubeworm *Riftia pachyptila*. *Nature* **366**: 338–340.

Hentschel U, Hand S, Felbeck H. (1996). The contribution of nitrate respiration to the energy budget of the symbiont-containing clam *Lucinoma aequizonata*: a calorimetric study. *J Exp Biol* **199**: 427–433.

Hugler M, Wirsen CO, Fuchs G, Taylor CD, Sievert SM. (2005). Evideince for autotrophic CO2 fixation via the reductive tricarboxylic acid cycle by members of the epsilon subdivision of Proteobacteria. *J Bacteriol* **187**: 3020–3027.

Huson DH, Mitra S, Ruscheweyh H-J, Weber N, Schuster SC. (2011). Integrative analysis of environmental sequences using MEGAN4. *Genome Res* **21**: 1552–1560.

Hügler M, Petersen JM, Dubilier N, Imhoff JF, Sievert SM. (2011). Pathways of carbon and energy metabolism of the epibiotic community associated with the deep-sea hydrothermal vent shrimp *Rimicaris exoculata*. *PLoS One* **6**: e16018.

Johnson KS, Beehler CL, Sakamoto-Arnold CM, Childress JJ. (1986). *In situ* measurements of chemical distributions in a deep-sea hydrothermal vent field. *Science* **231**: 1139–1141.

Kuwahara H, Yoshida T, Takaki Y, Shimamura S, Nishi S, Harada M *et al.* (2007). Reduced genome of the thioautotrophic intracellular symbiont in a deep-sea clam, *Calyptogena okutanii*. *Curr Biol* **17**: 881–886.

Lee RW, Robinson JJ, Cavanaugh CM. (1999). Pathways of inorganic nitrogen assimilation in chemoautotrophic bacteria-marine invertebrate symbioses: expression of host and symbiont glutamine synthetase. *J Exp Biol* **202**: 289–300.

Maezawa K, Shigenobu S, Taniguchi H, Kubo T, Aizawa S-i, Morioka M. (2006). Hundreds of flagellar basal bodies cover the cell surface of the endosymbiotic bacterium *Buchnera aphidicola* sp. strain APS. *J Bacteriol* **188**: 6539–6543.

Markert S, Gardebrecht A, Felbeck H, Sievert SM, Klose J, Becher D *et al.* (2011). Status quo in physiological proteomics of the uncultured *Riftia pachyptila* endosymbiont. *Proteomics* **11**: 3106–3117.

Meyer F, Paarmann D, D'Souza M, Olson R, Glass E, Kubal M *et al.* (2008). The metagenomics RAST server—a public resource for the automatic phylogenetic and functional analysis of metagenomes. *BMC Bioinformatics* **9**: 386.

Millikan DS, Ruby EG. (2004). *Vibrio fischeri* flagellin A is essential for normal motility and for symbiotic competence during initial squid light organ colonization. *J Bacteriol* **186**: 4315–4325.

Moran NA, Plague GR. (2004). Genomic changes following host restriction in bacteria. *Curr Opin Genet Dev* **14**: 627–633.

Mottl MJ, Seewald JS, Wheat CG, Tivey MK, Michael PJ, Proskurowski G *et al.* (2011). Chemistry of hot springs along the Eastern Lau Spreading Center. *Geochimica Et Cosmochimica Acta* **75**: 1013–1038.

Nakagawa S, Takai K. (2008). Deep-sea vent chemoautotrophs: diversity, biochemistry and ecological significance. *FEMS Microbiol Ecol* **65**: 1–14.
Nakagawa S, Takai K, Inagaki F, Hirayama H, Nunoura T, Horikoshi K *et al.* (2005). Distribution, phylogenetic diversity and physiological characteristics of epsilon-Proteobacteria in a deep-sea hydrothermal field. *Environ Microbiol* **7**: 1619–1632.
Newton ILG, Woyke T, Auchtung TA, Dilly GF, Dutton RJ, Fisher MC *et al.* (2007). The *Calyptogena magnifica* chemoautotrophic symbiont genome. *Science* **315**: 998–1000.
Nyholm SV, Stabb EV, Ruby EG, McFall-Ngai MJ. (2000). Establishment of an animal-bacterial association: Recruiting symbiotic vibrios from the environment. *Proc Natl Acad Sci* **97**: 10231–10235.
Petersen JM, Zielinski FU, Pape T, Seifert R, Moraru C, Amann R *et al.* (2011). Hydrogen is an energy source for hydrothermal vent symbioses. *Nature* **476**: 176–180.
Potter L, Angove H, Richardson D, Cole J. (2001). Nitrate reduction in the periplasm of gram-negative bacteria. *Adv Microb Physiol* **45**: 51–112.
Potter LC, Millington P, Griffiths L, Thomas GH, Cole JA. (1999). Competition between *Escherichia coli* strains expressing either a periplasmic or a membrane-bound nitrate reductase: does Nap confer a selective advantage during nitrate-limited growth? *Biochem J* **344**: 77–84.
Pruesse E, Quast C, Knittel K, Fuchs BM, Ludwig W, Peplies Jr *et al.* (2007). SILVA: a comprehensive online resource for quality checked and aligned ribosomal RNA sequence data compatible with ARB. *Nucleic Acids Res* **35**: 7188–7196.
Reeder J, Knight R. (2010). Rapidly denoising pyrosequencing amplicon reads by exploiting rank-abundance distributions. *Nat Meth* **7**: 668–669.
Reitzer L. (2003). Nitrogen assimilation and global regulation in *Escherichia coli*. *Annu Rev Microbiol* **57**: 155–176.
Robidart JC, Bench SR, Feldman RA, Novoradovsky A, Podell SB, Gaasterland T *et al.* (2008). Metabolic versatility of the *Riftia pachyptila* endosymbiont revealed through metagenomics. *Environ Microbiol* **10**: 727–737.
Robidart JC, Roque A, Song P, Girguis PR. (2011). Linking hydrothermal geochemistry to organismal physiology: physiological versatility in *Riftia pachyptila* from sedimented and basalt-hosted vents. *PLoS One* **6**: e21692.
Sievert SM, Scott KM, Klotz MG, Chain PSG, Hauser LJ, Hemp J *et al.* (2008). Genome of the epsilonproteobacterial chemolithoautotroph *Sulfurimonas denitrificans*. *Appl Environ Microbiol* **74**: 1145–1156.
Sievert SM, Vetriani C. (2012). Chemoautotrophy at deep-sea vents: past, present, and future. *Oceanography* **25**: 218–233.
Sikorski J, Munk C, Lapidus C, Djao ODN, Lucas S, Glavina Del Rio T *et al.* (2010). Complete genome sequence of Sulfurimonas autotrophica type strain (OK10). *Stand Genomic Sci* **3**: 194–202.
Stewart F, Dmytrenko O, DeLong E, Cavanaugh C. (2011). Metatranscriptomic analysis of sulfur oxidation genes in the endosymbiont of *Solemya velum*. *Front Microbiol* **2**: 134.
Stewart FJ, Newton ILG, Cavanaugh CM. (2005). Chemosynthetic endosymbioses: adaptations to oxic-anoxic interfaces. *Trends Microbiol* **13**: 439–448.
Stewart FJ, Ottesen EA, DeLong EF. (2010). Development and quantitative analyses of a universal rRNA-subtraction protocol for microbial metatranscriptomics. *ISME J* **4**: 896–907.
Suzuki Y, Kojima S, Sasaki T, Suzuki M, Utsumi T, Watanabe H *et al.* (2006). Host-symbiont relationships in hydrothermal vent gastropods of the genus *Alviniconcha* from the Southwest Pacific. *Appl Environ Microbiol* **72**: 1388–1393.
Suzuki Y, Sasaki T, Suzuki M, Nogi Y, Miwa T, Takai K *et al.* (2005). Novel chemoautotrophic endosymbiosis between a member of the Epsilonproteobacteria and the hydrothermal-vent gastropod *Alviniconcha* aff. *hessleri* (Gastropoda: Provannidae) from the Indian Ocean. *Appl Environ Microbiol* **71**: 5440–5450.
Takai K, Campbell BJ, Cary SC, Suzuki M, Oida H, Nunoura T *et al.* (2005). Enzymatic and genetic characterization of carbon and energy metabolisms by deep-sea hydrothermal chemolithoautotrophic isolates of epsilonproteobacteria. *Appl Environ Microbiol* **71**: 7310–7320.
Takai K, Suzuki M, Nakagawa S, Miyazaki M, Suzuki Y, Inagaki F *et al.* (2006). Sulfurimonas paralvinellae sp. nov., a novel mesophilic, hydrogen- and sulfur-oxidizing chemolithoautotroph within the Epsilonproteobacteria isolated from a deep-sea hydrothermal vent polychaete nest, reclassification of Thiomicrospira denitrificans as Sulfurimonas denitrificans comb. nov. and emended description of the genus Sulfurimonas. *Int J Syst Evol Micr* **56**: 1725–1733.
Tivey MK. (2007). Generation of seafloor hydrothermal vent fluids and associated mineral deposits. *Oceanography* **20**: 50–65.
Toft C, Fares MA. (2008). The evolution of the flagellar assembly pathway in endosymbiotic bacterial genomes. *Mol Biol Evol* **25**: 2069–2076.
Vignais PM, Billoud B. (2007). Occurrence, classification, and biological function of hydrogenases: an overview. *Chem Rev* **107**: 4206–4272.
Wendeberg A, Zielinski FU, Borowski C, Dubilier N. (2012). Expression patterns of mRNAs for methanotrophy and thiotrophy in symbionts of the hydrothermal vent mussel *Bathymodiolus puteoserpentis*. *ISME J* **6**: 104–112.
Wittenberg JB, Stein JL. (1995). Hemoglobin in the symbiont-harboring gill of the marine gastropod *Alviniconcha hessleri*. *Biol Bull* **188**: 5–7.
Woyke T, Teeling H, Ivanova NN, Huntemann M, Richter M, Gloeckner FO *et al.* (2006). Symbiosis insights through metagenomic analysis of a microbial consortium. *Nature* **443**: 950–955.
Yamamoto M, Takai K. (2011). Sulfur metabolisms in epsilon- and gamma-Proteobacteria in deep-sea hydrothermal fields. *Front Microbiol* **2192.**

Supplementary Information accompanies this paper on The ISME Journal website (http://www.nature.com/ismej)

Chapter 4

The uptake and excretion of partially oxidized sulfur broadens our understanding of the energy resources metabolized by hydrothermal vent symbioses

(formatted for journal submission)

Abstract

Symbioses between animals and chemoautotrophic bacteria predominate at hydrothermal vents. In these associations, symbiotic bacteria utilize chemical reductants for the energy to support autotrophy, providing primary nutrition for the host. It is well known that reductants in venting fluid (e.g., sulfide, methane, hydrogen) can fuel productivity by vent symbioses. At vents along the Eastern Lau Spreading Center (ELSC), partially oxidized sulfur (e.g., thiosulfate, polysulfides) has also been detected around communities of symbiotic molluscs. Thiosulfate is known to drive autotrophy in free-living sulfur oxidizing microbes as well as the epibiotic symbionts of some vent crustaceans, but has never been shown in a an intact association between animals and intracellular symbionts. To test this metabolism in vent endosymbioses, we used high-pressure, flow-through incubations to maintain three symbiotic molluscs from the ELSC - the snails *Alviniconcha* and *Ifremeria nautilei*, and the mussel *Bathymodiolus brevior* – at conditions mimicking those *in situ*. We assessed their productivity when oxidizing sulfide or thiosulfate via the incorporation of isotopically labeled inorganic carbon, while concurrently measuring their effect on sulfur flux from the aquaria with voltammetric microelectrodes. We found that the symbionts of all three genera supported carbon fixation while oxidizing thiosulfate as well as sulfide, though at different rates. Additionally, we showed that these symbioses excreted partially oxidized sulfur under highly sulfidic conditions, which illustrates that these symbioses could represent a source for partially oxidized sulfur in their habitat. Finally, by examining the rate at which individuals incorporated the isotopic label, we revealed spatial disparity in the rates of carbon fixation among the animals in our incubations that might have implications for the variability of productivity *in situ*. Altogether, this work demonstrates that thiosulfate may be an ecologically important energy source for vent symbioses and that, beyond the removal of vent-

derived sulfide, these symbioses may also impact the local geochemical regime through the excretion of sulfur compounds.

Introduction

Hydrothermal vents support dense assemblages of invertebrates, many of which rely on chemoautotrophic bacterial symbionts for nourishment. These microbial-animal associations aggregate around vent orifices so that their symbionts can utilize chemicals in venting fluid for the energy to support carbon fixation (Stewart et al. 2005). To date, the symbionts of animals from multiple phyla have been shown to use sulfide, methane and/or hydrogen from vent fluid as energy sources (Belkin et al. 1986; Nelson & Hagen 1995; Girguis & Childress 2006; Childress et al. 1991; Ponsard et al. 2012; Watsuji et al. 2012; Watsuji et al. 2010; Fisher et al. 1987; Robinson et al. 1998; Petersen et al. 2011). Though these are likely to be the most important forms of energy for vent symbioses (Amend et al. 2011), other reduced compounds can be present in and around venting fluid (Gartman et al. 2011; Luther et al. 2001; Luther Iii et al. 2001; Schmidt et al. 2008). In particular, the partially oxidized sulfur compounds polysulfide and thiosulfate, which are produced from the abiotic and/or biological oxidation of vent-derived sulfide (Mullaugh et al. 2008; Gartman et al. 2011), have been detected at some vent systems (Gartman et al. 2011; Mullaugh et al. 2008; Waite et al. 2008; Gru et al. 1998). These compounds are typically present away from vent outlets (Gartman et al. 2011; Mullaugh et al. 2008; Waite et al. 2008). Since competition among vent symbioses for vent-derived resources is likely to be intense, the use of reductants that are not sourced directly from vent fluid would be energetically advantageous. Moreover, since the proximity that is required for access to reductants in venting fluid requires exposure to high temperatures and toxic chemicals (e.g., sulfide), the exploitation of reductants that are not obtained directly from the vent could be

beneficial to symbioses that cannot tolerate such conditions. Thus, the use of partially oxidized sulfur has many ecological advantages for vent symbioses.

It is well known that partially oxidized sulfur compounds can be used as energy for carbon fixation by some free-living vent chemoautotrophs (Teske et al. 2000; Sievert & Vetriani 2012), as well as by chemoautotroph-animal symbioses from non-vent ecosystems (Dando et al. 1986; Scott & Cavanaugh 2007; Giere et al. 1988; Childress et al. 1998). Moreover, experimental studies have observed thiosulfate-driven carbon fixation among the epibiotic symbionts of vent crustaceans (Watsuji et al. 2012; Watsuji et al. 2010; Ponsard et al. 2012; Polz et al. 1998). A few studies have also measured thiosulfate oxidation in vitro by the intracellular symbionts of vent mussels and clams that were physically separated from their hosts (Belkin et al. 1986; Wilmot & Vetter 1990; Fisher et al. 1987; Childress et al. 1991; Nelson et al. 1995). To date, thiosulfate-driven carbon fixation has not been demonstrated in an intact symbiosis between a vent animal and intracellular symbionts; thus, the extent to which this metabolism is important for productivity many vent symbioses remains unclear.

The abundance of partially oxidized sulfur in the vent environment has been best characterized at vents along the Eastern Lau Spreading Center (ELSC), in the southwestern Pacific near the island of Tonga. Three molluscs dominate at these vent fields: the provannid snails *Alviniconcha* and *Ifremeria nautilei*, as well as the mussel *Bathymodiolus brevior*. Though each of these symbioses can support net carbon fixation with sulfide oxidation (Henry et al. 2008), they associate with different, phylogenetically distant lineages of symbiotic bacteria that are housed in in their gill tissue (Y. Suzuki, Kojima, Watanabe, et al. 2006b; Y. Suzuki, Kojima, Sasaki, et al. 2006a; Y. Suzuki, Sasaki, M. Suzuki, Tsuchida, et al. 2005b; Y. Suzuki, Sasaki, M. Suzuki, Nogi, et al. 2005a; Beinart et al. 2012; Dubilier et al. 1998; Stein et al. 1988). Interestingly, these animals typically form concentric patterns around vent orifices, with *Alviniconcha* found closest to

the outlet, followed by a zone of *I. nautilei*, and finally *B. brevior* at the very edges of the assemblages (Podowski et al. 2009; Podowski et al. 2010; Waite et al. 2008). It has been suggested that these zones reflect both preference for particular temperature and chemical regimes by the symbioses, and competitive interactions among them (Podowski et al. 2010; Sen et al. 2013). In addition to sulfide originating from the venting fluid, partially oxidized sulfur compounds are common in and around these aggregations; surveys with *in situ* voltammetric microelectrodes have detected thiosulfate and polysulfides at concentrations up to 1000 and 400 μM, respectively (Waite et al. 2008; Mullaugh et al. 2008; Gartman et al. 2011). Interestingly, the presence and abundance of these sulfur compounds correspond to the distribution of the mollusc genera, which might be indicative of specific exchanges between particular symbioses and the pools of partially oxidized sulfur compounds. In particular, the highest concentrations of thiosulfate in the aggregations are found over the zones of *B. brevior* (Waite et al. 2008; Mullaugh et al. 2008), while the highest concentrations of polysulfides are found among the *I. nautilei* (Gartman et al. 2011; Waite et al. 2008).

To determine whether these symbioses can use partially reduced sulfur compounds to support carbon fixation, we conducted a series of shipboard incubations with all three ELSC mollusc symbioses using high-pressure, flow-through aquaria. Inline voltammetric electrodes allowed us to assess total sulfur flux through the aquaria, while an isotopic tracer allowed us to quantify individual productivity during the incubations. The data presented here reveal which of these symbioses can support carbon fixation with thiosulfate, and demonstrate excretion of partially oxidized sulfur under highly sulfidic conditions. Additionally, the data suggest that there is variability in individual carbon fixation rates within an assemblage of these symbioses that may be related to competition for resources.

Methods

Animal collections

Animals were collected from the vent fields ABE (-20°45.8' by -176°11.5') or Tu'i Malila (-21°59.4' by -176°34.1') at the Eastern Lau Spreading Center (ELSC) by the remotely operated vehicle *JASON II* during expedition TM-235 in 2009 on board the R/V *Thomas G. Thompson*. Animals were brought to the ship in insulated containers and, once on board, were kept in 4°C seawater. *Alviniconcha* or *I. nautilei* that were responsive to touch and *B. brevior* that were tightly closed upon recovery were immediately placed in the flow-through, titanium aquaria that represent part of the high-pressure respirometry system (HPRS; described below). For each incubation, between 3 and 10 individuals of each genus were placed into three separate aquaria. Animals were situated upon perforated acrylic partitions so that they were stacked vertically in the cylindrical aquaria.

Incubation conditions and acclimation

Three incubations (hereafter 'rate experiments' or 'experiments') were performed to compare net sulfur uptake and excretion rates, as well as carbon fixation rates, by the three mollusc genera at three different conditions: 105 µM sulfide, 300 µM thiosulfate, and no sulfur compounds. During each rate experiment, an empty high-pressure aquarium (control) was run alongside the three animal-containing aquaria in order to account for systematic losses and enable the most robust mass specific rate determinations. In addition, two additional incubations (hereafter 'exposure treatments' or 'treatments') were performed to establish the extent of variation in carbon fixation rates among the animals within each vessel. Exposure treatments were run with a larger number of individuals per aquaria (sometimes double the number in the

rate experiments) at 350 µM sulfide or 300 µM thiosulfate (exposure treatments lack a control aquaria). Prior to the start of each experiment or treatment, all animals were incubated in aerated seawater at 15°C and 25 MPa for 8 hours prior to the addition of sulfur compounds and isotopic tracer. During the no sulfur experiment, animals were acclimated with ~300 µM sulfide before sulfur was stopped and isotopic tracer was added**.**

Incubations with the high-pressure respirometry system (HPRS)

To measure sulfur oxidation and carbon fixation rates under *in situ*-like conditions, rate experiments and exposure treatments were performed with the HPRS (Fig.4.1). The HPRS was housed in a temperature-controlled intermodal shipping container maintained at 15-17°C. Surface seawater from the ship's metal-free seawater systems was filtered to 0.2 µm via inline cartridge filters (Millipore Inc), then pumped into into a 40 L polypropylene carboy (Nalgene™). Filtered seawater was then amended with 1 g isotopically labeled sodium bicarbonate (as solution of 240 mM $Na^{13}CO_3$; 99.9% atom percent; Icon Services), to achieve a final $^{13}C/^{12}C$ atom percent of ~5% in the carboy. In addition, sodium nitrate ($NaNO_3$) was added to achieve a final concentration of 40 µM, comparable to deep ocean water.

For the thiosulfate experiment and treatment, 300 mM sodium thiosulfate (NaS_2O_3) was added to the amended seawater in carboy to achieve a final concentration of 300 µM. This was pumped into an acrylic gas equilibration column (Girguis et al. 2000), where it was bubbled with carbon dioxide, oxygen, nitrogen using mass flow controllers (Sierra Instruments Inc) to achieve concentrations of 4 mM, >300 µM, and 400 µM respectively (Table S4.1). The pH of the resulting input water was always 6-7. For the hydrogen sulfide experiment and treatment, the conditions were identical except for the absence of the thiosulfate, and the addition of gaseous

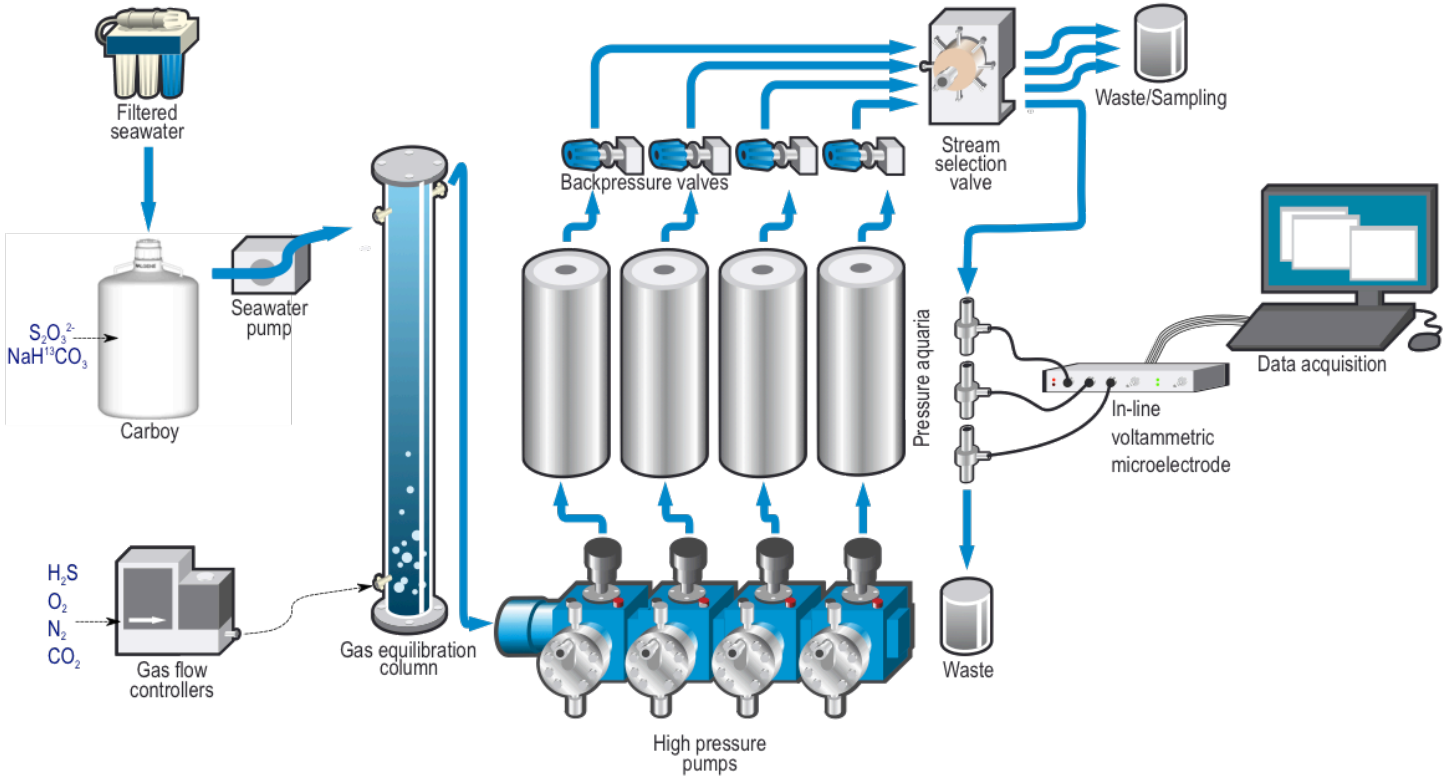

Figure 4.1 Schematic of the high-pressure respirometry system (HPRS). Filtered seawater is amended with chemicals to mimic *in situ* conditions, and then pumped through three titanium aquaria containing the symbiotic molluscs, and in some cases, through an additional, empty control aquaria. These aquaria are held at ~25 mPa with back-pressure valves. The input water and/or the aquaria effluent are directed, via a stream-selection valve, to an in-line voltammetric microelectrode system that measures the concentrations of sulfur compounds (modified from Nyholm et al., 2008).

5% H_2S/95% N_2 gas via a mass flow controller to achieve the target final concentrations (presented above).

In all incubations, the resulting seawater from the equilibration column was then supplied to four high-pressure metering pumps (Lewa GmbH) equipped with titanium wetted parts. The pumps generated ~25 mPa and delivered fluid into the three or four titanium high-pressure aquaria at a rate of 10-16 ml min^{-1}. Pressure was maintained via 316 stainless steel backpressure valves (StraVal Inc). The aquaria effluents and/or equilibration column seawater (hereafter 'input water') were directed toward an electronic, multi-position stream-selection valve (Valco Instruments Co. Inc.) that systematically sent each stream to analysis by a voltammetric microelectrode (see below), to collection for analyses on shore, or to waste.

Sulfur oxidation and excretion rates

To determine the net sulfur oxidation rates, as well as detect the excretion of partially oxidized sulfur compounds, the concentrations of sulfur compounds in the effluent of the experimental aquaria were compared to the concentrations in effluent from the empty control aquarium (rate experiments) or to the concentrations in input water (exposure treatments). Oxidation (or uptake) and excretion (or production) of sulfur compounds is defined here, respectively, as an observed net decrease or increase in the concentrations of sulfur compounds in the effluent of the aquaria relative to the control effluent or the input water. The concentrations of the sulfur compounds sulfide ($\sum H_2S$ and HS^-), thiosulfate and polysulfides were measured via voltammetric microelectrodes (Luther et al. 2001; Brendel & Luther 1995). Though we were unable to quantify oxygen concentrations during the incubations, the voltammetric microelectrodes (see below) were always able to detect oxygen in the aquaria effluent during all incubations (minimum detection limit is 5 µM; (Gartman et al. 2011)), suggesting that oxygen

was never completely depleted by the symbioses in the aquaria. The input and/or effluent water was measured in a cyclical series of 30 minute intervals throughout the duration of the experiment; one complete 2-hour series of 4 intervals starting with an experimental effluent and ending with either the control effluent or input water is hereafter referred to as a 'set'. Electrochemical scans were performed at a rate of 1 per ~43 s, resulting in 42 measurements per 30 min interval. The detection limits for the voltammetric microelectrodes were 30 µM thiosulfate and 0.2 µM sulfide and polysulfide. The electrodes were calibrated for measurement of sulfide concentrations with measurements made via discrete water samples from either the input water (exposure treatment) or the control vessel effluent (rate experiment) as described below (Fig.S4.1). The electrodes were calibrated for measurement of thiosulfate concentration based on the 300 µM concentration in the input water.

At 4 h intervals throughout the course of the experiments, 10 ml of input or control effluent water was also preserved with 1 M zinc acetate and stored at -20°C until analysis. Later, sulfide concentrations were determined via a colorimetric assay ((Cline 1969); Lamotte Co.) by comparing our unknowns to a standard curve varying from 1 to 500 µM on a Spectramax Plus 384 absorbance microplate reader (Molecular Devices, LLC).

Net sulfur oxidation rates were calculated using data obtained after at least 10 h into the experiment, as this allowed for three turnovers in the volume of water in the aquaria. To calculate the concentrations of each sulfur compound during each 30 min interval, the first 10 scans of each interval were removed (i.e., the first 24% of the total scans in each interval) to exclude the transitory scans that occurred after the switch to a different aquarium effluent. The concentrations resulting from the remaining scans were averaged, resulting in a single concentration value per interval (hereafter, 'interval concentration'). To calculate oxidation rates for each mollusc genus within a set, the interval concentration of the control effluent was

subtracted from the interval concentration of the experimental effluent, and these in turn were divided by the total gill mass of the animals in each aquarium.

DIC isotopic composition

To measure the exact amount of isotopic tracer $Na^{13}CO_3$ available during each experiment or treatment, input water was sampled 2-3 times over the course of each. Approximately 10 ml of input water taken directly from the gas equilibration column was filtered (0.2 µm) to remove particulate carbon. Dissolved inorganic carbon (DIC) in the samples was base-trapped with a solution of sodium hydroxide so that the final pH was >11 and stored frozen at -20°C in gas-tight, glass Hungate tubes until analysis. The atom percent of the DIC was measured at the Yale Institute of Biospheric Studies' Earth System Center for Stable Isotopic Studies, where 1 ml of thawed sample was injected into pre-flushed 12 ml exetainers containing H_3PO_4 to evolve DIC as CO_2 for analysis via a ThermoFinnigan Delta^{PLUS} Advantage mass spectrometer (Thermo Scientific) coupled to a Costech ECS 4010 EA elemental analyzer (Costech Analytical Technologies).

Sampling of experimental animals

At the conclusion of each experiment, the aquaria were depressurized and animals were quickly removed from the high-pressure aquaria, excised from their shells, and total wet weight for each individual was determined via a motion-compensated shipboard balance (Childress & Mickel 1980). From these weights, each individual's gill weight was estimated from linear equations derived from the regression of total body mass to gill mass (Fig.S2) for each genus. Gill and foot tissue was subsampled for isotopic analysis and frozen at -80°C until further processing.

In addition, subsamples of gill tissue were homogenized and preserved in Trizol™ (Life

Technologies) for extraction of nucleic acids. DNA was extracted from the Trizol™-preserved tissue samples following RNA extraction via the manufacturer's protocol. DNA was back-extracted from the resulting interphase with a buffer consisting of 4 M guanidine thiocyanate, 50 mM sodium citrate and 1 M Tris (free base). The DNA was then extracted again with chloroform:isoamyl alcohol and precipitated with isopropanol. The resulting DNA pellets were washed twice with 75% ethanol and air-dried. DNA pellets were resuspended in 8 mM sodium hydroxide, adjusted to pH 7-8 with 0.1 M HEPES and amended with 1 mM EDTA.

Symbiont identities

Symbiont 16S rRNA genes were directly amplified from diluted *I. nautilei* and *B. brevior* DNA extracts using the universal bacterial primers 27F and 1492R (Lane 1991). PCR reactions were performed with Crimson Taq DNA polymerase (New England Biolabs, Inc.) for 2 min at 95 °C, 30 cycles of 30 s at 95°C, 30 s at 55°C, 90 s at 68°C, followed by 5 min at 72°C. PCR products were subjected to electrophoresis on a 1.2% (wt/vol) agarose gel stained with SYBR Safe (Invitrogen, Inc.) to check the quantity and the quality of the products using a U:Genius UV transilluminator (Syngene, Inc.). PCR products were cleaned with ExoSAP-IT (Affymetrix, Inc.), then bidirectionally sequenced. Quality assessment of the sequences and assembly of forward and reverse reads were performed in Geneious v6.1.6 (BioMatters, Inc.). Sequences were aligned with other symbiont and free-living Proteobacterial sequences using the SILVA Incremental Aligner v1.2.11 (Pruesse et al. 2012). A Bayesian inference phylogeny was produced with MrBayes (Huelsenbeck & Ronquist 2001) implementing the GTR+I+G model of substitution. Three replicate runs of 5 x 10^7 generations were performed with sampling every 10^3 generations and burn-in of 12,500 samples. Quantitative and qualitative diagnostics were performed for each of

the three runs using the Coda package in R (Plummer et al. 2006), the three replicate runs were combined, and a 50% majority rule consensus tree was created in MrBayes.

Because *Alviniconcha* from the ELSC are known to host an assemblage of phylogenetically distinct symbionts (Beinart et al. 2012), direct amplification and sequencing of symbiont 16S rRNA genes was not performed. Instead, the symbiont populations associated with the experimental *Alviniconcha* were assessed as in Beinart *et al.* (2012), with three 16S rRNA gene quantitative PCR assays that are specific to their symbiont phylotypes. Briefly, we estimated the proportion of each symbiont phylotype in the diluted *Alviniconcha* gill DNA extracts by applying all the assays to 2 µl of each sample (in duplicate), which were compared against duplicate standard curves and no-template controls. A standard curve for each assay was constructed from linearized plasmid containing a representative 16S rRNA gene from the three symbiont phylotypes, diluted so that 10^1 to 10^7 gene copies were added per reaction.

Tracer incorporation into tissue samples and carbon fixation rates

Approximately 300 mg symbiont-containing gill and symbiont-free foot tissue were subsampled while frozen for carbon isotopic analysis. Samples were lyophilized for 24 h and then were acidified with 0.1 N HCl to remove any unincorporated $Na^{13}CO_3$ contamination. The samples were subsequently dried for 24–48 h at 50–60°C, weighed to determine the dry weight, homogenized to a fine powder, and ~1 mg sealed within tin capsules.

The carbon isotopic composition and percent carbon content was determined for foot tissue samples at Washington State University by combustion in an elemental analyzer (Eurovector, Inc.) and separating the evolved CO_2 by gas chromatography before introduction to a Isoprime™ isotope ratio mass spectrometer (Micromass Inc). Gill tissue samples were assayed at the Yale Institute of Biospheric Studies' Earth System Center for Stable Isotopic Studies using

a ThermoFinnigan Delta^{PLUS} Advantage mass spectrometer (Thermo Scientific) coupled to a Costech ECS 4010 EA elemental analyzer (Costech Analytical Technologies). Measurements of isotopic composition are expressed as the atomic percent (%A = [$^{13}C/(^{13}C+^{12}C)$] x 100%) and carbon contents expressed as a percentage of dry weight (%C).

To obtain the percentage of ^{13}C incorporated during these experiments (%$^{13}C_{inc}$), the following formula was used:

$$\%^{13}C_{inc} = \frac{(A\%_g - A\%_f)}{(A\%_w - A\%_f)}$$

where $A\%_g$ is the atomic percent of the gill tissue sample; $A\%_f$ is the atomic percent of the same individual's foot tissue sample; and $A\%_w$ is the atomic percent of the input water DIC. The average isotopic composition of the foot tissue of each genus from all experiments was comparable to the natural isotopic composition of these animals (Table S4.2), indicating that ^{13}C incorporation into foot tissue or contamination of the samples did not occur. Foot tissue was not sampled at the conclusion of the sulfide exposure treatment, so the average $A\%_f$ from the other experiments was used to calculate rates for the individuals in this experiment (averages 1.076%, 1.075%, and 1.075% for *Alviniconcha*, *I. nautilei* and *B. brevior*, respectively). For the *Alviniconcha* individuals in the sulfide exposure treatment that hosted ε-proteobacterial symbionts, the $A\%_f$ average from the previous experiments could not be used since *Alviniconcha* from the other experiments hosted γ-proteobacterial symbionts. For these individuals, the previously published average $A\%_g$ (1.093%; (Beinart et al. 2012)) for ε-proteobacteria-hosting individuals was used since gill tissue is typically a reasonable approximation of the $A\%_f$ in *Alviniconcha* (Y. Suzuki, Kojima, Sasaki, et al. 2006a).

The weight of incorporated carbon ($W^{13}C_{inc}$) was then calculated by multiplying the %$^{13}C_{inc}$ by the dry weight of the gill tissue (DW_g) and the carbon content of the sample (%C).

Carbon incorporation rates (C_{inc}) are expressed as umoles ^{13}C per gram of wet tissue per hour. This was first calculated as a rate of carbon incorporation expressed as umoles ^{13}C per gram of dry tissue per hour ($DryC_{inc}$) with the formula:

$$DryC_{inc} = \frac{[(W^{13}C_{inc} \mid MW_c) \times 1000]}{(DW_g \times t)}$$

where MW_c is the molecular weight of ^{13}C; and t is the duration of the experiment. C_{inc} was then converted to C_{inc} by multiplying $dryC_{inc}$ by the ratio of DW_g to the wet weight of that same sample (W_g).

Results

Symbiont identity

Via assessment of the symbiont populations through analysis of the 16S rRNA genes, we found that the symbionts of each host genus had low symbiont diversity. Except for a number of *Alviniconcha* from the sulfide exposure treatment, individuals from all three genera used in the incubations hosted γ-proteobacterial symbionts. *Alviniconcha* from the ELSC are known hosts to three phylotypes of symbionts: two γ-proteobacterial phylotypes (γ-1, γ-Lau) or an ε-proteobacterial phylotype. With the exception of some individuals in the sulfide exposure treatment, all experimental *Alviniconcha* were dominated by symbionts from one of the two γ-proteobacterial phylotypes (i.e., ≥93% of the detected 16S rRNA genes; Table S4.3). Most of these individuals hosted mainly γ-1 symbionts; only two individuals from the no sulfur experiment were dominated by γ-Lau symbionts. Among individuals of *I. nautilei* and *B. brevior*, there was low diversity in their symbionts as indicated by their 16S rRNA genes. Additionally, direct amplification and sequencing resulted in chromatograms with no evidence of mixed

symbiont populations within individuals (data not shown). Individuals of *I. nautilei* yielded six unique sequences that are at least 99.5% identical to one another, while *B. brevior* individuals yielded three unique sequences that are at least 98.8% identical to one another. Bayesian phylogenetic analysis (Fig.4.2) showed that the experimental *B. brevior* symbiont sequences fell in a well-supported clade consisting of symbionts from *Bathymodiolus* mussels and *Calyptogena* clams and a few free-living marine bacteria. Experimental *I. nautilei* symbiont sequences fell in a well-supported clade of *I. nautilei* symbionts from the Lau basin and other hydrothermal vent regions.

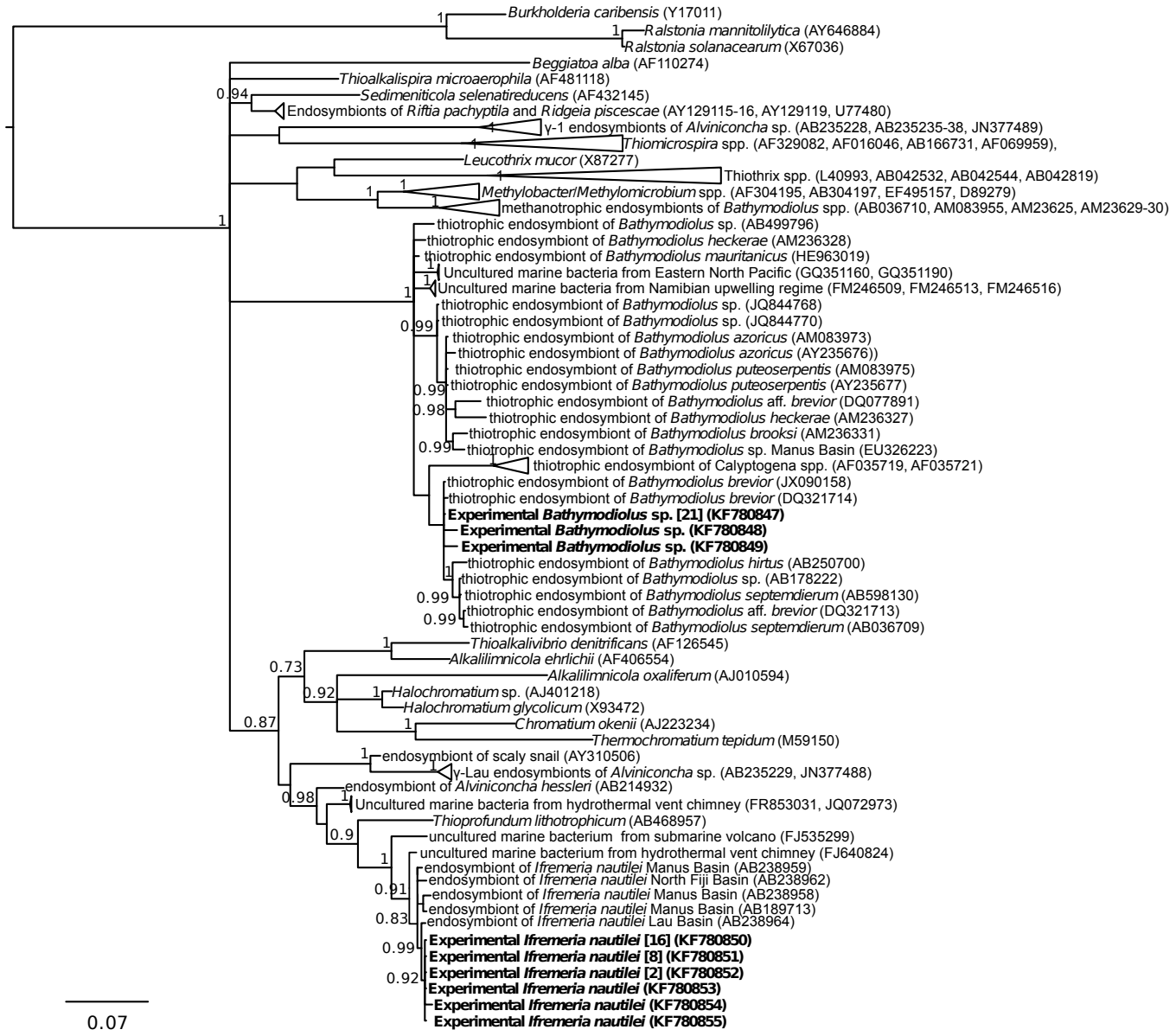

Figure 4.2: Bayesian inference phylogeny of γ-proteobacterial 16S rRNA gene sequences with β-proteobacterial outgroup. The symbionts of *B. brevior* and *I. nautilei* from all incubations are shown in bold with the number of individuals yielding that sequence indicated in brackets. Accession numbers are shown in parentheses. Posterior probabilities are indicated above the nodes if >0.7.

Table 4.1: Net sulfur uptake (oxidation) and excretion by the three mollusc genera. Number of individuals (n) and the total wet weight of gill tissue for each mollusc genus in each experiment, as well as the average (min, max) concentrations of sulfide, thiosulfate and polysulfides as measured via a voltammetric electrode in the effluent from each aquaria.

				Concentration in effluent (μM)		
Experiment	**Genus**	**n**	**Total gill wet weight (g)**	**Sulfide**	**Thiosulfate**	**Polysulfides**
No sulfur	Control	0	0	0.20 (0.20, 0.20)	30 (30,30)	0.20 (0.20, 0.20)
	Alviniconcha	5	15.9	0.20 (0.20, 0.20)	30 (30,30)	0.20 (0.20, 0.20)
	I. nautilei	5	18.8	0.20 (0.20, 0.20)	30 (30,30)	0.20 (0.20, 0.20)
	B. brevior	4	18.8	0.20 (0.20, 0.20)	30 (30,30)	0.20 (0.20, 0.20)
Sulfide	Control	0	0	66 (46, 107)	30 (30,30)	0.20 (0.20, 0.20)
	Alviniconcha	5	22.6	5.7 (2.7,9.7)	30 (30,30)	0.20 (0.20, 0.20)
	I. nautilei	5	20.5	5.8 (3.0, 8.6)	30 (30,30)	0.20 (0.20, 0.20)
	B. brevior	4	18.4	3.0 (1.4, 3.9)	30 (30,30)	0.20 (0.20, 0.20)
Thiosulfate	Control	0	0	0.32 (0.20, 1.1)	276 (216, 310)	0.20 (0.20, 0.20)
	Alviniconcha	3	21.4	0.22 (0.20, 0.36)	139 (30, 209)	0.20 (0.20, 0.20)
	I. nautilei	4	19.5	0.22 (0.20, 0.31)	42 (30, 70)	0.20 (0.20, 0.20)
	B. brevior	3	13.5	0.20 (0.20, 0.20)	140 (67,188)	0.20 (0.20, 0.20)

Sulfur metabolism and carbon fixation in rate experiments

All three symbioses demonstrated net sulfide and thiosulfate uptake (or oxidation; Table 4.1). Though seawater sulfur concentrations were depleted by the animals during the incubations (relative to the control vessel), measurable concentrations of sulfide and thiosulfate were detected in the vessel effluent during all experiments, suggesting that sulfur compounds did not become limiting in the experiments (sulfur limitation would prohibit the determination of mass-specific sulfur uptake rates). Average mass-specific net sulfide oxidation rates were comparable among the three genera at these experimental conditions (Fig.4.3a). The average mass-specific net thiosulfate oxidation rates varied more among the three genera, with *I. nautilei* having almost twice the average rate of *Alviniconcha* (Fig.4.3b). Additionally, net thiosulfate oxidation rates fluctuated more widely over the duration of the experiment than did net sulfide oxidation rates (Fig.4.3a,b). Other than the provided sulfur species, no sulfur compounds were detected the effluent of the three experiments, indicating that sulfur excretion did not occur at these conditions.

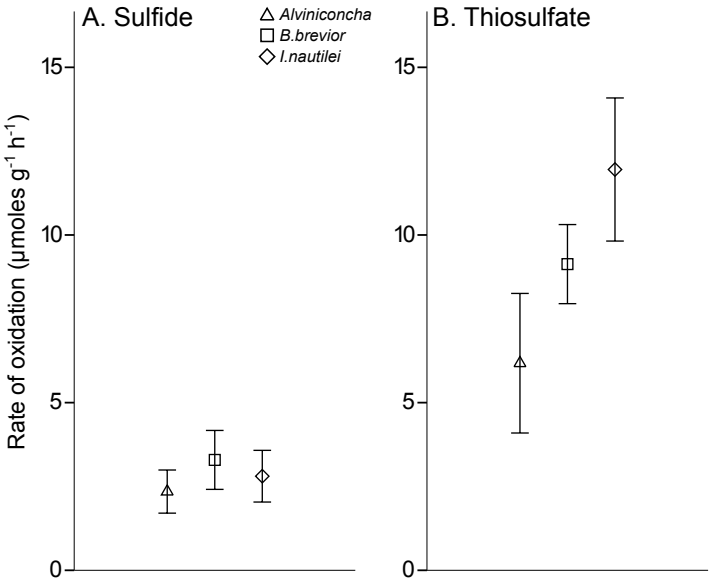

Figure 4.3: Average (±S.D.) mass specific net sulfur oxidation rates (μmoles of sulfur per gram of wet gill tissue per hour) during the sulfide (a) and thiosulfate (b) rate experiments for *Alviniconcha* (△), *B. brevior* (□), and *I. nautilei* (◇).

Carbon incorporation (or fixation) was stimulated in the gills of individuals from all three symbiotic genera when provided sulfide, but only in *Alviniconcha* and *I. nautilei* individuals when given thiosulfate (Fig.4.4, Fig.S4.3). When supplied sulfide, carbon incorporation rates among the

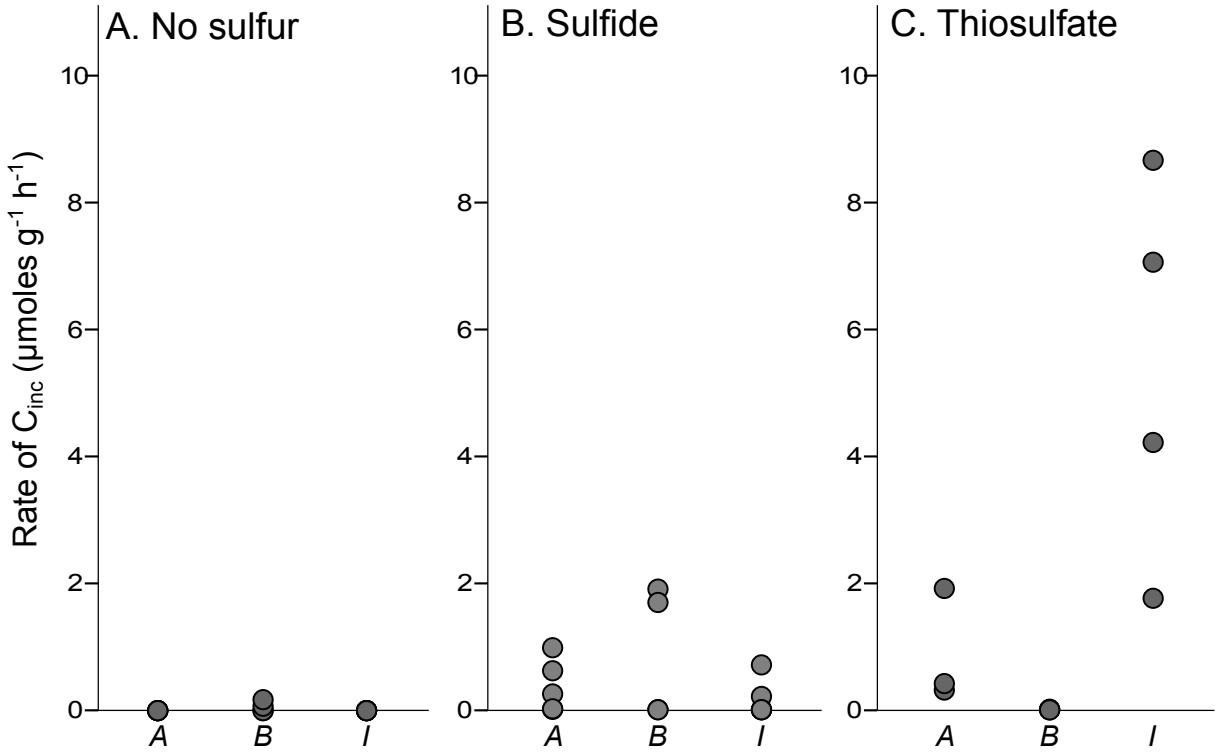

Figure 4.4: Individual mass-specific carbon incorporation rates (µmoles of ^{13}C per gram of wet gill tissue per hour) for *Alviniconcha* (A), *I. nautilei* (I), and *B. brevior* (B) during the no sulfur (a), sulfide (b), and thiosulfate (c) rate experiments.

genera did not differ significantly from one another (Kruskal-Wallis, p=0.424) (Fig.4.4b). Among all three experiments, the greatest rates of carbon fixation occurred in *I. nautilei* individuals supplied thiosulfate (Fig.4.4c), though *I. nautilei* did not differ significantly from *Alviniconcha* individuals in that experiment (Mann-Whitney U, p=0.114). Carbon fixation was not stimulated in *Alviniconcha* and *I. nautilei* individuals in the no sulfur (control) experiments, though minor carbon incorporation was detected in two of the four *B. brevior* individuals.

Sulfur metabolism and carbon fixation during exposure treatments

Both sulfide and thiosulfate concentrations were depleted in the effluents of the experimental aquaria relative to the input water in their respective exposure treatments (Table 4.2). As with the rate experiments, measurable concentrations of sulfide and thiosulfate were detected in the experimental effluent in their respective treatments, indicating that the symbioses did not completely exhaust these compounds in the aquaria. Mass-specific rates of uptake (oxidation) calculated relative to the input water were comparable among treatments, though the average rate of sulfide oxidation was greater than the average rate of thiosulfate oxidation for all three genera (Table 4.2). Sustained sulfur excretion was observed throughout the duration of the sulfide treatment, but not during the thiosulfate treatment (Table 4.2).

Table 4.2: Net sulfur uptake (oxidation) and excretion by the three mollusc genera during exposure treatments. Number of individuals (n); the sum total wet weight of gill tissue for each mollusc genus; average (min, max) concentrations of sulfide, thiosulfate and polysulfides as measured via a voltammetric electrode in the effluent from each aquaria; average (± S.D.) rates of net oxidation or excretion (indicated as negative or positive values, respectively) as µmoles per gram of wet gill tissue per hour.

	Genus	n	Total gill wet weight (g)		Sulfide	Thiosulfate	Polysulfides
Sulfide treatment	Input	NA	NA	Concentration (µM)	349 (329, 387)	30 (30,30)	0.20 (0.20, 0.20)
	Alviniconcha	10	36.9	Concentration (µM)	21 (19, 23)	73 (68, 77)	0.20 (0.20, 0.20)
				Rate (µmoles g^{-1} h^{-1})	*-6.8 ± 0.50*	*+0.92 ± 0.05*	*0*
	I. nautilei	5	34.1	Concentration (µM)	85 (76, 90)	30 (30,30)	78 (0.2, 126)
				Rate (µmoles g^{-1} h^{-1})	*-7.2 ± 0.75*	*0*	*+2.2 ± 1.5*
	B. brevior	6	39.9	Concentration (µM)	14 (12, 15)	34 (30, 40)	0.20 (0.20, 0.20)
				Rate (µmoles g^{-1} h^{-1})	*-7.4 ± 0.52*	*+0.10 ± 0.08*	*0*
Thiosulfate treatment	Input	NA	NA	*Concentration (µM)*	0.20 (0.20, 0.20)	302 (251, 404)	0.20 (0.20, 0.20)
	Alviniconcha	8	39.3	Concentration (µM)	0.20 (0.20, 0.20)	40 (30, 82)	0.20 (0.20, 0.20)
				Rate (µmoles g^{-1} h^{-1})	*0*	*-5.62 ± 1.22*	*0*
	I. nautilei	10	50.7	Concentration (µM)	0.20 (0.20, 0.20)	44 (30, 60)	0.20 (0.20, 0.20)
				Rate (µmoles g^{-1} h^{-1})	*0*	*-4.66 ± 0.93*	*0*
	B. brevior	6	45.3	Concentration (µM)	0.20 (0.20, 0.20)	103 (30, 162)	0.20 (0.20, 0.20)
				Rate (µmoles g^{-1} h^{-1})	*0*	*-4.02 ± 0.84*	*0*

Alviniconcha and *I. nautilei* individuals from both the sulfide and thiosulfate exposure treatments incorporated carbon (Fig.4.5a,c,d,f; Fig.S4.3). No carbon incorporation was observed by *B. brevior* in the sulfide treatment (Fig.4.5b, Fig.S4.3), though, two of the six *B. brevior* individuals from the thiosulfate exposure treatment incorporated carbon (Fig.4.5e, Fig. S4.3).

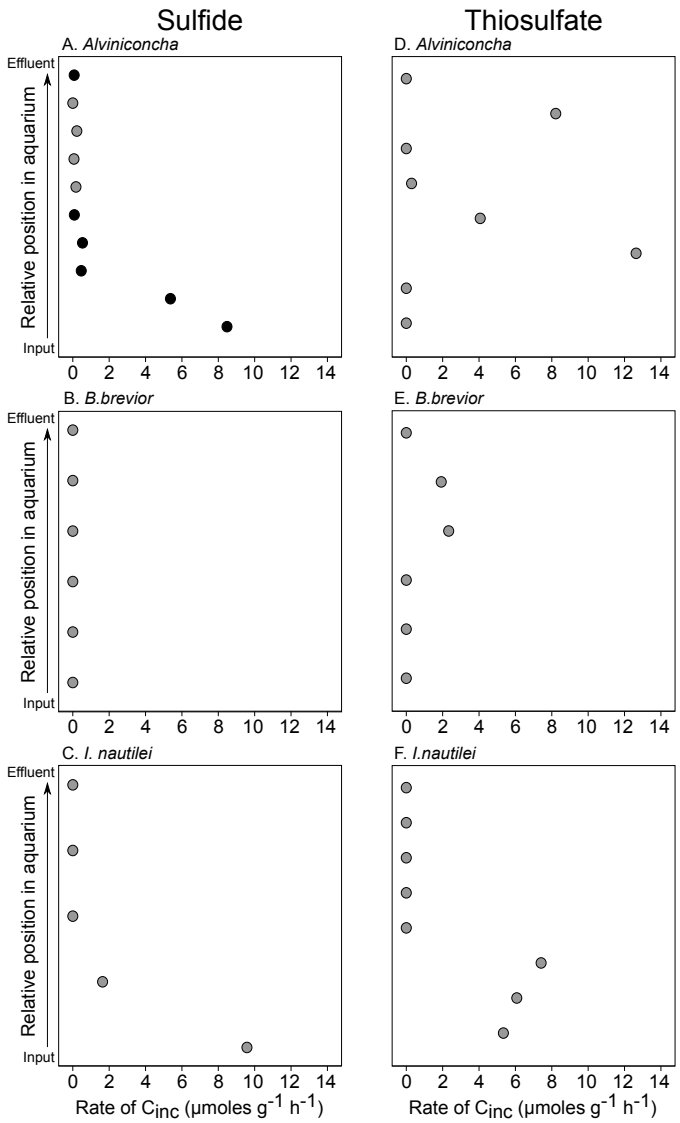

Figure 4.5 Individual mass-specific carbon incorporation rates (µmoles of ^{13}C per gram of wet gill tissue per hour) during the exposure treatments. Sulfide exposure treatment with *Alviniconcha* (a), *B. brevior* (b), and *I. nautilei* (c); thiosulfate exposure treatment with *Alviniconcha* (d), *B. brevior* (e), and *I. nautilei* (f). Black symbols indicate *Alviniconcha* hosting ε-proteobacterial symbionts. Individuals are shown according to their relative position in the HPRS aquaria.

In both treatments, carbon incorporation rates were greatly variable but likely related to substrate limitation in the aquaria. Animals positioned in the aquaria closest to the input of water generally had the highest carbon fixation rates, though this trend is more pronounced in the sulfide treatment then the thiosulfate treatment. Additionally, individuals from these treatments demonstrated the highest rates of carbon fixation among all of the animals in either the rate experiments or exposure treatments. *Alviniconcha* and *B. brevior* individuals from the thiosulfate exposure treatment showed the highest rates of carbon fixation among all individuals of their genus. Additionally, an individual from the sulfide exposure

treatment had the highest carbon fixation rate for any *I. nautilei*.

Discussion

The significance of thiosulfate oxidation for hydrothermal vent symbioses

Here, we demonstrated, for the first time, that exogenous thiosulfate drove carbon fixation in intact symbioses between vent animals and intracellular symbionts. This has only previously been tested in the intact vent tubeworm *Riftia pachyptila*, which does not oxidize thiosulfate (and carbon fixation was not measured; (Wilmot & Vetter 1990)). *In vitro* studies of the intracellular symbionts of *Bathymodiolus* mussels and *Calyptogena* clams show that they can support carbon fixation with thiosulfate oxidation (Belkin et al. 1986; Wilmot & Vetter 1990; Fisher et al. 1987; Childress et al. 1991; Nelson et al. 1995). However, since many animals produce thiosulfate from sulfide as a detoxification mechanism (Grieshaber & Völkel 1998), these experiments left it ambiguous whether these symbionts were only able to utilize endogenous thiosulfate produced by their host, or if the intact symbioses could take up and use thiosulfate from their surroundings. Our results demonstrated that these three mollusc symbioses were clearly able to support carbon fixation through the uptake of exogenous thiosulfate.

This discovery, along with previous work showing thiosulfate-based carbon fixation in the epibionts of vent crustaceans (Watsuji et al. 2012; Watsuji et al. 2010; Polz et al. 1998; Ponsard et al. 2012), expands our understanding the many ways in which vent symbioses can derive energy from chemical reductants. Sulfide oxidation is often considered the main driver of primary productivity by chemoautotrophs at these habitats (Amend et al. 2011). However, with respect to standard Gibbs free energies, the complete oxidation of thiosulfate with oxygen is comparable to the complete oxidation of HS^- (-738.7 and -732.6 kJ mol substrate^{-1}, respectively) (Kelly 1999). Moreover, in our experiments, individual, thiosulfate-dependent carbon fixation rates often met

or exceeded individual mass-specific rates with approximately the same concentration of sulfide. Furthermore, thiosulfate is non-toxic and may be readily concentrated within the host's or symbionts' cells, leading to higher Gibbs energies resulting from an elevated concentration of the substrate. Thus, thiosulfate has the potential to be an important energy source for some hydrothermal vent symbioses, though the extent to which the ELSC symbioses (or others) selectively use thiosulfate over sulfide remains to be determined.

The potential ecological importance of thiosulfate-fueled carbon fixation is emphasized by the results of our experiment without sulfur, which underscores that sustained access to exogenous reductants is necessary for the productivity of these symbioses. It has long been hypothesized that many vent symbioses can utilize stored, intracellular elemental sulfur granules when exogenous reductants are absent (Vetter 1985; Stein et al. 1988). However, we demonstrated that the absence of reduced sulfur compounds results in a cessation of carbon fixation in the ELSC symbioses. Instead of depending on stored compounds, flexible use of multiple sulfur compounds may enable vent symbioses to contend with the dynamic conditions at hydrothermal vents. Given the variability in access to vent fluid that they are likely to experience due to temporal and spatial fluid dynamics, the ability to use multiple reductants (e.g., both sulfide and thiosulfate) may relieve the energy limitation that could occur if a symbiosis was exclusively dependent on energy sources found only in venting fluid.

Sulfur oxidation by the mollusc symbioses at the ELSC

Our experiments showed that all three tested symbiotic mollusc genera used both sulfide and thiosulfate to fuel carbon fixation, though their capacities for these metabolisms varied. The specific rates of sulfide oxidation we report are comparable to the previous findings of Henry *et al.* (2008). Our mass-specific sulfide oxidation rates were similar in magnitude to those reported with

conditions analogous to our incubations, though our *I. nautilei* mass-specific carbon fixation rates were higher than previously reported. Since their rates are based on the net uptake of carbon dioxide, high rates of respiration by *I. nautilei* may have masked higher rates of carbon fixation in their experiments. Our isotopic labeling experiments suggest that *I. nautilei* may be as productive as *Alviniconcha* at our experimental conditions, e.g., when sulfide and oxygen are replete.

Previous work on the distribution of ELSC symbioses has suggested that the use of thiosulfate by the mussel *B. brevior* may play a role in its distribution. In particular, it was hypothesized that thiosulfate may be especially important for *B. brevior* physiological intolerance to high sulfide concentrations or temperature may prevent it from inhabiting areas of high fluid exposure (Waite et al. 2008). Consequently, thiosulfate oxidation may enable exploitation of habitat away from the venting fluid, where sulfide concentrations are typically low to undetectable but thiosulfate concentrations are elevated. While we observed that *B. brevior* can indeed use thiosulfate to power carbon fixation, only two of the nine total individuals tested incorporated the tracer (Fig.4.3,4.4), suggesting an inefficient coupling between the metabolisms. Therefore, determining the relative significance of this energy source to *B. brevior*'s overall productivity will require further work.

We did, however, observe relatively high mass-specific rates of thiosulfate-dependent carbon fixation in both *I. nautilei* and *Alviniconcha*. These snails typically live in closer proximity to the venting source, where sulfide is more abundant and thiosulfate concentrations are low (Podowski et al. 2010; Waite et al. 2008; Gartman et al. 2011). Regardless, the data clearly reveal a robust coupling between thiosulfate oxidation and carbon fixation in *I. nautilei* and *Alviniconcha*. Consequently, the observation that *I. nautilei* and *Alviniconcha* commonly inhabit regions of low thiosulfate may simply reflect removal of thiosulfate via oxidation. This supposition is supported

by the observed increase in thiosulfate concentrations when *Alviniconcha* and *I. nautilei* were removed from snail and mussel aggregations *in situ* (Mullaugh et al. 2008).

Variability in carbon fixation rate and substrate limitation in the aquaria

Use of an isotopic label to assess carbon fixation rates among the population of individuals in each exposure treatment revealed striking patterns in the carbon fixation rates that likely reflect substrate limitation in the aquaria seawater. Most previous experiments measuring the rates of carbon fixation by intact hydrothermal vent symbioses have been performed on low numbers of individuals, most often one at a time (Girguis & Childress 2006; Childress et al. 1991; Wilmot & Vetter 1990; Henry et al. 2008), and used the resulting change in chemical composition and the total biomass to estimate mass-specific metabolic rates. Here, the use of stable isotopically labeled inorganic carbon in our aquarium seawater allowed us to examine the variability in productivity among individuals; in our exposure treatments, we interrogated the mass-specific rates of carbon fixation for between five and ten individuals per genus. We found that the most productive animals in each aquarium likely accounted for much of the sulfur oxidation occurring in each during the exposure treatments. Using the molar ratios of 6.21 and 6.64 for the amount of carbon fixed per sulfide or thiosulfate (Kelly 1999) with an assumed 10% efficiency of energy conservation, we calculated the predicted rate of sulfur oxidation by the most productive animals in each aquarium from their individual rates of carbon fixation. In the sulfide exposure treatment, sulfide oxidation by the two most productive individuals may have accounted for 27% and 51% of the total oxidation in the *Alviniconcha* and *I. nautilei* aquaria, respectively. In the thiosulfate exposure treatment, oxidation by the productive individuals (all other individuals showed no carbon incorporation) may have accounted for 100% and 64% (*Alviniconcha* and *I. nautilei*, respectively) of the total oxidation in each aquarium.

The striking disparity in mass-specific carbon fixation rates among individuals was unlikely to be linked to biological diversity (e.g., differences in symbiont populations), but alternatively may be due to individual differences in access to resources in the aquaria. Based on 16S rRNA gene sequences, all *I. nautilei* and *B. brevior* symbionts were very closely related. Except for some symbionts in the sulfide exposure treatment and no sulfur rate experiment, the symbionts of the *Alviniconcha* in our incubations were from one phylotype (γ-1). Instead, we discovered that the individuals closest to the input of water incorporated the greatest amount of carbon, and those near the outflow showed no measurable carbon incorporation, indicating that the most productive individuals near the input were limiting some substrate for those downstream. This pattern was clearly seen in the exposure treatments (Fig.4.4). Because both sulfur and oxygen were not completely depleted in the effluent, it is unclear which of these substrates, or any other substrate for that matter, was restricting the productivity of the symbioses. Moreover, it is plausible that waste-products from the more productive individuals may have inhibited productivity by those located downstream, though it is unclear what those waste-products might be (the predominant waste-products of chemoautotrophic sulfide oxidation are oxidized sulfur compounds and hydrogen ions) (Girguis, Childress, Freytag, et al. 2002; Girguis & Childress 1998).

Our results have important implications for our understanding of total productivity of assemblages of these organisms in their habitats, particularly if the observed variability in carbon fixation rates is due to sulfur limitation. Large communities of these symbioses are often found piled around hydrothermal vent orifices, often two to seven animals deep (C. Fisher, pers. comm.). In these piles, an individual's access to sulfide (or any vent-derived substrate) is governed by the confluence of end-member concentration, fluid flow rate, and animal/microbial uptake rate. *In situ* populations are likely experiencing gradients in vent-derived geochemistry resulting

from the net effect of biotic and abiotic factors. Our data suggest that competition for vent-derived resources, which is tied to spatial position in the fluid flow relative other individuals, may be significant for these symbioses. Interestingly, these results also provide another perspective from which to view thiosulfate-driven autotrophy in these ecosystems. At the tops of the assemblages, where vent-derived reductants may be depleted by the activity of those below, use of an energy source that is not sourced from venting fluid could sustain productivity. Therefore, metabolic flexibility has the potential to relieve competition for vent-derived reductants, both within and between genera.

Excretion of sulfur compounds

Though links between the distribution of particular ELSC symbioses and elevated concentrations of partially oxidized sulfur may indicate a preference for that particular geochemical niche, it is also possible that such correlation may be the result from excretion of that compound by the associated symbioses. To address the potential for sulfur excretion by the ELSC symbioses, we measured the production of partially oxidized sulfur in our incubations. Our sulfide exposure treatment showed that these symbioses have the potential to contribute to the partially oxidized sulfur pools in their environment. During the ~350 μM sulfide exposure treatment, the snail *I. nautilei* released polysulfides (as previously described in Gartman *et al.*, (2011). Additionally, both *Alviniconcha* and *B. brevior* excreted thiosulfate, though the mass-specific rate was nine times higher in *Alviniconcha*. Since our incubations were performed on intact symbioses, we are unable to discern which partner, host or symbiont, is the source of the excreted sulfur. Many invertebrates, even those without chemoautotrophic symbionts, detoxify sulfide via oxidation to thiosulfate with their mitochondria (Grieshaber & Völkel 1998). Because we did not observe sulfur excretion in the other incubation with a lower sulfide concentration (i.e., the rate

experiment with a ~105 μM sulfide), this could be the case. Additionally, *B. brevior* did not fix carbon when exposed to ~350 μM sulfide, though sulfide oxidation was observed. The sulfide concentration in this treatment was much higher than what *B. brevior* would experience *in situ* (Podowski et al. 2009; Podowski et al. 2010; Sen et al. 2013), thus it is possible that it was oxidizing sulfide to thiosulfate as a detoxification mechanism.

It is also conceivable that the excreted partially oxidized sulfur was the product of sulfide oxidation by the symbionts of these animals. Experiments with the sulfur-oxidizing isolate *Thiobacillus thioparus* showed that both thiosulfate and polysulfides can be produced via sulfide oxidation when oxygen is limiting (van den Ende & Gemerden 1993). Though >5 μM oxygen was always detected in the effluent of the aquaria (data not shown), respiration by the high biomass in the exposure treatment could have caused low concentrations in the aquaria, resulting in high sulfide to oxygen ratios. In addition, the symbionts of the vent tubeworm *Riftia pachyptila* produce polysulfides from the oxidation of sulfide *in vitro* (Wilmot & Vetter 1990), though this is thought to be a normal intermediate during the production of sulfur granules as it is with other sulfide oxidizers (Dahl & Prange 2006).

Regardless of the partner of origin, net excretion of partially oxidized sulfur by these symbioses reveals a biological source for these compounds *in situ*. High polysulfide concentrations are detected around *I. nautilei* and *Alviniconcha* at the ELSC, while high thiosulfate concentrations are found around *B. brevior* (Gartman et al. 2011; Waite et al. 2008; Mullaugh et al. 2008). It was suggested previously that these partially oxidized sulfur compounds result from the abiotic oxidation of sulfide in venting fluid by aqueous iron or rocky substrate, or from biological oxidation by the symbioses. Here, we demonstrate that biological oxidation may influence the presence of these sulfur compounds, ultimately affecting the local sulfur regime. Since both free-living microbes and vent symbioses can use these compounds for autotrophy, biological sulfur

transformations have the potential to affect the distribution and activities of many organisms within these ecosystems.

Conclusions

The extent to which vent symbioses can use exogenous thiosulfate to drive autotrophy remains unknown, though genomic analyses of the symbionts of vent organisms has revealed that many possess the metabolic pathway for the oxidation of sulfur, including thiosulfate (Kleiner et al. 2012; Newton et al. 2007; Kuwahara et al. 2007; Robidart et al. 2008; Nakagawa et al. 2013; Gardebrecht et al. 2011). Thiosulfate concentrations at vent habitats have only been extensively surveyed at the ELSC. However, given the rapid abiotic oxidation of sulfide to thiosulfate in the presence of certain metals (Santos Afonso & Stumm 1992; Pyzik & Sommer 1981), as well as the potential for some symbioses to contribute to pools of partially oxidized sulfur, it is likely that it is also present in other systems. Thiosulfate-fueled autotrophy has ecological benefits, particularly for symbioses that cannot be near the high concentrations of reductants in venting fluid, either due to physiological intolerance to high temperatures or toxic vent chemicals, or because of competitive exclusion. Additionally, flexible use of multiple reductants may help vent symbioses cope with periods of low exposure to reductants in vent fluid that result from the temporal and spatial inconsistency of these habitats. Though we showed that access to particular sulfur compounds differentially affects the productivity of these symbioses, the ability of all three, coexisting genera to fuel autotrophy with both sulfide and thiosulfate indicates that metabolic flexibility has important advantages in these ecosystems.

Altogether, these experiments broaden our understanding of sulfur metabolism in animal-bacterial symbioses at hydrothermal vents. Though it has long been expected that vent symbioses can alter the local geochemical regime through the uptake and oxidation of sulfide, the observed

excretion of partially oxidized sulfur suggests a new mode for these associations to affect their ecosystem. Since the discovery of hydrothermal vents, sulfide has been known to play a fundamental role in structuring and supporting vent assemblages (Fisher et al. 2007); here, our data suggests that the influence of vent symbioses on sulfur biogeochemical cycling extends beyond the acquisition and oxidation of sulfide, and the resulting production of sulfate. Rather, these symbioses may be influencing the availability of partially oxidized sulfur compounds that are of energetic value to the free-living microbes that live in these ecosystems. While tubeworm symbioses have previously been described as ecosystems engineers for the role they play in shaping the physical structure of their environment, these data extend that role and illustrate the extent to which they might govern the local sulfur regime.

Acknowledgements

This material is based upon work supported by the National Science Foundation (GRF grant no. DGE-1144152 to RAB, OCE-0732439 to GWL, and OCE-0732369 to PRG). We are grateful for the crews of the *RV Thomas G. Thompson* and the *ROV JASON II* for their support. We thank A. Thomsen, R. Hussey and T. Galyean for their assistance with the sulfide measurements from our discrete samples; and G. Hunsinger from the Yale Institute of Biospheric Studies' Earth System Center for Stable Isotopic Studies.

References

Amend, J.P. et al., 2011. Catabolic and anabolic energy for chemolithoautotrophs in deep-sea hydrothermal systems hosted in different rock types. Geochimica Et Cosmochimica Acta, 75(19), pp.5736–5748.

Beinart, R.A. et al., 2012. Evidence for the role of endosymbionts in regional-scale habitat partitioning by hydrothermal vent symbioses. Proceedings of the National Academy of Sciences. Online only.

Belkin, S., Nelson, D.C. & Jannasch, H.W., 1986. Symbiotic assimilation of CO_2 in the two hydrothermal vent animals, the mussel *Bathymodiolus thermophilus* and the tubeworm *Riftia pachyptila*. Biol Bull, 170(1), pp.110–121.

Brendel, P.J. & Luther, G., 1995. Development of a gold amalgam voltammetric microelectrode for the determination of dissolved Fe, Mn, O_2, and S (-II) in porewaters of marine and freshwater sediments. Environmental Science & Technology, 29(3), pp.751-761

Childress, J.J. & Mickel, T.J., 1980. A motion compensated shipboard precision balance system. Deep Sea Research Part A. Oceanographic Research Papers, 27(11), pp.965–970.

Childress, J.J. et al., 1991. Sulfide and carbon dioxide uptake by the hydrothermal vent clam, *Calyptogena magnifica*, and its chemoautotrophic symbionts. Physiological Zoology, 64(6), pp.1444–1470.

Childress, J.J. et al., 1998. The role of a zinc-based, serum-borne sulphide-bidning component in the uptake and transport of dissolved sulphide by the chemoautotrophic symbiont-containing clam *Calyptogena elongata*. J Exp Biol, 179(1), pp.131–158.

Cline, J.D., 1969. Spectrophotometric determination of hydrogen sulfide in natural waters. Limnol. Oceanogr., 14, pp.454–458.

Dahl, C. & Prange, A., 2006. Bacterial sulfur globules: occurrence, structure and metabolism. Inclusions in Prokaryotes. Shively, J.M. (ed.). Heidelberg: Springer-Verlag, pp. 21–51.

Dando, P.R., Southward, A.J. & Southward, E.C., 1986. Chemoautotrophic symbionts in the gills of the bivalve mollusc *Lucinoma borealis* and the sediment chemistry of its habitat. Proceedings of the Royal Society B-Biological Sciences, 227(1247), pp.227–247.

Dubilier, N., Windoffer, R. & Giere, O., 1998. Ultrastructure and stable carbon isotope composition of the hydrothermal vent mussels *Bathymodiolus brevior* and *B.* sp. affinis *brevior* from the North Fiji Basin, western Pacific. Marine Ecology Progress Series, 165, pp.187–193.

Fisher, C.R. et al., 1987. The importance of methane and thiosulfate in the metabolism of the bacterial symbionts of two deep-sea mussels. Marine Biology, 96(1), pp.59–71.

Fisher, C.R., Takai, K. & Le Bris, N., 2007. Hydrothermal vent ecosystems. Oceanography,

20(1), pp.14–23.

Gardebrecht, A. et al., 2011. Physiological homogeneity among the endosymbionts of *Riftia pachyptila* and *Tevnia jerichonana* revealed by proteogenomics. 6(4), pp.766–776.

Gartman, A. et al., 2011. Sulfide oxidation across diffuse flow zones of hydrothermal vents. Aquatic Geochemistry, 17(4-5), pp.583–601.

Giere, O. et al., 1988. Contrasting effects of sulfide and thiosulfate on symbiotic CO_2-assimilation of *Phallodrilus leukodermatus* (Annelida). Marine Biology, 97(3), pp.413–419.

Girguis, P.R. & Childress, J.J., 1998. H^+ equivalent elimination by the tube-worm *Riftia pachyptila*. Cahiers De Biologie Marine, 39(3-4), pp.295–296.

Girguis, P.R. & Childress, J.J., 2006. Metabolite uptake, stoichiometry and chemoautotrophic function of the hydrothermal vent tubeworm *Riftia pachyptila*: responses to environmental variations in substrate concentrations and temperature. Journal of Experimental Biology, 209(18), pp.3516–3528.

Girguis, P.R. et al., 2000. Fate of nitrate acquired by the tubeworm *Riftia pachyptila*. Applied and Environmental Microbiology, 66(7), pp.2783–2790.

Girguis, P.R., Childress, J.J., Freytag, J.K., et al., 2002. Effects of metabolite uptake on proton-equivalent elimination by two species of deep-sea vestimentiferan tubeworm, *Riftia pachyptila* and *Lamellibrachia* cf *luymesi*: proton elimination is a necessary adaptation to sulfide-oxidizing chemoautotrophic symbionts. Journal of Experimental Biology, 205(19), pp.3055–3066.

Grieshaber, M.K. & Völkel, S., 1998. Animal adaptations for tolerance and exploitation of poisonous sulfide. Annual Review of Physiology, 60, pp.33–53.

Gru, C. et al., 1998. Determination of reduced sulfur compounds by high-performance liquid chromatography in hydrothermal seawater and body fluids from Riftia pachyptila. The Analyst, 123(6), pp.1289–1293.

Henry, M.S., Childress, J.J. & Figueroa, D., 2008. Metabolic rates and thermal tolerances of chemoautotrophic symbioses from Lau Basin hydrothermal vents and their implications for species distributions. Deep Sea Research Part I: Oceanographic Research Papers, 55(5), pp.679–695.

Huelsenbeck, J.P. & Ronquist, F.R., 2001. MRBAYES: Bayesian inference of phylogeny. Bioinformatics, 17, pp.754–755.

Kelly, D.P., 1999. Thermodynamic aspects of energy conservation by chemolithotrophic sulfur bacteria in relation to the sulfur oxidation pathways. Archives of Microbiology, 171(4), pp.219–229.

Kleiner, M., Petersen, J.M. & Dubilier, N., 2012. Convergent and divergent evolution of metabolism in sulfur-oxidizing symbionts and the role of horizontal gene transfer. Current

Opinion in Microbiology, 15(5), pp.621–631.

Kuwahara, H. et al., 2007. Reduced Genome of the Thioautotrophic Intracellular Symbiont in a Deep-Sea Clam, *Calyptogena okutanii*. Current Biology, 17(10), pp.881–886.

Lane, D.J., 1991. 16S/23S rRNA sequencing E. Stackebrandt, M. Goodfellow, & undefined author, eds., New York: J. Wiley and Sons.

Luther III, G.W. et al., 2001. Sulfur speciation monitored in situ with solid state gold amalgam voltammetric microelectrodes: polysulfides as a special case in sediments, microbial mats and hydrothermal vent waters. Journal of Environmental Monitoring, 3(1), pp.61–66.

Luther III, G.W. et al., 2001. Chemical speciation drives hydrothermal vent ecology. Nature, 410(6830), p.813.

Mullaugh, K.M. et al., 2008. Voltammetric (Micro)Electrodes for the In Situ Study of Fe^{2+} Oxidation Kinetics in Hot Springs and S_2O Production at Hydrothermal Vents. Electroanalysis, 20(3), pp.280–290.

Nakagawa, S. et al., 2013. Allying with armored snails- the complete genome of gammaproteobacterial endosymbiont. pp.1–12.

Nelson, D.C. & Hagen, K.D., 1995. Physiology and biochemistry of symbiotic and free-living chemoautotrophic sulfur bacteria. Amer. Zool., 35(2), pp.91–101.

Nelson, D.C., Hagen, K.D. & Edwards, D.B., 1995. The gill symbiont of the hydrothermal vent mussel *Bathymodiolus thermophilus* is a psychrophilic, chemoautotrophic, sulfur bacterium. Marine Biology, 121(3), pp.487–495.

Newton, I.L.G. et al., 2007. The *Calyptogena magnifica* chemoautotrophic symbiont genome. Science (New York, N.Y.), 315(5814), pp.998–1000.

Petersen, J.M. et al., 2011. Hydrogen is an energy source for hydrothermal vent symbioses. Nature, 476(7359), pp.176–180.

Plummer, M. et al., 2006. CODA: convergence diagnosis and output analysis for MCMC. R News, 6(1), pp.7–11.

Podowski, E.L. et al., 2010. Biotic and abiotic factors affecting distributions of megafauna in diffuse flow on andesite and basalt along the Eastern Lau Spreading Center, Tonga. Marine Ecology Progress Series, 418, pp.25–45.

Podowski, E.L. et al., 2009. Distribution of diffuse flow megafauna in two sites on the Eastern Lau Spreading Center, Tonga. Deep-Sea Research Part I, 56(11), pp.2041–2056.

Polz, M.F. et al., 1998. Trophic ecology of massive shrimp aggregations at a Mid-Atlantic Ridge hydrothermal vent site. Limnology and Oceanography, 43(7), pp.1631–1638.

Ponsard, J. et al., 2012. Inorganic carbon fixation by chemosynthetic ectosymbionts and

nutritional transfers to the hydrothermal vent host-shrimp *Rimicaris exoculata*. The ISME journal, 7(1), pp.96–109.

Pruesse, E., Peplies, J. & Glöckner, F.O., 2012. SINA: accurate high-throughput multiple sequence alignment of ribosomal RNA genes. Bioinformatics.

Pyzik, A.J. & Sommer, S.E., 1981. Sedimentary iron monosulfides: Kinetics and mechanism of formation. Geochimica Et Cosmochimica Acta.

Robidart, J.C. et al., 2008. Metabolic versatility of the *Riftia pachyptila* endosymbiont revealed through metagenomics. Environmental microbiology, 10(3), pp.727–737.

Robinson, J.J. et al., 1998. Physiological and immunological evidence for two distinct C1-utilizing pathways in *Bathymodiolus puteoserpentis* (Bivalvia: Mytilidae), a dual endosymbiotic mussel from the Mid-Atlantic Ridge. Marine Biology, 132(4), pp.625–633.

Santos Afonso, Dos, M. & Stumm, W., 1992. Reductive dissolution of iron (III)(hydr) oxides by hydrogen sulfide. Langmuir, 8, pp.1671–1675

Schmidt, C. et al., 2008. Geochemical energy sources for microbial primary production in the environment of hydrothermal vent shrimps. Marine Chemistry, 108(1-2), pp.18–31.

Scott, K.M. & Cavanaugh, C.M., 2007. CO2 Uptake and Fixation by Endosymbiotic Chemoautotrophs from the Bivalve Solemya velum. Applied and Environmental Microbiology, 73(4), pp.1174–1179.

Sen, A. et al., 2013. Distribution of mega fauna on sulfide edifices on the Eastern Lau Spreading Center and Valu Fa Ridge. Deep Sea Research Part I: Oceanographic Research Papers, 72, pp.48–60.

Sievert, S. & Vetriani, C., 2012. Chemoautotrophy at deep-sea vents: past, present, and future. Oceanography, 25(1), pp.218–233.

Stein, J.L. et al., 1988. Chemoautotrophic symbiosis in a hydrothermal vent gastropod. Biological Bulletin, 174(3), pp.373–378.

Stewart, F.J.F., Newton, I.L.G.I. & Cavanaugh, C.M.C., 2005. Chemosynthetic endosymbioses: adaptations to oxic-anoxic interfaces. Trends in Microbiology, 13(9), pp.439–448.

Suzuki, Y., Kojima, S., Sasaki, T., et al., 2006a. Host-symbiont relationships in hydrothermal vent gastropods of the genus *Alviniconcha* from the Southwest Pacific. Applied and Environmental Microbiology, 72(2), pp.1388–1393.

Suzuki, Y., Kojima, S., Watanabe, H., et al., 2006b. Single host and symbiont lineages of hydrothermal vent gastropods *Ifremeria nautilei* (Provannidae): biogeography and evolution. Marine Ecology Progress Series, 315, pp.167–175.

Suzuki, Y., Sasaki, T., Suzuki, M., Nogi, Y., et al., 2005a. Novel chemoautotrophic

endosymbiosis between a member of the Epsilonproteobacteria and the hydrothermal-vent gastropod *Alviniconcha* aff. *hessleri* (Gastropoda : Provannidae) from the Indian Ocean. Applied and Environmental Microbiology, 71(9), pp.5440–5450.

Suzuki, Y., Sasaki, T., Suzuki, M., Tsuchida, S., et al., 2005b. Molecular phylogenetic and isotopic evidence of two lineages of chemo auto trophic endosymbionts distinct at the subdivision level harbored in one host-animal type: The genus *Alviniconcha* (Gastropoda : Provannidae). Fems Microbiology Letters, 249(1), pp.105–112.

Teske, A. et al., 2000. Diversity of thiosulfate-oxidizing bacteria from marine sediments and hydrothermal vents. Applied and Environmental Microbiology, 66(8), pp.3125–3133.

van den Ende, F.P. & Gemerden, H.V., 1993. Sulfide oxidation under oxygen limitation by a *Thiobacillus thioparus* isolated from a marine microbial mat. FEMS Microbiology Ecology, 13(1), pp.69–77.

Vetter, R.D., 1985. Elemental sulfur in the gills of three species of clams containing chemoautotrophic symbiotic bacteria: a possible inorganic energy storage compound. Marine Biology.

Waite, T.J. et al., 2008. Variation in sulfur speciation with shellfish presence at a Lau Basin diffuse flow vent site. Journal of Shellfish Research, 27(1), pp.163–168.

Watsuji, T.-O. et al., 2010. Diversity and function of epibiotic microbial communities on the galatheid crab, *Shinkaia crosnieri*. Microbes and Environments, 25(4), pp.288–294.

Watsuji, T.-O., et al., 2012. Cell-Specific Thioautotrophic Productivity of Epsilon-Proteobacterial Epibionts Associated with *Shinkaia crosnieri* S. Bertilsson, ed. PLoS ONE, 7(10), p.e46282.

Wilmot, D.B., Jr & Vetter, R.D., 1990. The bacterial symbiont from the hydrothermal vent tubeworm *Riftia pachyptila* is a sulfide specialist. Marine Biology, 106(2), pp.273–283.

Chapter 5

Intracellular Oceanospirillales among the chemosynthetic symbionts of the hydrothermal vent snail *Alviniconcha*: secondary symbionts or parasites?

(formatted for journal submission)

Summary

Associations between bacteria from the γ-proteobacterial order Oceanospirillales and invertebrates are increasingly recognized as common in marine habitats. Members of the Oceanospirillales exhibit a diversity of interactions with their various hosts, ranging from the catabolism of complex compounds that benefit host growth to attacking and bursting host nuclei. Here, we describe the association between a novel, intracellular Oceanospirillales phylotype and the hydrothermal vent snail *Alviniconcha*. *Alviniconcha* typically harbor chemoautotrophic γ- or ε-proteobacterial symbionts, but we also observed (via fluorescence *in situ* hybridization and transmission electron microscopy) this *Alviniconcha* Oceanospirillales phylotype (AOP) among the dense populations of proteobacterial symbionts that *Alviniconcha* host inside their gill cells. Notably, AOP were separately contained in membrane-bound vacuoles. Using AO-specific quantitative PCR, we surveyed 283 *Alviniconcha* individuals, and found that AOP occurred more frequently and at greater abundance in *Alviniconcha* hosting γ-proteobacterial symbionts. However, the population size of AOP was always minor relative to those of the canonical symbionts. The high incidence of AOP in γ-proteobacteria hosting *Alviniconcha* implies that it could play a significant ecological role for these snails either as a host parasite or as an additional symbiont with unknown physiological capacities.

Introduction

In recent years, lineages from the γ-proteobacterial order Oceanospirillales have emerged as widespread associates of marine invertebrates. In shallow-water habitats, Oceanospirillales are common and even dominant members of the tissue and mucus-associated microbiota of temperate and tropical corals (Bourne et al., 2013; Bayer, Arif, et al., 2013; Bayer, Neave, et al., 2013; La Rivière et al., 2013; Sunagawa et al., 2010; Chen et al., 2013) and sponges (Bourne et

al., 2013; Nishijima et al., 2013; Bayer, Arif, et al., 2013; Kennedy et al., 2008; Bayer, Neave, et al., 2013; Flemer et al., 2011; La Rivière et al., 2013; Sunagawa et al., 2010; Chen et al., 2013), and they have been detected in the gills of commercially important shellfish (Costa et al., 2012), as well as invasive oysters (Zurel et al., 2011). In deep-water habitats, Oceanospirillales have been found in association with hydrothermal vent and hydrocarbon seep bivalves (Jensen et al., 2010; Zielinski et al., 2009), polychaete worms and gastropods from whale carcasses (Johnson et al., 2010; Goffredi et al., 2005; Verna et al., 2010). In almost all cases, the nature of these animal-bacterial relationships remains undetermined. Cultivated members of the Oceanospirillales are heterotrophs known for their abilities to degrade complex organic compounds (Garrity et al., 2005). Thus, hypotheses about the function of animal-associated Oceanospirillales have ranged from parasitic consumers of host tissue to beneficial symbionts that assist in the metabolism or cycling of organic compounds.

Two well-characterized examples from the deep-sea show that Oceanospirillales can be either beneficial or harmful to their hosts. In bone-eating *Osedax* worms found at whale-falls, Oceanospirillales are intracellular symbionts thought to assist in the digestion of bone-derived organic compounds (Goffredi et al., 2005). In contrast, bacteria from another lineage of Oceanospirillales are parasites of *Bathymodiolus* mussels from hydrothermal vent and cold seeps, proliferating in and bursting host nuclei (Zielinski et al., 2009). These cases demonstrate the range of interactions that Oceanospirillales can mediate with marine invertebrates.

Here, we report a novel Oceanospirillales phylotype discovered in a general survey of the bacterial community associated with gill tissue of the hydrothermal vent snail *Alviniconcha*. *Alviniconcha* are dominant members of the animal communities at hydrothermal vents in the south-western Pacific and Indian Ocean (Desbruyeres et al., 1994; Podowski et al., 2009; 2010; Van Dover et al., 2001; Ramirez-Llodra et al., 2007). This symbiotic genus is comprised of at

least five lineages (likely species) that are supported by the productivity of chemoautotrophic bacterial symbionts, which utilize the reductants in emitted fluid for the energy to fix inorganic carbon (Henry et al., 2008; Y. Suzuki, Sasaki, M. Suzuki, Tsuchida, et al., 2005; Y. Suzuki, Sasaki, M. Suzuki, Nogi, et al., 2005; Y. Suzuki et al., 2006; Sanders et al., 2013). Dense populations of the bacterial symbionts reside intracellularly in *Alviniconcha* gill tissue and provide the bulk of host nutrition (Y. Suzuki, Sasaki, M. Suzuki, Tsuchida, et al., 2005; Y. Suzuki, Sasaki, M. Suzuki, Nogi, et al., 2005). *Alviniconcha* snails are typically dominated by one γ- or ε-proteobacterial phylotype according to their species, although individuals from one of these species harbor relatively equal populations of two distinct γ-proteobacterial phylotypes (Beinart et al., 2012). On the basis of molecular surveys and microscopic examination, we describe the phylogenetic relationship of a novel, *Alviniconcha*-associated Oceanospirillales phylotype to other lineages in this order, localize it inside the gill cells of *Alviniconcha*, and report its frequency and abundance across a population of *Alviniconcha* from hydrothermal vents at the Eastern Lau Spreading Center.

Results and Discussion

Identification and phylogeny of an Oceanospirillales phylotype in Alviniconcha

Alviniconcha specimens were obtained from four Lau Basin hydrothermal vent fields, which are separated by 10s of kilometers along the approximately 300 kilometer north-south Eastern Lau Spreading Center (ELSC). The bacterial communities associated with the gills of ELSC *Alviniconcha* were surveyed by amplifying and sequencing 16S rRNA gene sequences from the pooled tissue DNA of 30 individuals recovered from two vent fields (as described in Beinart et al., 2012). While sequences with affiliation to previously known *Alviniconcha* ε- and γ-proteobacterial symbiont phylotypes dominated the survey (Beinart et al., 2012), we also observed a novel

phylotype from the γ-proteobacterial order Oceanospirillales (hereafter referred to as 'AOP' for '*Alviniconcha* Oceanospirillales phylotype'). To augment the clone library, we used BLASTN (Altschul et al., 1990) to search for AOP in 16S rRNA pyrosequence libraries from four *Alviniconcha* individuals (Sanders et al., 2013). This revealed only one matching operational taxonomic unit (OTU) that comprised of sequences with ≥ 97% identity to our AOP sequence. One other OTU was taxonomically characterized as an Oceanospirillales, but only comprised of two, comparatively short sequence reads (94% identity to the AOP sequence).

To ascertain the relationship of AOP to other Oceanospirillales (and, more broadly, the γ-proteobacteria), Bayesian inference was used to construct a phylogeny of 16S rRNA genes (Fig.5.1). AOP falls within a well-supported clade of Oceanospirillales that have all, with the exception of one clone, been found in association with diverse marine invertebrates from various habitats. The closest relatives of AOP are clones recovered from tropical, shallow-water corals from the Caribbean (Sunagawa et al., 2010) and the Great Barrier Reef (Bourne and Munn, 2005). The few cultivated representatives from this clade are members of the genera *Endozoicomonas* and *Spongiobacter*, which have been isolated from sea slugs (Kurahashi and Yokota, 2007), corals (Bayer, Arif, et al., 2013; Yang et al., 2010; Raina et al., 2009), and sponges (Nishijima et al., 2013; Flemer et al., 2011). Though there is increasing evidence that this clade of Oceanospirillales is specific to marine invertebrates, the relationship between its members and their animal hosts, as well as their location in or on host tissue, is, as yet, uncharacterized. A notable exception is "*Candidatus* Endonucleobacter bathymodiolii", a parasite of hydrothermal vent mussels that has been shown to infect host nuclei, multiply and eventually burst from the organelle (Zielinski et al., 2009). The AOP 16S rRNA gene has 95% sequence identity to a "*Ca.* E. bathymodiolii" 16S rRNA gene sequence recovered from a Gulf of Mexico cold seep mussel.

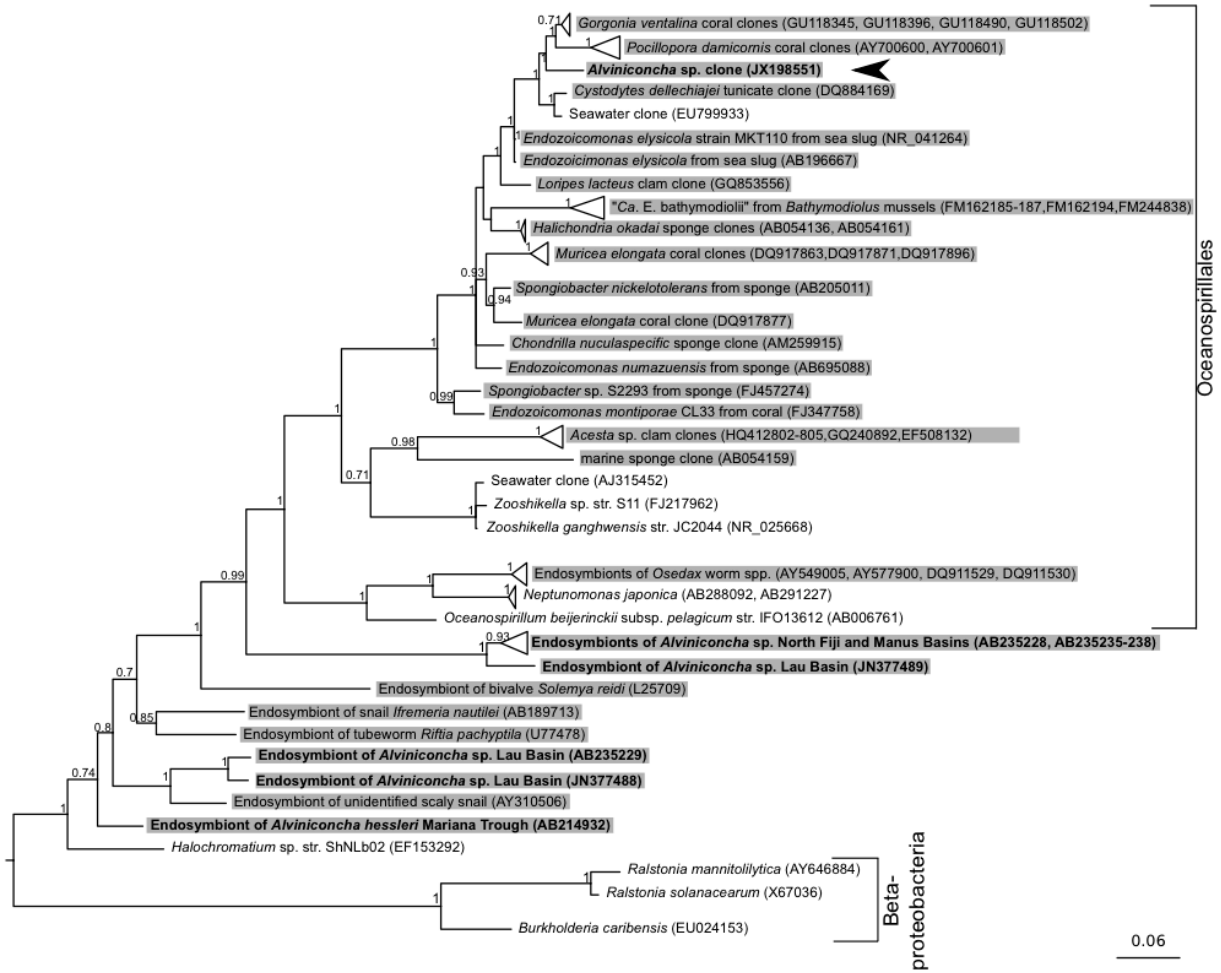

Figure 5.1: A Bayesian inference phylogeny of 16S rRNA gene sequences showing the relationship of AOP (indicated with an arrow) to other Oceanospirillales, the chemoautotrophic symbionts of *Alviniconcha* and other animals, and the sequences from the out-group β-proteobacteria. All *Alviniconcha*-associated sequences are shown in bold. Gray highlighting indicates that the clone or strain has been found in association with a marine invertebrate. Posterior probabilities are indicated above the nodes if >0.7.

Localization of AOP in Alviniconcha *gill tissue*

To localize AOP in *Alviniconcha* gill tissue, we examined *Alviniconcha* individuals via fluorescence in situ hybridization (FISH) using universal bacterial and AOP-specific probes targeting 16S rRNA (Fig.5.2), as well as used transmission electron microscopy (TEM) to describe its morphology in association with *Alviniconcha* gills (Fig.5.3, 5.4). Three animals hosting γ-proteobacterial symbionts and three animals hosting ε-proteobacterial symbionts were selected for these analyses.

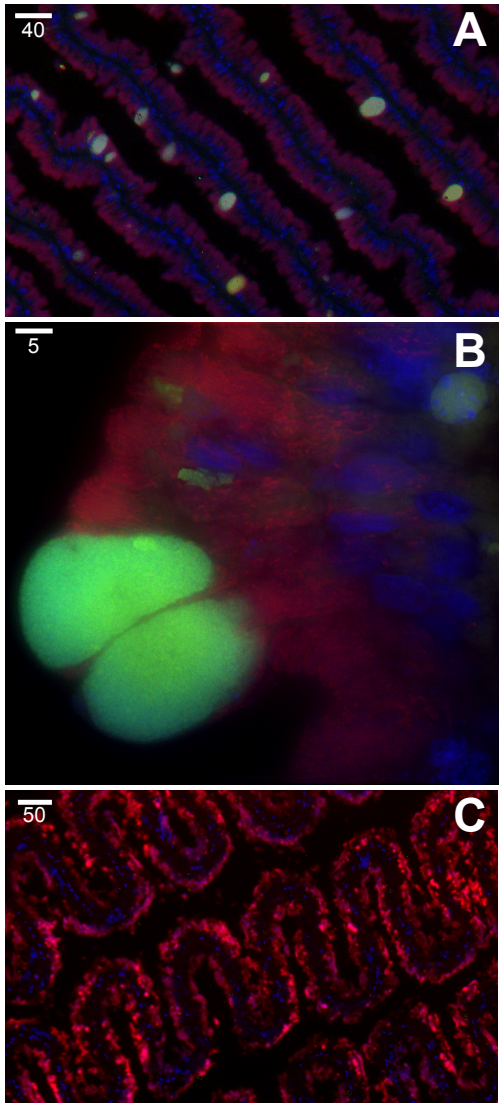

Figure 5.2: Identification of AOP (yellow) and all bacteria (red), including the chemoautotrophic symbionts, in *Alviniconcha* gill tissue with fluorescence *in situ* hybridization. Additionally, DNA-containing organelles or cells were stained with DAPI and shown in blue. (A) Gill filaments of *Alviniconcha* hosting γ-proteobacterial symbionts with AOP-containing vacuoles distributed sporadically. (B) A typical AOP vacuole. (C) Gill filament of *Alviniconcha* hosting ε-proteobacterial symbionts, with no AOP-containing vacuoles. All scale bars are shown in μm.

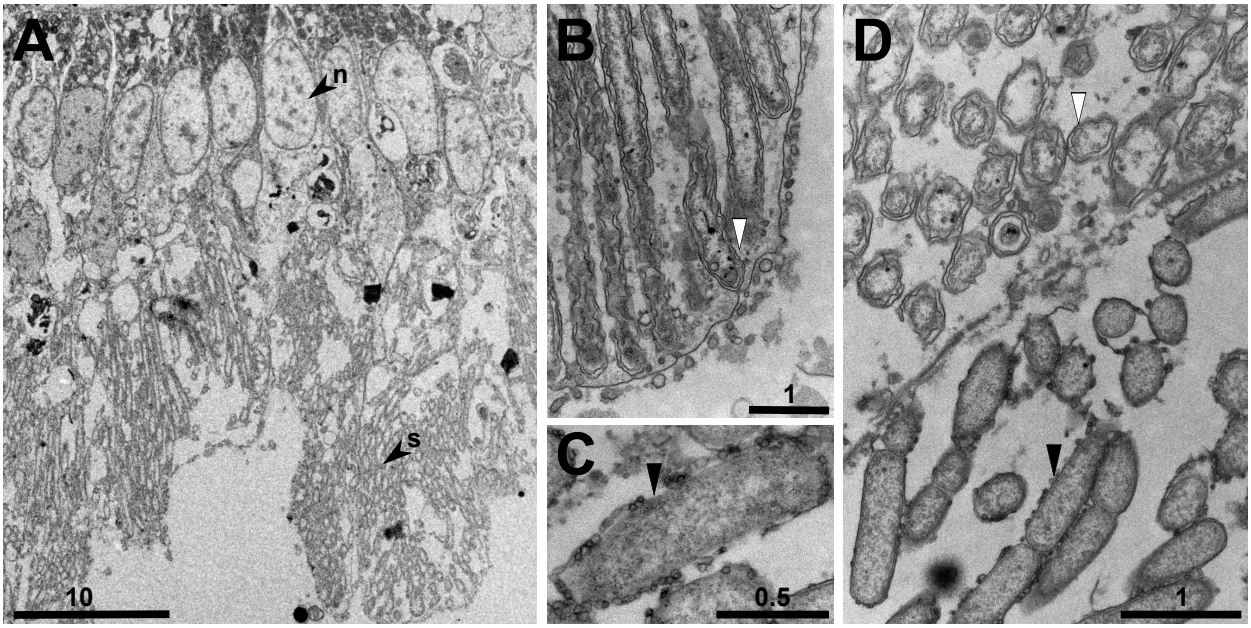

Figure 5.3: Transmission electron micrographs of the γ-proteobacterial symbionts of *Alviniconcha*. (A) One side of a gill filament, showing bacteriocytes, but no suspected AOP-containing vacuoles. n, host nuclei; s, symbiont cells. (B), (C) and (D) show the two symbiont morphotypes, distinguished by white and black arrows. All scale bars are shown in μm.

Examination of *Alviniconcha* gills using FISH confirmed the presence of AOP inside host cells, though there was no evidence of their presence in host nuclei (Fig.5.2a,b). Via FISH, AOP was found to be present only in the gills of the γ-proteobacteria-hosting snails and not in the ε-hosting individuals (Fig.5.2a,c). We consistently found AOP populations localized in vacuoles, approximately 10 - 40 μm in diameter, which were sporadically distributed throughout the gill filaments in symbiont-containing cells (bacteriocytes). Unlike the filamentous and rod-shaped symbionts that dominate gill filaments, the AOP-cells inside these vacuoles appear to be coccoid. The AOP-containing vacuoles were never observed in symbiont-free cells near the dorsal ends of the filaments where they attach to the snail's mantle (not shown). This contrasts sharply with the exclusive infection of "*Ca.* E. bathymodiolii" in the nuclei of symbiont-free intercalary cells in the gills of their mussel hosts (Zielinski et al., 2009).

We also used TEM to examine the structure and morphology of the bacteria inhabiting *Alviniconcha* gill tissue, revealing membrane-bound vacuoles likely containing AOP. Inspection of the gill tissue of a γ-proteobacteria-hosting individual showed that gram-negative, filamentous and rod-shaped bacterial symbionts were densely packed at the apical ends of the cells (Fig.5.3a), consistent with previous descriptions of *Alviniconcha* gill morphology (Endow and Ohta, 1989; Stein et al., 1988; Urakawa et al., 2005). Our examination clearly showed that these canonical symbionts consist of two morphotypes (Fig.5.3b,c,d), which are either free in the host cytoplasm or contained within individual vacuoles (challenges with preservation makes it difficult to distinguish their precise position). These two distinct morphologies very likely represent the two γ-proteobacterial symbiont phylotypes, though they could also reflect morphological variation within a single symbiont phylotype. As we observed via FISH, we found vacuoles containing a third bacterial morphotype–likely the AOP phylotype- distributed sporadically throughout the gill tissue (Fig.5.4). These membrane-bound compartments are full of small (~1 μm), coccoid, gram-negative bacterial cells that contain electron-dense particles, that are somewhat similar to those observed in "*Ca.* E. bathymodiolii" via TEM (Zielinski et al., 2009).

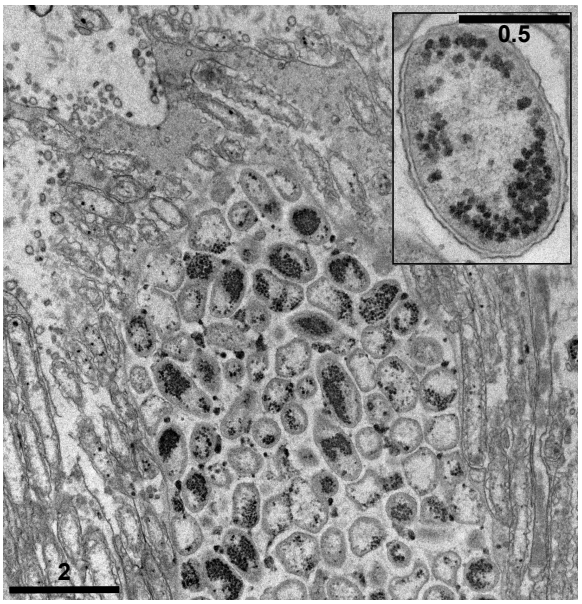

Figure 5.4: A transmission electron micrograph of a suspected AOP vacuole inside a bacteriocyte of a γ-proteobacteria-hosting *Alviniconcha*. Inset shows a single cell inside the suspected AOP vacuole. All scale bars are shown in μm.

Distribution and abundance of AOP in ELSC Alviniconcha

Because our microscopic examination of AOP in gill tissue suggested specificity for *Alviniconcha* types hosting γ-proteobacteria, we used quantitative PCR (qPCR) to examine the distribution and abundance of AOP in 283 *Alviniconcha* from across four vent fields at the ELSC (Supporting Methods). We had previously genotyped these *Alviniconcha* host individuals by sequencing their mitochondrial cytochrome-c oxidase gene and quantified the proportions of the three chemoautotrophic symbiont phylotypes in each using qPCR of their 16S rRNA genes (Beinart et al., 2012). This survey demonstrated that there are three genetically distinct *Alviniconcha* host types (likely undescribed species), which form specific associations with three proteobacterial phylotypes. Host types I and III mainly associate with two γ-proteobacterial phylotypes (γ-1, γ-Lau) and host type II primarily associates with an ε-proteobacterial phylotype (Beinart et al., 2012). Among the three host types, each individual snail is typically dominated by either γ- or ε-proteobacterial symbionts, with only one of the three phylotypes representing >99% of the detected symbiont 16S rRNA genes in a single individual. Minor, co-occurring populations of one of the other phylotypes are sometimes detected, and a small number of γ-proteobacteria-hosting individuals associate with equal proportions of the two γ-proteobacterial phylotypes.

Using qPCR primers targeting AOP's 16S rRNA gene (Supporting Methods), we determined the proportion of AOP relative to the canonical symbiont populations within each snail, as well as their prevalence according to host type (Tables S5.1, S5.2). AOP was detected in 63% of the surveyed *Alviniconcha* individuals but consistently represented only a minor proportion of the total detected bacterial 16S rRNA genes (0-36%, median 0.53%) (Table S5.1, S5.2). As seen with FISH, the prevalence of AOP differed between *Alviniconcha* dominated by ε- and γ-proteobacterial symbionts. In *Alviniconcha* hosting primarily γ-proteobacteria of either or both

phylotypes (host type I and III), AOP was detected in the large majority (96%) of individuals. In contrast, AOP was detected in only 5 of the 102 *Alviniconcha* individuals hosting primarily ε-proteobacteria (mainly host type II, a few host type I).

Along with a greater frequency, we also found a greater relative abundance of AOP 16S rRNA genes in *Alviniconcha* that host γ-proteobacteria (Mann-Whitney U $p<0.0001$, SPSS v20). Similarly, our search of 16S rRNA gene pyrosequences from *Alviniconcha* hosting γ- or ε-proteobacteria (Sanders et al, 2013) revealed that sequences allied to AOP were only detected in *Alviniconcha* that host γ-proteobacteria (0.3 and 2% of the sequence reads). No sequences classified as Oceanospirillales were detected in the *Alviniconcha* hosting ε-proteobacteria. Additionally, when we compared the proportion of AOP 16S rRNA genes among *Alviniconcha* dominated by each symbiont phylotype, excluding the 8 individuals with approximately equal proportions of the two γ-proteobacterial phylotypes, we also observed a significant difference (data not shown; Kruskal-Wallis $p<0.0001$, SPSS v20). Individuals dominated by either the γ-1 or the γ-Lau phylotypes had significantly greater proportions of AOP than individuals dominated by the ε-proteobacterial symbiont (Post-hoc Mann-Whitney U $p<0.0001$ for both, Bonferroni corrected $\alpha=0.0167$, SPSS v20) but were not significantly different than one another (Mann-Whitney U $p=0.027$, Bonferroni corrected $\alpha=0.0167$, SPSS v20). Even within the single host type (III) that can be dominated by either of the γ-proteobacterial phylotypes, we found no significant difference in AOP proportion between individuals dominated by the γ-1 or γ-Lau (Mann-Whitney U $p=0.352$, SPSS v20).

These patterns demonstrated that AOP predominantly associated with *Alviniconcha* hosting γ-proteobacteria and was only rarely detected in *Alviniconcha* hosting ε-proteobacteria. This specificity was relatively consistent throughout *Alviniconcha* from the four ELSC vent fields (Table S5.3), despite the fact that γ- and ε-proteobacteria hosting *Alviniconcha* are conversely

dominant at geographically distant vent fields separated by 10s to 100s of kilometers (Beinart et al., 2012). For example, of the 10 ε-proteobacteria hosting individuals from ABE, a vent field that is inhabited by mostly γ-proteobacteria hosting *Alviniconcha* with typical levels of AOP, only one had detectable AOP. Thus, even at a vent field where most of their neighbors are hosting AOP, *Alviniconcha* hosting ε-proteobacteria still have an apparent low frequency of association. This indicates that geography is not structuring the frequency of AOP in the ELSC *Alviniconcha* population, but rather that biological determinants are more important.

Overall, the observed pattern of correspondence with the γ-proteobacterial symbionts implies that AOP interacts with these particular symbionts and/or has specificity for the two host types that associate with them. It is difficult to resolve these two options, since host and symbiont identity are linked. However, to address this issue, we compared the abundance of AOP among individuals of host type I, which can either associate with γ-proteobacterial or ε-proteobacterial symbionts, and found that there was no significant difference between individuals hosting the different symbiont classes (Mann-Whitney U $p=0.092$, SPSS v20). This must be interpreted with caution, however, since there is a large difference in sample size between host type I individuals hosting ε-proteobacteria ($n=6$) and those hosting γ-proteobacteria ($n=93$). With that caveat, it appears that host type may be more important than symbiont class in determining infection by the AOP.

Potential Modes of Interaction between AOP and Alviniconcha

Here we present two possibilities that represent ends of the spectrum of animal-bacterial associations, from parasitic to beneficial, and consider the degree to which these data are consistent with both scenarios. In terms of parasitism, AOP is closely related to the intranuclear parasites of hydrothermal vent mussels (95% 16S rRNA gene identity). However, we never

definitively observed AO in host nuclei. Even if it is not nuclear-specific, it is possible that AOP represents a parasite or pathogen of *Alviniconcha* that is contained inside a membrane-bound vacuole, as is common with other intracellular pathogens (Goebel and Gross, 2001; Casadevall, 2008; Kumar and Valdivia, 2009). Alternatively, AOP may be mutualistically associated with *Alvinivoncha*. AOP appears to be lower in abundance than the canonical symbionts. As such, AOP may represent a minor, secondary symbiont of *Alviniconcha* that provides beneficial function directly (e.g., the breakdown of an organic compound) or indirectly (e.g., by facilitating the metabolism of the other symbionts). Among insects, secondary symbionts, although an order of magnitude lower in abundance than the primary symbionts, can confer ecologically important advantages for their hosts (Mira and Moran, 2002; Oliver et al., 2010). It is worth noting that AOP is most closely related to *Endozoicomonas*-like phylotypes found in association with tropical, shallow-water corals (Bourne and Munn, 2005; Sunagawa et al., 2010). Recent efforts have led to the cultivation of *Endozoicomonas*-like isolates from corals, and have shown that they can degrade dimethylsulfoniopropionate (DMSP) (Raina et al., 2009) that is produced by the algal symbionts of corals (Van Alstyne et al., 2008). This suggests that *Endozoicomonas* play an important role in sulfur cycling within or around the host corals. Though DMSP production is thought to be specific to marine algae, AOP could similarly play a role in sulfur cycling in *Alviniconcha*.

Conclusions

The discovery of symbioses between chemoautotrophic bacteria and invertebrates led to a watershed of research on these types of associations from many habitats, with much of the focus on the canonical, chemoautotrophic symbionts (Dubilier et al., 2008; Cavanaugh et al., 2006). Throughout 40 years of research, there has been little evidence for the presence of minor microbial associates (i.e., microbes that form specific associations with their hosts but are present

in low abundance, including non-chemoautotrophs). Here, through a combination of phylogenetics, microscopy and qPCR surveys, we have established that AOP are minor, but specific and frequent, associates of *Alviniconcha*. While the precise nature of the interaction remains to be determined, the data presented herein further extends the diversity –and potentially the functional role- of intracellular bacteria associated with *Alviniconcha*. This is the first description of an Oceanospirillales associating with *Alviniconcha* or any other hydrothermal vent gastropod and the second description of an Oceanospirillales associating with a symbiotic, hydrothermal vent mollusc. With growing awareness of the significance of microbes, either as parasites or mutualists, to organismal health and function, investigations of minor microbial associates across the known diversity of invertebrate-chemoautotrophic symbioses are warranted.

Experimental Procedures

Alviniconcha *collections:*

Animals were recovered with the remotely operated vehicle *JASON II* during expedition TM-235 in 2009 on-board the RV *Thomas G. Thompson.* Upon recovery, *Alviniconcha* snails were placed into ice-cold seawater and kept at 4 °C prior to sampling. Gill tissue was excised and preserved for molecular and microscopic analysis of the bacterial populations associated with *Alviniconcha.* See (Beinart et al., 2012) for details of *Alviniconcha* collected for 16S rRNA gene sequencing and the quantitative PCR survey. In addition to these specimens, the gills of six other *Alviniconcha* were fixed for microscopy. The ε-proteobacterial-hosting individuals were collected from the vent field Tow Cam (Dive 432) on June 7, 2009. The γ-proteobacterial-hosting individuals were collected from the vent field ABE (Dive J2-435) on June 14, 2009.

Phylogenetic Analysis

16S rRNA gene sequences were recovered from the pooled DNA of 30 *Alviniconcha* individuals from two vent fields (as described in Beinart et al., 2012). Briefly, the 16S rRNA gene was amplified using the universal bacterial primers 27F and 1492R, cloned with the TOPO TA cloning kit (Invitrogen Inc., Carlsbad, CA USA) and sequenced unidirectionally. BLASTN (Altschul et al., 1990) of all recovered sequences revealed that two of the clones held novel 16S rRNA gene sequences from the Order Oceanospirillales. One clone from this pair was bidirectionally sequenced and deposited in Genbank with accession number JX198551 and the other partial sequence with accession number JX206825. An alignment of 16S rRNA gene sequences was created with the NAST Alignment tool in GreenGenes (DeSantis, Hugenholtz et al. 2006), trimmed to the shortest sequence (1264 positions) with Geneious (Drummond AJ, Ashton B et al. 2011), then used to produce a Bayesian inference phylogeny with MrBayes (Altekar, Dwarkadas et al. 2004) implementing the GTR+I+G model of substitution. Three replicate runs of 10^7 generations each were performed with sampling every 10^3 generations and burn-in of 2500 samples. Quantitative and qualitative diagnostics were performed for each of the three runs using the Coda package in R (Plummer, Best et al. 2006), the three replicate runs were combined and a 50% majority rule consensus tree was created in MrBayes.

Fluorescence in situ hybridization

An oligonucleotide FISH probe (AOP 5'CCGTACTCCAGCCACCCA) targeting the AOP 16S rRNA gene sequences was created by modifying the FISH probe Bnix643 that was previously designed to target the closely related Oceanospirillales found to infect the vent mussels of the genus *Bathymodiolus* (Zielinski et al., 2009). Specific hybridization conditions for the AOP probe were found by varying the concentration of formamide in the hybridization buffer.

Dual FISH hybridizations were performed using a Cy3-labeled, AOP-specific probe (5'CCGTACTCCAGCCACCCA) and Cy5-labeled, universal bacterial EUB338(I-III) probes (Amann et al., 1990). Subsamples of *Alviniconcha* gill tissues were fixed for 12-24 hours at 4°C in 1X phosphate buffered saline (PBS: 137 mM NaCl, 2.7 mM KCl, 10 mM Na_2HPO_4, 2 mM KH_2PO_4) containing 2% paraformaldehyde. Gill samples were subsequently washed three times in 1X PBS, transferred to storage solution of equal parts 1X PBS and ethanol and kept at 4°C until embedding. Gill samples were dehydrated in an ascending ethanol series, washed twice in xylene, then embedded in paraffin. Paraffin blocks were sectioned with a microtome into 5 µm thick sections. The sections were placed onto Super-Frost slides (Fisher Scientific, Waltham, MA USA), dewaxed in three successive baths of xylene for 10 min each and a descending ethanol series (96%, 80%, 70%, 50%) for 5 min each and finally air dried. Each section was circled with a wax pen (PAP-pen, Kisker Biotech, Steinfurt, Germany), then covered with 30% formamide hybridization buffer (Pernthaler et al., 2002) containing fluorescently labeled oligonucleotide probes (5 ng μl^{-1} final concentration). Hybridization, washing, DAPI staining and mounting of sections on slides was performed as in (Jillian et al., 2010). Negative controls to account for background autofluorescence were performed with NON338 (Wallner et al., 1993). Sections were examined and photographed using the fluorescence microscope Axioskop2 mot plus (Carl Zeiss, Inc., Göttingen, Germany). The ImageJ software plugin DeconvolutionLab (Vonesch and Unser, 2008) was used for deconvolution of the images, and ImageJ used for contrast adjustment, and assignment of colors to the different wavelengths.

Transmission Electron Microscopy

Subsamples of the paraformaldehyde fixed gills (see FISH preservation) were post-fixed in a solution of 1% osmium tetroxide and 0.8% potassium ferricyanide in 0.1M sodium cacodylate

with 0.375M NaCl for 1.5 hr at 4°C, then washed in distilled water, dehydrated through an ascending ethanol series, cleared in 100% acetone, and embedded in an epoxy mixture of Embed 812 (Electron Microscopy Sciences, Hatfield, PA USA) and Araldite 506 (Ernest Fulham Inc., Albany, NY USA). Thin sections (80 nm) were obtained using a diamond knife on a LKB Ultramicrotome V followed by staining with 2% uranyl acetate and Reynold's lead citrate, and viewed with a FEI Tecnai Biotwin G2 Spirit electron microscope (Hillsboro, OR USA) operated at 80 kV. The contrast of the micrographs was adjusted in Adobe Photoshop Elements.

Quantitative PCR Survey

A SYBR-green quantitative PCR (qPCR) assay was designed to target the AOP 16S rRNA genes. QPCR was performed with the primers AOP-F (5' TTTCCAGAGATGGATGGGTGCCTT) and AOP-R (5' ACCCAAAGTGCTGGTAACTGAGGA) at a final concentration of 300 μM. The proportion of AOP was estimated in each individual *Alviniconcha* as in (Beinart et al., 2012) using a standard curve made of 10 to 10^7 copies of linearized plasmid containing the 16S rRNA AOP representative sequence. Via tests against plasmid-based standard curves containing the 16S rRNA genes of the other *Alviniconcha* symbiont phylotypes, the AOP-specific qPCR assay was found to cause slight non-specific amplification with the 16S rRNA gene of the *Alviniconcha* symbiont γ-Lau. The maximum number of γ-Lau 16S rRNA gene copies, in any given sample, was on the order of 10^6, which we found would result in non-specific amplification equal to that of 10 copies of AOP. Therefore, to ensure that the number of AOP 16S rRNA gene copies was not overestimated due to this non-specific amplification, 10 copies were subtracted from the AOP counts for all samples. Additionally, all quantities were also adjusted for amplification inhibition as in (Beinart et al., 2012).

Acknowledgements

This material is based upon work supported by the National Science Foundation (GRF grant no. DGE-1144152 to RAB, IOS-0958006 to SVN, and OCE-0732369 to PRG). SVN was also supported by the University of Connecticut Research Foundation. ND is grateful for funding from the Max Planck Society and the DFG Cluster of Excellence 'The Ocean in the Earth System' at MARUM, Bremen. We would like to thank the crews of the *RV Thomas G. Thompson* and the *ROV JASON II* for their support. We thank the Histology Core at the Beth Israel Deaconess Medical Center for embedding the tissue for FISH microscopy, and S. Wetzel of the Max Planck Institute for Marine Microbiology for assistance with FISH sample processing and imaging. Additionally, we are grateful to S. Daniels of the University of Connecticut Electron Microscopy facility for preparation and transmission electron microscopy imaging. We also thank D. Richardson of the Harvard Center for Biological Imaging for assistance with image deconvolution. We also thank A. Knoll, C. Cavanaugh and C. Marx for their comments that improved the quality of this manuscript.

References

Altschul,S.F. et al. (1990) Basic local alignment search tool. *Journal of Molecular Biology* **215**: 403–410.

Amann,R.I. et al. (1990) Combination of 16S rRNA-targeted oligonucleotide probes with flow cytometry for analyzing mixed microbial populations. *Appl. Environ. Microbiol.* **56**: 1919–1925.

Bayer,T., Arif,C., et al. (2013) Bacteria of the genus Endozoicomonas dominate the microbiome of the Mediterranean gorgonian coral Eunicella cavolini. *Mar. Ecol. Prog. Ser.* **479**: 75–84.

Bayer,T., Neave,M.J., et al. (2013) The microbiome of the Red Sea coral Stylophora pistillata is dominated by tissue-associated Endozoicomonas bacteria. *Appl. Environ. Microbiol.*

Beinart,R.A. et al. (2012) Evidence for the role of endosymbionts in regional-scale habitat partitioning by hydrothermal vent symbioses. *Proceedings of the National Academy of Sciences*.

Bourne,D.G. and Munn,C.B. (2005) Diversity of bacteria associated with the coral Pocillopora damicornis from the Great Barrier Reef. *Environ. Microbiol.* **7**: 1162–1174.

Bourne,D.G. et al. (2013) Coral reef invertebrate microbiomes correlate with the presence of photosymbionts. 1–7.

Casadevall,A. (2008) Evolution of Intracellular Pathogens. *Annu. Rev. Microbiol.* **62**: 19–33.
Cavanaugh,C. et al. (2006) Marine Chemosynthetic Symbioses. In, *The Prokaryotes*. pp. 475–507.
Chen,M.H. et al. (2013) Corallomonas stylophorae gen. nov., sp. nov., a halophilic bacterium isolated from the reef-building coral Stylophora pistillata. *International Journal of Systematic and Evolutionary Microbiology* **63**: 982–988.
Costa,P.M. et al. (2012) Molecular detection of prokaryote and protozoan parasites in the commercial bivalve Ruditapes decussatus from southern Portugal. *Aquaculture* **370-371**: 61–67.
Desbruyeres,D. et al. (1994) Deep-sea hydrothermal communities in southwestern Pacific back-arc basins (The North Fiji and Lau Basins) - composition, microdistribution and food-web. *Marine Geology* **116**: 227–242.
Dubilier,N. et al. (2008) Symbiotic diversity in marine animals: the art of harnessing chemosynthesis. *Nat Rev Micro* **6**: 725–740.
Endow,K. and Ohta,S. (1989) The symbiotic relationship between bacteria and a mesogastropod snail, Alviniconcha hessleri, collected from hydrothermal vents of the Mariana back-arc basin. *Bulletin of the Japanese Society of Microbial Ecology* **3**: 73–82.
Flemer,B. et al. (2011) Diversity and antimicrobial activities of microbes from two Irish marine sponges, Suberites carnosus and Leucosolenia sp. *Journal of Applied Microbiology* **112**: 289–301.
Garrity,G.M. et al. (2005) Oceanospirillales ord. nov. In, Brenner,D.J. et al. (eds), *Bergey's Manual® of Systematic Bacteriology*. Springer, New York, pp. 270–323.
Goebel,W. and Gross,R. (2001) Intracellular survival strategies of mutualistic and parasitic prokaryotes. *Trends in Microbiology* **9**: 267–273.
Goffredi,S.K. et al. (2005) Evolutionary innovation: a bone-eating marine symbiosis. *Environ. Microbiol.* **7**: 1369–1378.
Henry,M.S. et al. (2008) Metabolic rates and thermal tolerances of chemoautotrophic symbioses from Lau Basin hydrothermal vents and their implications for species distributions. *Deep Sea Research Part I: Oceanographic Research Papers* **55**: 679–695.
Jensen,S. et al. (2010) Intracellular Oceanospirillales bacteria inhabit gills of Acesta bivalves. *FEMS Microbiology Ecology* **74**: 523–533.
Jillian,M.P. et al. (2010) Dual symbiosis of the vent shrimp Rimicaris exoculata with filamentous gamma-and epsilonproteobacteria at four Mid-Atlantic Ridge hydrothermal vent fields. *Environ. Microbiol.* **9999**:.
Johnson,S.B. et al. (2010) Rubyspira, New Genus and Two New Species of Bone-Eating Deep-Sea Snails With Ancient Habits. *The Biological Bulletin* **219**: 166–177.
Kennedy,J. et al. (2008) Diversity of microbes associated with the marine sponge, Haliclona simulans, isolated from Irish waters and identification of polyketide synthase genes from the sponge metagenome. *Environ. Microbiol.* **10**: 1888–1902.
Kumar,Y. and Valdivia,R.H. (2009) Leading a Sheltered Life: Intracellular Pathogens and Maintenance of Vacuolar Compartments. *Cell Host and Microbe* **5**: 593–601.
Kurahashi,M. and Yokota,A. (2007) Endozoicomonas elysicola gen. nov., sp. nov., a γ-proteobacterium isolated from the sea slug Elysia ornata. *Systematic and Applied Microbiology* **30**: 202–206.
La Rivière,M. et al. (2013) Transient Shifts in Bacterial Communities Associated with the Temperate Gorgonian Paramuricea clavata in the Northwestern Mediterranean Sea. *PLoS ONE* **8**: e57385.
Mira,A. and Moran,N.A. (2002) Estimating Population Size and Transmission Bottlenecks in Maternally Transmitted Endosymbiotic Bacteria. *Microb Ecol* **44**: 137–143.

Nishijima,M. et al. (2013) Endozoicomonas numazuensis sp. nov., a gammaproteobacterium isolated from marine sponges, and emended description of the genus Endozoicomonas Kurahashi and Yokota 2007. *International Journal of Systematic and Evolutionary Microbiology* **63**: 709–714.

Oliver,K.M. et al. (2010) Facultative Symbionts in Aphids and the Horizontal Transfer of Ecologically Important Traits. *Annu. Rev. Entomol.* **55**: 247–266.

Pernthaler,A. et al. (2002) Fluorescence In Situ Hybridization and Catalyzed Reporter Deposition for the Identification of Marine Bacteria. *Appl. Environ. Microbiol.* **68**: 3094–3101.

Podowski,E.L. et al. (2010) Biotic and abiotic factors affecting distributions of megafauna in diffuse flow on andesite and basalt along the Eastern Lau Spreading Center, Tonga. *Mar. Ecol. Prog. Ser.* **418**: 25–45.

Podowski,E.L. et al. (2009) Distribution of diffuse flow megafauna in two sites on the Eastern Lau Spreading Center, Tonga. *Deep-Sea Research Part I* **56**: 2041–2056.

Raina,J.B. et al. (2009) Coral-Associated Bacteria and Their Role in the Biogeochemical Cycling of Sulfur. *Appl. Environ. Microbiol.* **75**: 3492–3501.

Ramirez-Llodra,E. et al. (2007) Biodiversity and Biogeography of Hydrothermal Vent Species Thirty Years of Discovery and Investigations. *Oceanography* **20**: 30–41.

Sanders,J.G. et al. (2013) Metatranscriptomics reveal differences in in situ energy and nitrogen metabolism among hydrothermal vent snail symbionts. *ISME J* 1–12.

Stein,J.L. et al. (1988) Chemoautotrophic symbiosis in a hydrothermal vent gastropod. *Biol. Bull.* **174**: 373–378.

Sunagawa,S. et al. (2010) Threatened corals provide underexplored microbial habitats. *PLoS ONE* **5**: e9554.

Suzuki,Y. et al. (2006) Host-symbiont relationships in hydrothermal vent gastropods of the genus Alviniconcha from the Southwest Pacific. *Appl. Environ. Microbiol.* **72**: 1388–1393.

Suzuki,Y., Sasaki,T., Suzuki,M., Nogi,Y., et al. (2005) Novel chemoautotrophic endosymbiosis between a member of the Epsilonproteobacteria and the hydrothermal-vent gastropod Alviniconcha aff. hessleri (Gastropoda : Provannidae) from the Indian Ocean. *Appl. Environ. Microbiol.* **71**: 5440–5450.

Suzuki,Y., Sasaki,T., Suzuki,M., Tsuchida,S., et al. (2005) Molecular phylogenetic and isotopic evidence of two lineages of chemo auto trophic endosymbionts distinct at the subdivision level harbored in one host-animal type: The genus Alviniconcha (Gastropoda : Provannidae). *FEMS Microbiology Letters* **249**: 105–112.

Urakawa,H. et al. (2005) Hydrothermal vent gastropods from the same family (Provannidae) harbour epsilon- and gamma-proteobacterial endosymbionts. *Environ. Microbiol.* **7**: 750–754.

Van Alstyne,K.L. et al. (2008) Is dimethylsulfoniopropionate (DMSP) produced by the symbionts or the host in an anemone–zooxanthella symbiosis? *Coral Reefs* **28**: 167–176.

Van Dover,C.L. et al. (2001) Biogeography and ecological setting of Indian Ocean hydrothermal vents. *Science* **294**: 818–823.

Verna,C. et al. (2010) High symbiont diversity in the bone-eating worm Osedax mucofloris from shallow whale-falls in the North Atlantic. *Environ. Microbiol.* **12**: 2355–2370.

Vonesch,C. and Unser,M. (2008) A fast thresholded Landweber algorithm for wavelet-regularized multidimensional deconvolution. *Image Processing*.

Wallner,G. et al. (1993) Optimizing fluorescent in situ hybridization with rRNA-targeted oligonucleotide probes for flow cytometric identification of microorganisms. *Cytometry* **14**: 136–143.

Yang,C.S. et al. (2010) Endozoicomonas montiporae sp. nov., isolated from the encrusting pore

coral Montipora aequituberculata. *International Journal of Systematic and Evolutionary Microbiology* **60**: 1158–1162.

Zielinski,F.U. et al. (2009) Widespread occurrence of an intranuclear bacterial parasite in vent and seep bathymodiolin mussels. *Environ. Microbiol.* **11**: 1150–1167.

Zurel,D. et al. (2011) Composition and dynamics of the gill microbiota of an invasive Indo-Pacific oyster in the eastern Mediterranean Sea. *Environ. Microbiol.* **13**: 1467–1476.

Appendix 1

Chapter 1 Supplemental Material

Supporting Information

Beinart et al. 10.1073/pnas.1202690109

SI Methods

Vent Fluid End-Member Calculations. The isobaric gastight samplers used for sampling vent effluent are precharged with a small amount of seawater to fill the dead volume, and varying amounts of ambient seawater may be entrained inadvertently during sampling. The proportions of seawater and vent end-member fluid in the samples were determined via the concentrations of dissolved magnesium ions (Mg^{2+}), because seawater contains abundant Mg^{2+}, whereas end-member hydrothermal fluids exiting the vent orifice typically contain nearly zero Mg^{2+} concentrations (1). End-member vent-fluid composition then is calculated by assuming conservative mixing and extrapolating the measured concentration of a given species to a zero-Mg^{2+} value using a least squares linear regression forced through seawater composition.

PCR Amplification, Sequencing, and Phylogenetic Analyses of the Host Mitochondrial Cytochrome Oxidase 1 Genes. The cytochrome oxidase 1 (CO1) mitochondrial gene was amplified using universal invertebrate primers LCO1490 and HCO2198 (2) in association with the TW2 and Gastro 3 primers (3). PCRs were performed with EconoTaq DNA Polymerase (Lucigen, Inc.), with 5 min at 95 °C, 40 cycles of 40 s at 94°c, 60 s at 50 °C, 90 s at 72 °C, followed by 5 min at 72 °C. PCR products were run on a 1% (wt/vol) agarose gel stained with ethidium bromide to check the quantity and the quality of the products and then were purified with ExoSAP-IT (Affymetrix, Inc.). Purified PCR products for the mitochondrial gene CO1 were sequenced bidirectionally with BigDye chemistry (version 3.1) (Applied Biosystems, Inc.) on an ABI 3730xl capillary sequencer (Applied Biosystems, Inc.). Quality of the sequence reads and alignment of the sequences were assessed with Chromas 2.22 (Technelysium Pty. Ltd.) and Geneious Pro-5 (4). Sequences were aligned with MUSCLE (5) in Mesquite v2.75 (6) and trimmed to 192 characters, the length for which all samples had unambiguous sequence. Bayesian inference phylogenies were produced with BEAST (7) using the SRD06 model of nucleotide evolution (8), which partitions protein coding sequence into first plus second and third codon positions, estimating parameters for each. Three replicate runs of 50 million generations were performed with sampling every 1,000 generations, thinning to every 3,000 generations with a burn-in of 3,000 samples. Quantitative and qualitative diagnostics were performed for each of the three runs using the Coda package in R (9), the three replicate runs were combined using LogCombiner, and a tree was created with TreeAnnotator (7). Host CO1 gene sequences used for phylogenetics were deposited in GenBank; accession numbers can be found in Table S1.

PCR Amplification, Sequencing, and Phylogenetic Analyses of the Symbiont 16S rRNA Genes. 16S rRNA genes were amplified from 30 individual snails from three collections: ABE-1, KM-1, and KM-2. PCR reactions were performed with High Fidelity Platinum Taq polymerase (Invitrogen, Inc.), using universal bacterial 27F and 1492R primers (10), 2 mM $MgSO_4$ for 2 min at 95 °C, 30 cycles of 30 s at 95 °C, 30 s at 55 °C, 90 s at 72 °C, followed by 5 min at 72 °C. PCR products were subjected to electrophoresis on a 1.2% (wt/vol) agarose gel stained with SYBR Safe (Invitrogen, Inc.) to check the quantity and the quality of the products using a U:Genius UV transilluminator (Syngene, Inc.). Then 5 μL of product from each reaction were combined in separate pools for each collection. Pooled PCR products were cleaned and concentrated with the QIAQuick PCR Purification kit (Qiagen, Inc.) and then were cloned with the TOPO TA Cloning kit (Invitrogen, Inc.). Partial sequences from each collection were obtained by sequencing unidirectionally. The resulting 16S rRNA gene sequences were trimmed of vector using Sequencher 4.10 (Gene Codes, Inc.) and classified into phylotypes based on their affiliation, via BLAST (11), with known *Alviniconcha* symbiont phylotypes. Partial sequences were deposited in GenBank under accession nos. JX206808–JX206824, JX206826, and JX206827. Representative longer sequences were aligned with other symbiont and free-living Proteobacterial sequences using the NAST Alignment tool in GreenGenes (12). Bayesian inference phylogenies using separate 1,240-position alignments of the γ- and ε-proteobacteria (with β- and δ-proteobacterial sequences as the outgroups, respectively) were produced with BEAST (7) implementing the GTR+I+G model of substitution. For the ε-proteobacterial tree, three replicate runs of 10 million generations each were performed with sampling every 1,000 generations and burn-in of 3,000 samples. For the γ-proteobacterial tree, three replicate runs of 50 million generations each were performed with sampling every 1,000 generations, thinning to every 5,000 generations (to reduce autocorrelation), and a burn-in of 3,000 samples. Quantitative and qualitative diagnostics were performed for each of the three runs using the Coda package in R (9), the three replicate runs were combined using LogCombiner, and a tree was created with TreeAnnotator (7).

Design and Optimization of Quantitative PCR Assays Targeting the Symbiont 16S rRNA Genes. Primers were designed and initially checked for specificity to *Alviniconcha* symbiont phylotypes by comparison with all available 16S rRNA gene sequences with Primer-BLAST (13). All assays were performed on a Stratagene MX3005p sequence detector (Stratagene, Inc.) in 96-well optical-grade plates and seals. Each assay was optimized using standard curves created from linearized plasmids (pCR2.1; Invitrogen) with the 16S rRNA gene from each symbiont type inserted (same clones as used in phylogenetic analysis). These standard curves spanned seven orders of magnitude and were designed to allow the addition of 10^1–10^7 gene copies as 2 μL of template in each PCR. Twenty-microliter reactions were used, with a final concentration of 1× Perfecta SYBR Green FastMix, low ROX (Quanta BioSciences, Inc.), and varying concentrations of primers (Table S2). PCR cycling conditions were 3 min at 95 °C, then 40 cycles of 30 s at 95 °C, 1 min at 65 °C, and 30 s at 72 °C. Data analyses were carried out with the system software MXPro (Stratagene Inc.). The potential cross-reactivity of each assay for nontarget symbiont sequences was evaluated by comparing the amplification of nontarget controls (plasmids containing nontarget 16S sequences at 10^7 and 10^6 plasmid copies per reaction) with a standard curve (plasmids containing the target 16S sequence) for each quantitative PCR (qPCR) assay. No cross-reactivity was found among any combination of qPCR assay and nontarget plasmids.

Assessment of and Accounting for Amplification Inhibition in qPCR Reactions. To assess potential influences of PCR inhibition on the amplification of the diluted *Alviniconcha* DNA samples, γ-1 qPCR reactions with each diluted DNA sample were spiked with 10^4 copies of target sequence (plasmids containing the target γ-1 16S rRNA gene). An increase in the cycle threshold (C_t) of the positive control caused by inhibition by the diluted DNA extract was detected by comparison with the Ct of the positive control alone. The PCR efficiency was calculated as in ref. 14. The average efficiency for all samples was 98.8% ± 0.07%.

Assessing Symbiont Genome Equivalents with 16S rDNA qPCR. The interpretation of qPCR targeting the 16S rRNA gene can be complicated by the fact that bacterial genomes can contain multiple copies of this gene. Both ε- and γ-proteobacteria have multiple 16S rRNA genes (2.58 copies and 5.81 copies, respectively) (15). However, these averages are likely overestimates for the symbionts of *Alviniconcha*, because the genomes of all chemosynthetic endosymbionts sequenced to date of have been found to contain a single copy of this gene (16–18). Additionally, the differences in the number of detected 16S rRNA genes in the different symbiont phylotypes within a single individual typically were found to be at least one order of magnitude. Therefore, any differences in 16S rRNA gene copy number (if they exist) are not likely to alter the trends found here significantly.

Analysis of Similarity. All multivariate statistics were performed with the software package PRIMER-E (v6) (19). Analysis of similarity tests yield a test statistic, R, that can range from −1 to 1. A value of zero indicates the null hypothesis: that there is equal dissimilarity within and between groups. A value greater than 0 indicates that there is greater dissimilarity among groups than within them, and an R value less than 0 indicates greater dissimilarity within groups than between them. Values of R, if significant, can be compared, because R values are an absolute measure of dissimilarity between groups.

1. Von Damm KL (1995) Controls on the chemistry and temporal variability of seafloor hydrothermal fluids. *Seafloor Hydrothermal Systems: Physical, Chemical, Biological, and Geological Interactions,* Geophys Monogr Ser (American Geophysical Union, Washington, DC), 91:222–247.
2. Folmer O, Black M, Hoeh W, Lutz R, Vrijenhoek R (1994) DNA primers for amplification of mitochondrial cytochrome c oxidase subunit I from diverse metazoan invertebrates. *Mol Mar Biol Biotechnol* 3(5):294–299.
3. Kojima S, et al. (2001) Phylogeny of hydrothermal-vent-endemic gastropods *Alviniconcha* spp. from the western Pacific revealed by mitochondrial DNA sequences. *Biol Bull* 200(3):298–304.
4. Drummond AJ, et al. (2010) Geneious Pro v5.1. Available at www.geneious.com. Accessed February 2012.
5. Edgar RC (2004) MUSCLE: Multiple sequence alignment with high accuracy and high throughput. *Nucleic Acids Res* 32(5):1792–1797.
6. Maddison WP, Maddison DR (2011) Mesquite: A modular system for evolutionary analysis. Version 2.75. Available at http://mesquiteproject.org.
7. Drummond AJ, Rambaut A (2007) BEAST: Bayesian evolutionary analysis by sampling trees. *BMC Evol Biol* 7(1):214.
8. Shapiro B, Rambaut A, Drummond AJ (2006) Choosing appropriate substitution models for the phylogenetic analysis of protein-coding sequences. *Mol Biol Evol* 23(1):7–9.
9. Plummer M, Best N, Cowles K, Vines K (2006) CODA: Convergence diagnosis and output analysis for MCMC. *R News* 6(1):7–11.
10. Lane DJ (1991) 16S/23S rRNA sequencing. *Nucleic Acid Techniques in Bacterial Systematics,* eds Stackebrandt E, Goodfellow M (Wiley and Sons, New York), pp 115–175.
11. Altschul SF, Gish W, Miller W, Myers EW, Lipman DJ (1990) Basic local alignment search tool. *J Mol Biol* 215(3):403–410.
12. DeSantis TZ, Jr., et al. (2006) NAST: A multiple sequence alignment server for comparative analysis of 16S rRNA genes. *Nucleic Acids Res* 34(Web Server issue):suppl 2):W394-9.
13. Rozen S, Skaletsky H (1999) *Primer3 on the WWW for General Users and for Biologist Programmers. Bioinformatics Methods and Protocols, Methods in Molecular Biology*, eds Misener S, Krawetz SA (Humana, Totowa, NJ), Vol 132, pp 365–386.
14. Short SM, Zehr JP (2005) Quantitative analysis of *nifH* genes and transcripts from aquatic environments. *Methods in Enzymology*, ed Jared RL (Academic Press, San Diego) Vol 397, pp 380–394.
15. Lee ZM-P, Bussema C III, Schmidt TM (2009) rrnDB: Documenting the number of rRNA and tRNA genes in bacteria and archaea. *Nucleic Acids Res* 37(Database issue):suppl 1):D489–D493.
16. Robidart JC, et al. (2008) Metabolic versatility of the *Riftia pachyptila* endosymbiont revealed through metagenomics. *Environ Microbiol* 10(3):727–737.
17. Woyke T, et al. (2006) Symbiosis insights through metagenomic analysis of a microbial consortium. *Nature* 443(7114):950–955.
18. Newton ILG, et al. (2007) The *Calyptogena magnifica* chemoautotrophic symbiont genome. *Science* 315(5814):998–1000.
19. Clarke KR, Gorley RN (2006) *Primer v6: User Manual/Tutorial* (*PRIMER-E*, Plymouth, United Kingdom).

Table S1. Contextual information regarding the sample collection sites, including dive numbers, number of individuals (*Alv*), coordinates, habitat type, and oxygen, temperature, and sulfide from cyclic voltammetry scans

Vent field	Dive	Dive date (2009)	*Alv* (*n*)	Collection ID	Latitude and longitude	Habitat	Cyclic voltammetry scan sets (*n*)	Oxygen, μM average (median)	Oxygen, μM minimum (maximum)	Temperature, °C average (median)	Temperature, °C minimum (maximum)	Sulfide, μM average (median)	Sulfide, μM minimum (maximum)
Kilo Moana	J2-J2-421	19 May	4	KM-1	20 3.18′ S, 176 8.02′ W	Chimney wall	0						
	J2-J2-433	6 June	31	KM-2	20 3.23′ S, 176 8.01′ W	Chimney wall	6	88.2 (92.2)	50.5 (118)	6.9 (6.9)	4.8 (9.9)	54.4 (43.4)	29.8 (126)
Total Kilo Moana			35				6						
Tow Cam	J2-422	20 May	15	TC-1	20 19.00′ S, 176 8. 19′ W	Chimney wall	0						
	J2-432*	5 June	27	TC-2	20 18.97′ S, 176 8.19′ W	Chimney wall	0						
	J2-432*	6 June	23	TC-3	20 18.98′ S, 176 8.19′ W	Diffuse flow	2	2.5 (2.5)	2.5 (2.5)	15.6 (15.6)	14.0 (17.2)	70.8 (70.8)	66.6 (75.0)
Total Tow Cam			65				2						
ABE	J2-423	22 May	8	ABE-1	20 45.79′ S, 176 11.47′ W	Chimney wall	0						
	J2-425*,†	25 May	42	ABE-2	20 45.80′ S, 176 11.48′ W	Diffuse flow	4	13.1 (2.5)	2.5 (45.0)	40.9 (47.0)	9.2 (60.2)	239.2 (281)	38.8 (356)
	J2-426*	27 May	9	ABE-3	20 45.80′ S, 176 11.48′ W	Diffuse flow	0						
	J2-431*,†	3 June	15	ABE-4	20 45.80′ S, 176 11.48′ W	Diffuse flow	1						
Total ABE			74				5						
Tu′i Malila	J2-428	28 May	45	TM-1	21 59.36′ S, 176 34.10′ W	Chimney wall	12	55.2 (62.8)	2.5 (91.1)	11.3 (8.9)	5.1 (34.6)	26.5 (15.4)	7.1 (128)
	J2-428	29 May	47	TM-2	21 59.37′ S, 176 34.11′ W	Diffuse flow	0						
	J2-430	1 June	22	TM-3	21 59.35′ S, 176 34.09′ W	Diffuse flow	4	32.9 (29.1)	2.5 (71.0)	16.9 (14.7)	10.9 (27.3)	25.1 (21.4)	7.9 (49.5)
Total Tu′i Malila			114				16						
Total			288				29						

*These collections were <10 m from the other marked collections within the same vent field but are ecologically distinct habitats.
†These collections are from the same site.

Table S2. *Alviniconcha* host mitochondrial CO1 haplotypes, with number of individuals according to vent field

Haplotype	Accession No.	No. of individuals				
		Kilo Moana	Tow Cam	ABE	Tu'i Malila	Total
Host type I 3	JQ624364			1		1
6	JQ624367				1	1
8	JQ624369			2		2
9	JQ624370			1		1
10	JQ624371				1	1
13	JQ624374			1		1
16	JQ624377			5	2	7
17	JQ624378		1	11	4	16
22	JQ624383			1		1
23*	AB235211	1	4	24	13	42
24	JQ624384		1			1
27	JQ624387				1	1
28	JQ624388	5		5	1	11
39	JQ624397				1	1
40	JQ624398		1	5	5	11
41	JQ624399			2		2
49	JQ624407			1		1
51	JQ624408	1				1
53	JQ624410			1		1
55	JQ624412				1	1
Host type II 4	JQ624365		1			1
7	JQ624368		1			1
15	JQ624376		1			1
18	JQ624379		1			1
20	JQ624381		1			1
21	JQ624382			1		1
31	JN402310	7	8	1		16
32	JQ624391		1			1
37	JQ624395			1		1
38	JQ624396	1				1
42	JQ624400	5	6	1		12
44	JQ624402		1			1
48	JQ624406	1				1
56*	AB235212	14	36	4		54
Host type III 1	JQ624362				1	1
2	JQ624363				1	1
5	JQ624366				6	6
11	JQ624372				2	2
12	JQ624373				1	1
14	JQ624375				1	1
19	JQ624380				1	1
25	JQ624385				1	1
26	JQ624386				1	1
29	JQ624389				6	6
30	JQ624390				1	1
33	JQ624392				1	1
34	JQ624393				1	1
35	JN402311				8	8
36	JQ624394				1	1
43	JQ624401				1	1
45	JQ624403				1	1
46	JQ624404				2	2
47	JQ624405				1	1
50*	AB235215				2	2
52	JQ624409				1	1
54	JQ624411			1	35	36

*Haplotypes found in previous studies as well as here.

Table S3. Carbon-stable isotopic values of gill tissues according to dominant symbiont phylotype

Vent field	Symbiont phylotype	*n*	δ^{13}C average ± SD
Kilo Moana	ε	7	−11.5 ± 0.2
Tow Cam	ε	5	−11.4 ± 0.5
	γ-1	2	−29.2
ABE	ε	5	−11.8 ± 0.5
	γ-1	9	−29.5 ± 1.6
Tu'i Malila	γ-1	10	−28.9 ± 1.1
	γ-Lau	25	−26.2 ± 3.2
	γ-Both	8	−26.8 ± 1.9

ε, ε-proteobacteria; γ-1, γ-proteobacteria type 1; γ-Lau, γ-proteobacteria type Lau; γ-Both, snails that have γ-1 and γ-Lau in approximately equal proportions.

Table S4. qPCR primer sets designed to target *Alviniconcha* symbiont phylotypes

Symbiont genotype		Primers (5′–3′)	Amplicon length (bp)	Primers (nM)	Average % efficiency ± SD	Average R^2 ± SD
γ-1	Forward	ACGGAATAAAGGTGGCCTCTGGTT	108	300	90 ± 0.06	0.996 ± 0.002
	Reverse	TGGATCGTCGCCTTGGTAGACCT				
γ-Lau	Forward	CCTTCGGGAGTGAGTAGAGTG	58	300	94 ± 0.04	0.996 ± 0.003
	Reverse	TACTGGGCAGATTTCCACGCGTTA				
ε	Forward	AACGCCGCGTGGAGGATGAC	163	100	90 ± 0.06	0.982 ± 0.016
	Reverse	TACGTGTCCTTTACGCCCAGTGAT				

Average efficiencies and R^2 for plasmid standard curves are shown. Symbiont phylotypes: ε, ε-proteobacteria; γ-1, γ-proteobacteria type 1; γ-Lau, γ-proteobacteria type Lau.

Table S5. Intragill comparison of symbiont proportions

Individual	Vent field (dive)	Gill section	% γ-1	% γ-Lau	% ε
1	Tow Cam (J2-432)	A	0.00	0.00	100.00
		B	0.00	0.00	100.00
		C	0.00	0.00	99.99
2	Tow Cam (J2-432)	A	INH	INH	INH
		B	0.00	0.00	100.00
		C	0.00	0.00	100.00
3	Tow Cam (J2-432)	A	INH	INH	INH
		B	0.00	0.00	100.00
		C	0.00	0.00	100.00
4	ABE (J2-435)*	A	99.99	0.00	0.01
		B	99.92	0.00	0.08
		C	99.84	0.00	0.16
5	ABE (J2-435)*	A	99.96	0.00	0.04
		B	99.92	0.00	0.08
		C	99.97	0.00	0.03
6	ABE (J2-435)*	A	99.99	0.00	0.01
		B	99.87	0.05	0.08
		C	99.87	0.00	0.13

A, adjacent to pallial margin; B, middle gill; C, posterior gill end; J2-435 from cruise TM-235, June–July 2009; INH, amplification was inhibited, thus sample was not measurable; symbiont phylotypes: ε, ε-proteobacteria; γ-1, γ-proteobacteria type 1; γ-Lau, γ-proteobacteria type Lau.

Appendix 2

Chapter 3 Supplemental Material

Supplementary Methods:

***In situ* homogenization**

To effectively preserve holobiont RNA *in situ*, we designed a combined sample container/homogenizer capable of operation at depth, hereafter referred to as the In-Situ Mussel And Snail Homogenizer (ISMASH; Fig. 1). ISMASH consists of a stainless steel cylinder of approximately 1L volume, wherein the cylinder bottom contains a rotating blade assembly (Waring Inc.) and preservative inlet. One-half inch diameter nylon rods are affixed to the interior sides of the blender to disrupt fluid flow and improve blending performance. The rotating blade assembly is coupled via a custom-machined coupling to a hydraulic motor (.218 cubic inch displacement gerotor, max 5000 RPM / 12 HP power / 35 in-lbs torque; Model # MGG20010, Parker Hannifin, Youngstown, OH). Based on approximate hydraulic flow rates from the Jason 2 submersible and motor manufacturer data, we estimate actual blade rotation speeds of approximately 2000-3000 RPM.

The top of the blender chamber is sealed by a detachable lid with an o-ring that seals against the upper flange of the cylinder. The lid is held in place by six pairs of neodymium magnets, one set of which is mounted on the lid while the other set is affixed to the cylinder flange. The lid also includes a polypropylene rope for ease of removal and emplacement by the robotically operated vehicle, as well as a one-way plastic diaphragm-style check valve with a low cracking pressure. The preservative inlet also includes a one-way, low cracking-pressure spring-operated check valve to isolate blender contents, and a compression fitting for connection to the preservative reservoir, a plastic collapsible 10 L container.

For sample collection, the collapsible container is cleaned and filled with the preservative RNALater™ (Ambion Inc), which has been dyed using FD&C red no. 5 food coloring. The preservative container is then affixed to the robotically operated vehicle (ROV) and connected to the inlet at the base of the blender body. Individual samples are collected using the ROV's manipulators, deposited in the cylinder, and the magnetically latched lid is closed by the ROV operator. RNALater™ is pumped into the cylinder by compressing the collapsible container *in situ* using the ROV manipulator, displacing the less-dense seawater through the lid's check valve. Once the cylinder is flooded (as indicated by the color and visible differences in density and refractive index of the effluent emitted from the lid check valve), the hydraulic motor is actuated to homogenize the sample. The time from collection of the sample to homogenization is typically around seven minutes. Upon completion, the sample is left in the chamber until recovery at the surface. One-way check valves on the inlet and outlet, and the robust latching of the lid to the cylinder, ensure that the sample has minimal contact with the surrounding seawater. At the surface, samples are carefully transferred to sterile glass jars and incubated per the manufacturer's instructions prior to freezing for shipment to the laboratory.

Supplementary Figures:

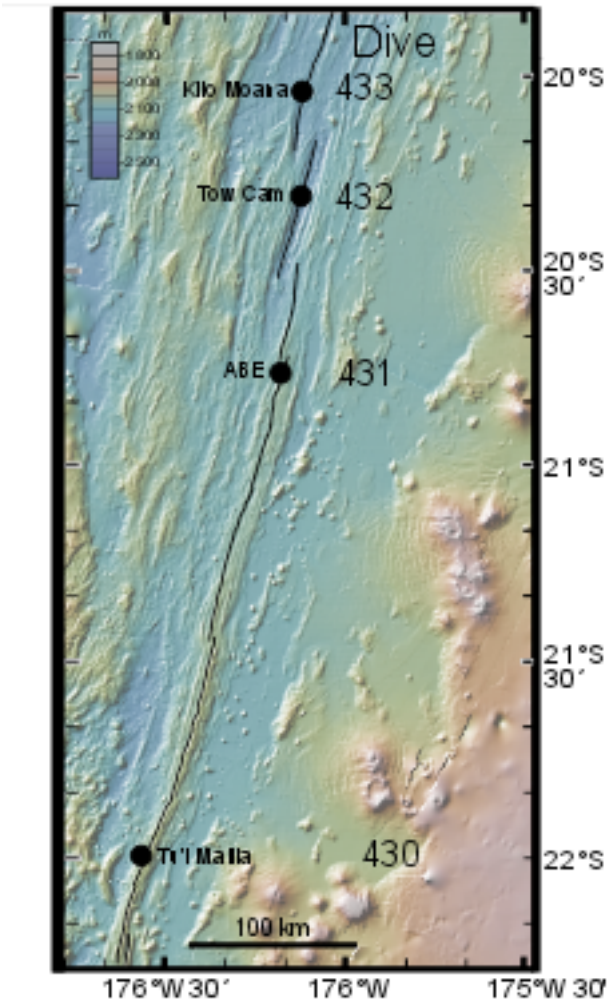

Figure S1: Map of the Eastern Lau Spreading Center, with four vent fields from which *Alviniconcha* were sampled with the ISMASH. Dive numbers associated with each sample are shown next to each vent field.

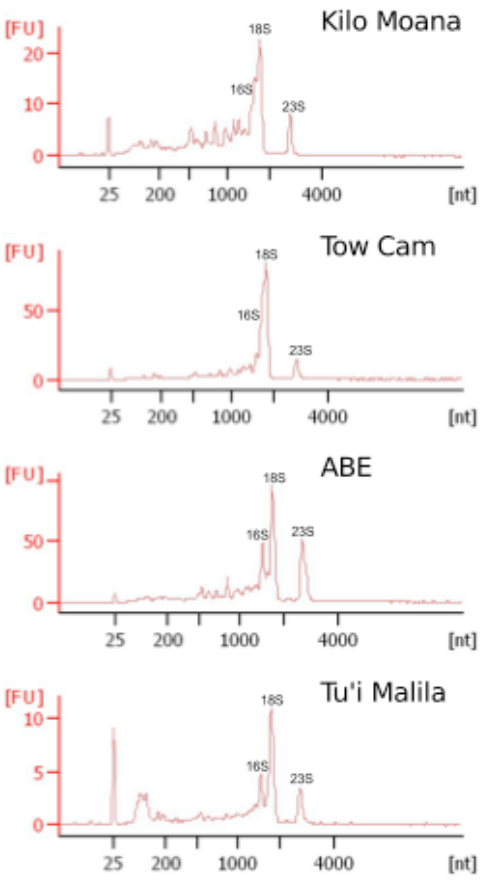

Figure S2: Agilent Bioanalyzer traces of total ISMASH RNA from each sample. Peaks are labeled for bacterial (symbiont) 16S and 23S rRNA and snail host 18S rRNA. In the snails, as with most protostomes, the 28S RNA is post-transcriptionally fragmented into two large pieces that are attached *in vivo* via hydrogen bonds. During extraction, most of these separate and migrate with the 18S rRNA.

Supplementary Table:

Table S1: Normalized read counts for pathways and gene categories discussed here. Annotation was performed in MGRAST using SEED/Subsystems unless indicated by an asterisk (*), which designates MGRAST IMG annotation. † indicates that one or more (non-normalized) reads for this gene was assigned to the non-dominant symbiont class (e.g., assigned to ε-proteobacteria in a γ-dominated metatranscriptome) in MEGAN. "% reads" = the percentage of reads that were allied to the non-dominant symbiont class in that category.

		KM	TC	ABE	TM
MGRAST SEED/Subsystems	EC #	ε	ε	γ	γ
Sulfur Oxidation					
% reads		*0.0*	*0.0*	*1.9*	*0.0*
Sox multienzyme complex					
Sulfur oxidation protein SoxA		1	4	1†	0
Sulfur oxidation protein SoxB		7	10	1†	0
Sulfur oxidation molybdopterin C protein SoxC		104	74	0	0
Sulfite dehydrogenase cytochrome subunit SoxD		6	15	0	0
Sulfur oxidation protein SoxX		0	16	9	9
Sulfur oxidation protein SoxY		3	18	3	2
Sulfur oxidation protein SoxZ		2	15	3	1
Reverse DSR					
Sulfite reductase alpha subunit DsrA	1.8.99.1	0	0	41†	16
Sulfite reductase beta subunit DsrB	1.8.99.1	1	0	47	20
Sulfite reductase, dissimilatory-type gamma subunit DsrC	1.8.99.3	0	0	34	37
DsrE*		0	0	23	18
DsrF*		0	0	2	0
DsrH*		0	0	8	6
Sulfite reduction-associated complex DsrMKJOP multiheme protein DsrJ (=HmeF)		0	0	0	1
Sulfite reduction-associated complex DsrMKJOP protein DsrK (=HmeD)		0	0	25	20
Similar to glutamate synthase [NADPH] small chain, clustered with sulfite reductase DsrL		0	0	26	28
Sulfite reduction-associated complex DsrMKJOP protein DsrM (= HmeC)		0	0	10	19
Sulfite reduction-associated complex DsrMKJOP iron-sulfur protein DsrO (=HmeA)		0	0	4	3
Sulfite reduction-associated complex DsrMKJOP protein DsrP (= HmeB)		0	0	6	13
DsrR*		0	0	0	2

Indirect sulfite oxidation pathway					
Sulfate adenylyltransferase, dissimilatory-type Sat	2.7.7.4	6	1	7†	1
Adenylylsulfate reductase alpha-subunit AprA	1.8.99.2	0	0	54	12
Adenylylsulfate reductase beta-subunit AprB	1.8.99.2	0	0	5	0
Adenylylsulfate reductase membrane anchor	1.8.99.2	0	0	12	3
Sulfide dehydrogenase					
Sulfide dehydrogenase [flavocytochrome C] flavoprotein chain precursor FccB	1.8.2.-	0	0	1	4
sulfide dehydrogenase, flavoprotein subunit FccB	1.8.2.-	0	0	1	0
Sulfide quinone (oxido)reductase					
sulfide qunione (oxido)reductase Sqr		41	66	22†	55
Hydrogen oxidation					
% reads		*0.0*	*0.0*	*0.0*	*0.0*
Hydrogenases					
Uptake hydrogenase cytochrome	1.12.99.6	13	10	1	0
Uptake hydrogenase large subunit	1.12.99.6	19	16	1	0
Uptake hydrogenase small subunit or precursor	1.12.99.6	11	12	1	2
Hydrogen-sensing hydrogenase large subunit		0	1	3	2
Hydrogen-sensing hydrogenase small subunit		0	0	1	0
Dissimilatory nitrogen metabolism					
% reads		*0.0*	*0.0*	*2.5*	*0.0*
Nitrate respiration					
Assimilatory nitrate reductase large subunit NapA	1.7.99.4	19	17	9†	10
Periplasmic nitrate reductase precursor NapA	1.7.99.4	83	52	13	10
Nitrate reductase cytochrome c550-type subunit NapB		58	48	0	0
Cytochrome c-type protein NapC		0	0	8	7
Periplasmic nitrate reductase component NapD		1	0	0	0
Ferredoxin-type protein NapF (periplasmic nitrate reductase)		0	0	1	1
Ferredoxin-type protein NapG (periplasmic nitrate reductase)		19	15	10	6
Polyferredoxin NapH (periplasmic nitrate reductase)		49	39	19	9
Periplasmic nitrate reductase component NapL		0	0	0	0
Denitrification					
Cytochrome cd1 nitrite reductase NirS	1.7.2.1	85	69	2†	3
Nitric-oxide reductase subunit B NorB	1.7.99.7	57	33	23	10
Nitric-oxide reductase subunit C NorC	1.7.99.7	12	12	6	3
Nitric oxide reductase activation protein NorE		0	0	1	2
Nitric oxide reductase activation protein NorD		0	0	6	3
Nitric oxide reductase activation protein NorQ		0	0	4	2
Nitrous-oxide reductase NosZ	1.7.99.6	50	28	7	10
Nitrous oxide reductase maturation protein NosD		2	3	2	2
Nitrous oxide reductase maturation protein NosF (ATPase)		0	2	0	1

Nitrous oxide reductase maturation transmembrane protein NosY		1	3	1	5
Nitrous oxide reductase maturation protein, outer-membrane lipoprotein NosL		0	0	0	0
Nitrogen assimilation					
% reads		*0.0*	*0.0*	*0.0*	*0.0*
Assimilatory nitrite reduction					
Nitrate/nitrite transporter NarK		3	17	3	1
Nitrite reductase [NAD(P)H] large subunit NirB	1.7.1.4	0	0	14	2
Nitrite reductase [NAD(P)H] small subunit NirD	1.7.1.4	0	0	1	2
Ferredoxin--nitrite reductase NirA	1.7.7.1	1	4	0	0
Ammonia assimilation					
Ammonium transporter		17	49	15	21
Glutamine synthetase type I	6.3.1.2	51	57	10	9
Glutamate synthase [NADPH] large chain	1.4.1.13	16	23	50	21
Glutamate synthase [NADPH] small chain	1.4.1.13	18	19	4	13
Carbon Fixation					
Calvin-Benson Cycle					
Triosephosphate isomerase	5.3.1.1	1	1	12	10
Transketolase	2.2.1.1	10	15	56	27
Ribulose-phosphate 3-epimerase	5.1.3.1	1	0	8	8
Ribulose bisphosphate carboxylase	4.1.1.39	0	0	16	6
Ribose 5-phosphate isomerase B	5.3.1.6	2	7	0	0
Ribose 5-phosphate isomerase A	5.3.1.6	0	0	3	6
Phosphoribulokinase	2.7.1.19	0	0	5	8
Phosphoglycerate kinase	2.7.2.3	7	12	19	15
NADPH-dependent glyceraldehyde-3-phosphate dehydrogenase	1.2.1.13	0	0	14	8
NAD-dependent glyceraldehyde-3-phosphate dehydrogenase	1.2.1.12	8	5	4	8
Fructose-bisphosphate aldolase Class II	4.1.2.13	5	4	19	10
Fructose-bisphosphate aldolase class I	4.1.2.13	1	0	0	0
Fructose-1,6-bisphosphatase, type 1	3.1.3.11	2	6	0	0
Fructose-1,6-bisphosphatase, GlpX type	3.1.3.11	2	0	0	1
Reverse TCA Cycle					
Pyruvate:ferredoxin oxidoreductase, alpha subunit	1.2.7.1	24	15	0	0
Pyruvate:ferredoxin oxidoreductase, beta subunit	1.2.7.1	28	22	0	0
Pyruvate:ferredoxin oxidoreductase, gamma subunit	1.2.7.1	5	8	0	0
Pyruvate:ferredoxin oxidoreductase, delta subunit	1.2.7.1	2	1	0	0
Citrate lyase, subunit 1	2.3.3.8	15	7	0	0
Citrate lyase, subunit 2	2.3.3.8	38	49	1	0
2-oxoglutarate oxidoreductase, alpha subunit	1.2.7.3	30	35	1	0
2-oxoglutarate oxidoreductase, beta subunit	1.2.7.3	6	3	0	0
2-oxoglutarate oxidoreductase, gamma subunit	1.2.7.3	19	21	1	0
2-oxoglutarate oxidoreductase, delta subunit	1.2.7.3	33	24	1	0

Flagellum					
Flagellar L-ring protein FlgH		3	1	0	0
Flagellar M-ring protein FliF		8	8	0	0
Flagellar P-ring protein FlgI		0	7	0	0
Flagellar basal-body rod modification protein FlgD		1	5	0	0
Flagellar basal-body rod protein FlgB		4	2	0	0
Flagellar basal-body rod protein FlgC		2	4	0	0
Flagellar basal-body rod protein FlgF		1	0	0	0
Flagellar basal-body rod protein FlgG		4	3	0	1
Flagellar biosynthesis protein FlhA		2	5	0	0
Flagellar biosynthesis protein FlhB		3	2	0	0
Flagellar biosynthesis protein FlhF		1	4	0	0
Flagellar biosynthesis protein FliP		1	1	0	0
Flagellar biosynthesis protein FliQ		0	1	0	0
Flagellar biosynthesis protein FliR		1	1	0	0
Flagellar biosynthesis protein FliS		1	1	0	0
Flagellar hook protein FlgE		5	11	1	0
Flagellar hook-associated protein FlgK		6	4	1	0
Flagellar hook-associated protein FlgL		0	0	1	0
Flagellar hook-associated protein FliD		2	0	0	0
Flagellar hook-basal body complex protein FliE		6	4	0	0
Flagellar hook-length control protein FliK		29	47	0	0
Flagellar motor rotation protein MotA		0	1	1	0
Flagellar motor rotation protein MotB		1	3	1	1
Flagellar motor switch protein FliG		4	3	0	0
Flagellar motor switch protein FliM		4	2	0	0
Flagellar motor switch protein FliN		10	7	0	0
Flagellar protein FlbB		1	0	0	0
Flagellar regulatory protein FleQ		0	0	1	1
Flagellar synthesis regulator FleN		2	1	1	0
Flagellin protein FlaA		31	32	0	1
Flagellin protein FlaB		6	0	0	1
Flagellum-specific ATP synthase FliI		1	2	0	0
Sulfur reduction					
Polysulphide reductase		0	0	1	3

Appendix 3

Chapter 4 Supplemental Material

Table S4.1: Input water conditions for all experiments and treatments. Mean (min, max) sulfide concentrations as determined via a colorimetric assay as applied to discrete water samples of input water; partial pressure of O_2 and calculated concentration of O_2 in input water; mean (min, max); and atom percent of ^{13}C in dissolved inorganic carbon (DIC).

Incubation	Mean [sulfide] (min, max) (µM)	pO_2 (%)	$[O_2]$ (µM)*	Mean A% DIC (min, max)
No sulfur	NA	50	562	5.08 (4.22, 5.59)
Sulfide	105 (57, 137)	27.5	310	5.44 (5.25, 5.75)
Thiosufate	0 (0,0)	54.8	618	4.83 (3.70, 5.63)
Sulfide treatment	388 (338,459)	54.5	615	6.45 (6.28, 6.62)
Thiosulfate treatment	0 (0,0)	52.3	590	3.38 (2.89, 3.74)

*Concentration of O_2 calculated based on concentration of 100% pO_2 in seawater at 20°C, 35 psu (Weiss et al., 1970)

Table S4.2: The average (± S.D.) of the stable isotopic composition of experimental foot and natural tissue expressed as $\delta^{13}C$ (‰).

	Experimental Foot	Natural
Alviniconcha	-27.0 ± 1.16	-27.6 ± 2.30[a]
I. nautilei	-28.0 ± 0.95	-28.5[b]
B. brevior	-28.1 ± 1.93	-30.6 ± 2.52[c]

[a] gill tissue values, Lau Basin, from Beinart et al., 2012
[b] gill tissue value, Lau Basin from Suzuki et al., 2006
[c] foot tissue values, North Fiji Basin from Dubilier et al., 1998

Table S4.3: Proportions of symbiont phylotypes associating with *Alviniconcha* as assessed via quantitative PCR.

Experiment/Treatment	Individual	%γ-1	%γ-Lau	%ε
No sulfur	1	100	0	0
	2	99	1	0
	3	100	0	0
	4	3	97	0
	5	3	96	0
Sulfide	1	100	0	0
	2	100	0	0
	3	93	7	1
	4	99	1	0
	5	96	0	4
Thiosulfate	1	100	0	0
	2	99	0	1
	3	100	0	0
Sulfide treatment	1	0	0	100
	2	99	0	1
	3	99	0	1
	4	100	0	0
	5	100	0	0
	6	0	0	100
	7	0	0	100
	8	0	0	100
	9	0	0	100
	10	0	0	100
Thiosulfate treatment	1	100	0	0
	2	100	0	0
	3	100	0	0
	4	100	0	0
	5	99	0	1
	6	100	0	0
	7	100	0	0
	8	100	0	0

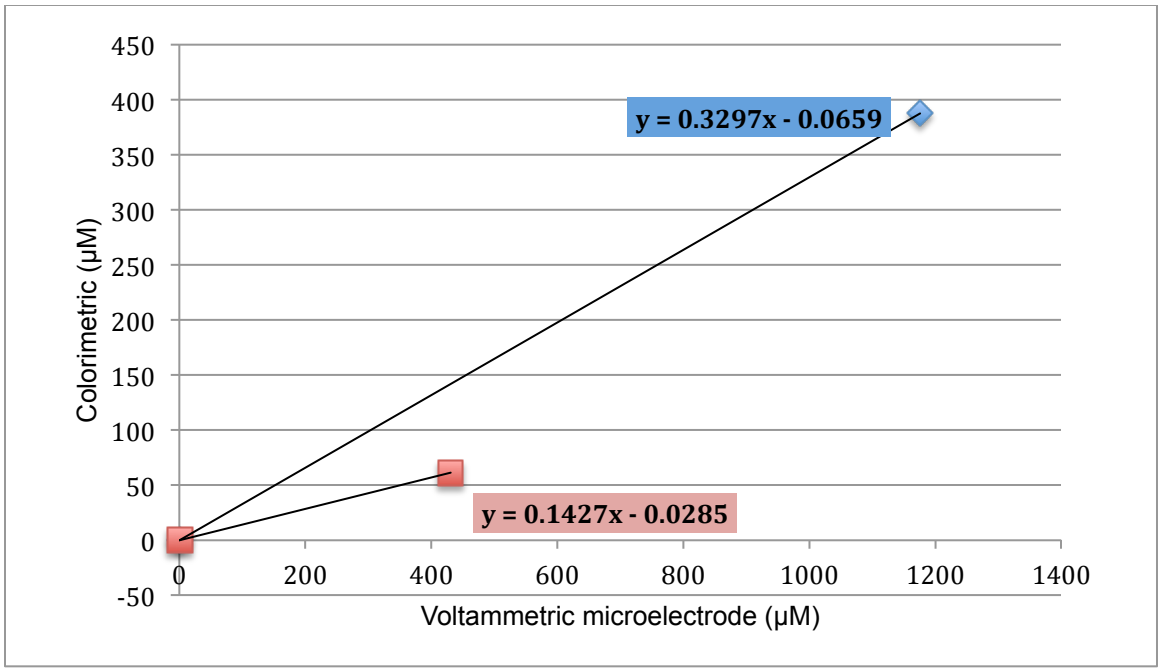

Figure S4.1: Two-point calibration of voltammetric microelectrodes with the average [sulfide] as determined via a colorimetric assay applied to discrete water samples from input water (exposure treatment; blue) or control effluent (rate experiment; red).

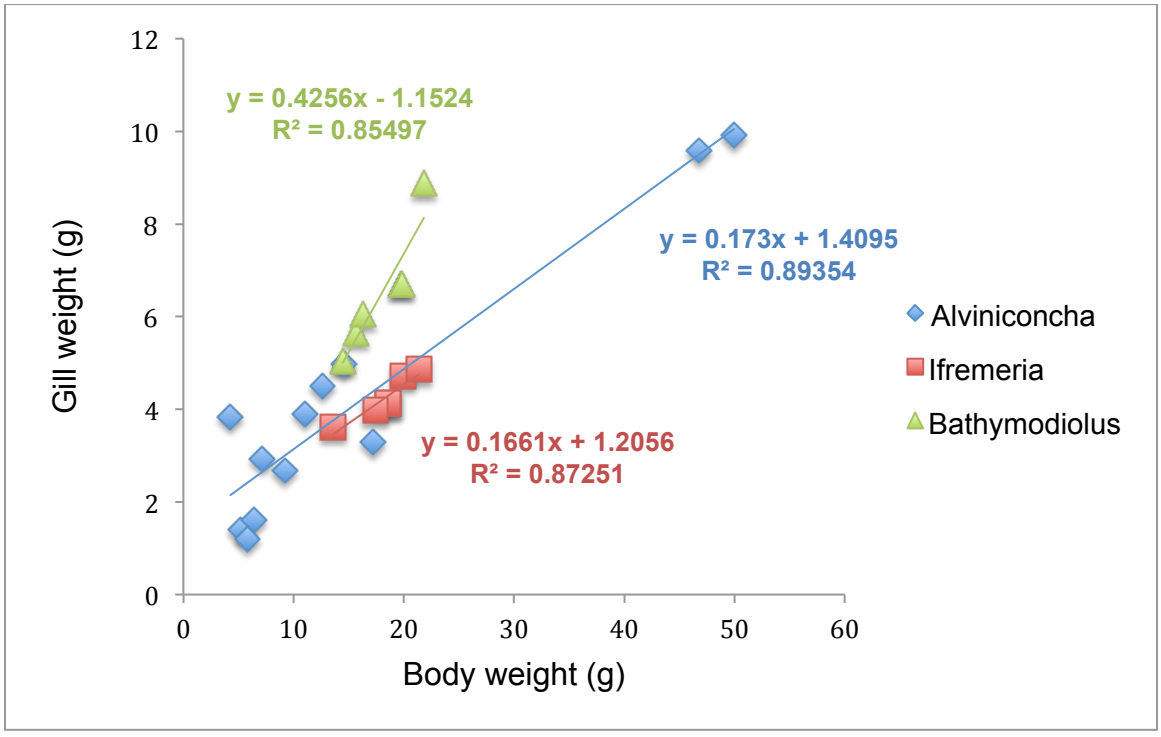

Figure S4.2: Linear regression of gill weight to body weight for each of the three mollusc genera.

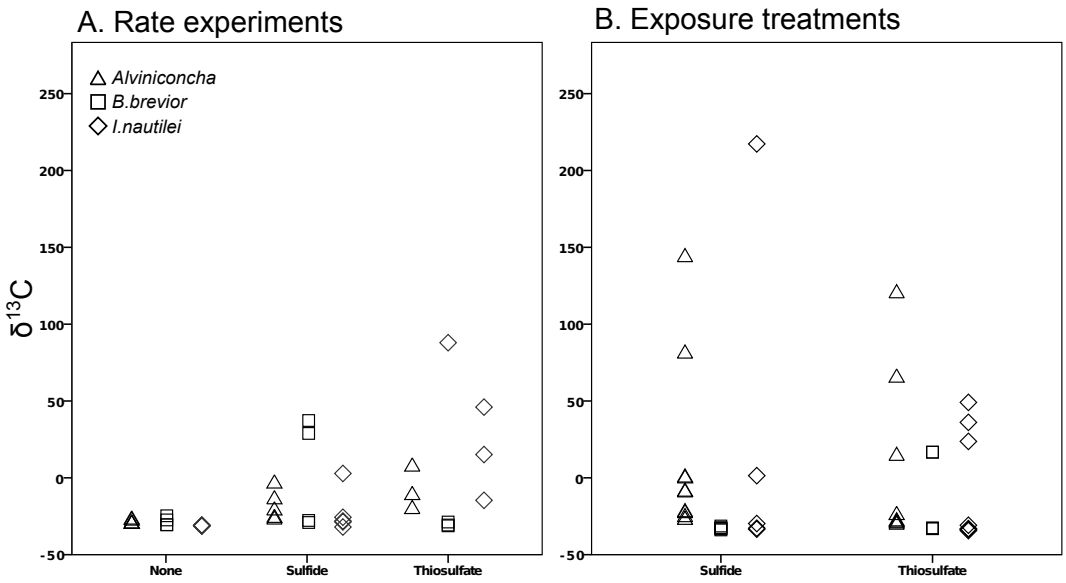

Figure S4.3 Stable carbon isotopic composition of *Alviniconcha* (△), *B. brevior* (□), and *I. nautilei* (◇) gill tissue after rate experiments and exposure treatments.

Supplemental References

Beinart, R.A. et al., 2012. Evidence for the role of endosymbionts in regional-scale habitat partitioning by hydrothermal vent symbioses. *Proceedings of the National Academy of Sciences*. Online Only.

Dubilier, N., Windoffer, R. & Giere, O., 1998. Ultrastructure and stable carbon isotope composition of the hydrothermal vent mussels Bathymodiolus brevior and B. sp. affinis brevior from the North Fiji Basin, western Pacific. *Marine Ecology Progress Series*, 165, pp.187–193.

Suzuki, Y. et al., 2006. Host-symbiont relationships in hydrothermal vent gastropods of the genus Alviniconcha from the Southwest Pacific. *Applied and Environmental Microbiology*, 72(2), pp.1388–1393.

Weiss, R.F., 1970. The solubility of nitrogen, oxygen and argon in water and seawater. *Deep Sea Research and Oceanographic Abstracts*. 17(4), pp.721-735.

Appendix 4

Chapter 5 Supplemental Material

Supporting Table 5.1: Number of *Alviniconcha* individuals in which AOP was detected/not detected via 16S rRNA gene qPCR according to majority symbiont class and host type.

	Host type				
Majority symbiont	*I*	*II*	*III*	*Undetermined*	*All*
ε	2/4	3/85	NA	0/8	**5/97**
γ	88/5	NA	74/3	11/0	**173/8**
All	**90/9**	**3/85**	**74/3**	**11/8**	***178/105***

Supporting Table 5.2: Proportion of AOP 16S rRNA genes, relative to the 16S rRNA genes of the symbionts, in *Alviniconcha* individuals according to their majority symbiont class and host type. Percentages are shown as median (minimum, maximum).

	Host type				
Majority symbiont	*I*	*II*	*III*	*Undetermined*	*All*
ε	0 (0, 7.5)	0 (0, 2.5)	NA	0 (0,0)	**0 (0, 7.5)**
γ	1.6 (0, 36)	NA	1.2 (0,15)	1.83 (0.09, 21.6)	**1.3 (0, 36)**
All	**1.5 (0, 36)**	**0 (0, 2.5)**	**1.2 (0,15)**	**NA**	***0.53 (0, 36)***

Supporting Table 5.3: Proportion of AOP 16S rRNA genes, relative to the 16S rRNA genes of the symbionts, in *Alviniconcha* individuals at the four vent fields at the ELSC, shown north to south in descending order. Percentages are shown as median (minimum, maximum). Dominant symbiont phylotypes and host types for the *Alviniconcha* communities inhabiting each vent field are indicated (Beinart et al., 2012).

Vent field	**%AOP**	**Dominant symbiont**	**Dominant host**
Kilo Moana	0 (0,0)	*ε*	II
Tow Cam	0 (0,35)	*ε*	II
ABE	1.5 (0,36)	*γ-1*	I
Tu'i Malila	1.3 (0,22)	*γ-1, γ-Lau*	I, III

Supporting References:

Beinart,R.A. et al. (2012) Evidence for the role of endosymbionts in regional-scale habitat partitioning by hydrothermal vent symbioses. *Proceedings of the National Academy of Sciences*.

Zielinski,F.U. et al. (2009) Widespread occurrence of an intranuclear bacterial parasite in vent and seep bathymodiolin mussels. *Environ. Microbiol.* **11**: 1150–1167.